NON-NEURONAL AND NON-ENZYMATIC ROLE OF ACETYLCHOLINESTERASE IN BONE REMODELING AND DISORDER

LUO XIAOHE

PhD

The Hong Kong Polytechnic University

2022

The Hong Kong Polytechnic University
Department of Biomedical Engineering

Non-Neuronal and Non-Enzymatic Role of Acetylcholinesterase in Bone Remodeling and Disorder

LUO Xiaohe

A thesis submitted in partial fulfilment of the requirements for the degree of Doctor of Philosophy

September 2021

CERTIFICATE OF ORIGINALITY

I hereby declare that this thesis is my own work and that, to the best of my knowledge and belief, it reproduces no material previously published or written, nor material that has been accepted for the award of any other degree or diploma, except where due acknowledgement has been made in the text.

Signed _____

LUO Xiaohe

Abstract

Osteoporosis is a multifactor degenerative bone loss disease characterized by the uncoupling of bone formation and bone resorption. As one of the leading causes of disability and even death in the elderly, osteoporosis poses enormous societal burdens to the whole world. Although several FDA-approved drugs are available, osteoporotic fractures remain an unresolved problem.

The positive correlation between Alzheimer's disease and osteoporosis has been noticed for a long time. Recently, the use of AChE inhibitors has been reported to associate with reduced risk of hip fractures, elevated healing of osteoporotic fractures, and decreased overall mortality in Alzheimer's disease patients. Meanwhile, it has been reported that the expression of AChE and other cholinergic components existed not only in the nervous system but also in the bone system. AChE and other cholinergic components have also been recently proposed to be correlated with the regulation of bone homeostasis. These cues indicate a possible role of AChE and its inhibitors in the treatment of osteoporosis.

The roles and the underlying mechanism of AChE, however, in osteoblast senescence and osteoclastogenesis under pathological conditions remain unclear. We aimed to determine the roles of AChE and its inhibitors in osteoblast senescence, osteoclastogenesis, and osteoblast-osteoclasts crosstalk in osteoporosis development as well as the feasibility of employing AChE inhibitors for osteoporosis treatment.

In this study, we first demonstrated that the AChE expression increased during the **natural aging process** in the mice model. For the *in vitro* study, we found that osteoblasts could form an autocrine loop of AChE and amplify the senescence of osteoblast continuously. We firstly confirmed an upregulated expression of AChE with an increased level of p21 and p16INK4a in an H2O2-induced senescence model of osteoblastic cells. Moreover, with the incubation with recombinant AChE protein or heat-inactivated AChE protein, a higher level of early senescent marker p21 in osteoblastic cells was observed. Additionally, the treatment of dual-bind AChE inhibitor donepezil but not catalytic inhibitor galantamine could partly rescue the H2O2 induced senescence in osteoblasts.

We also found that AChE played an important role in regulating osteoclastogenesis. We first confirmed that the AChE secreted by senescent osteoblasts could trigger the migration of osteoclast precursors. Secondly, our results suggested that both intact AChE and heat-inactivated AChE (HAChE) protein could promote the adhesion of osteoclast precursors. Thirdly, AChE and HAChE treatments accelerated the process of osteoclast fusion. The expression of AChE was also elevated during osteoclastic differentiation. Reversely, we observed that genetic silence of AChE led to a lower differentiation ratio of osteoclasts. Moreover, dual binding AChE inhibitor donepezil but not catalytic AChE inhibitor galantamine suppressed osteoclastogenesis *in vitro*, further suggesting that the non-enzymatic function and peripheral anionic site of AChE got involved in the regulation of osteoclast differentiation.

To investigate the protective effect of AChE inhibitors for the treatment of osteoporosis, we used the OVX mice as an osteoporotic *in vivo* model. We demonstrated that the expression of AChE protein increased in OVX induced postmenopausal osteoporosis *in vivo*. The pharmaceutical inhibition of AChE could rescue postmenopausal bone loss *in vivo*. In particular, the BBB (blood-brain barrier)-impermeable AChE inhibitor ambenonium indicated a comparable rescue effect to BBB-permeable inhibitor donepezil, which suggested that targeting peripheral AChE protein could also rescue OVX-induced bone loss.

In short, with the aging and bone degeneration development, higher expression of AChE occurred in senescent osteoblasts and further accelerated osteoblast aging. The elevated AChE was deposited in the bone matrix and was released to the bone microenvironment during osteoclast-mediated bone resorption. These released AChE proteins stimulated increased osteoclastogenesis. This study, for the first time, implicated the roles of AChE, a hydrolytic enzyme of choline ester, in bone homeostasis and disease. AChE inhibitor donepezil could be an emerging drug for osteoporosis treatment. This study will lead to the discovery of dual-acting AChE inhibitors as an alternative for the treatment of osteoporosis, which will open a new avenue for osteoporosis treatment via repositioning the AChE inhibitors.

List of Publications

Journal Articles

Chen, Z., **Luo, X.**, Zhao, X., Yang, M., & Wen, C. (2019). Label-free cell sorting strategies via biophysical and biochemical gradients. *Journal of orthopaedic translation*.

Chen, Z., Jiang, K., **Luo, X.**, Zou, Z., Lim, C., & Wen, C. (2020). High-throughput and label-free isolation of senescent murine mesenchymal stem cells. *Biomicrofluidics*.

Lin, L. J., Ge, Y. M., Tian, Y., Liu, N., **Luo, X. H.**, Xue, Y. T., ... & Tang, B. (2020). Multi-scale mechanical investigation of articular cartilage suffered progressive pseudorheumatoid dysplasia. *Clinical biomechanics*, 79, 104947.

Luo, X., Lauwers, M., Layer, P. G., & Wen, C. (2021). Non-neuronal Role of Acetylcholinesterase in Bone Development and Degeneration. *Frontiers in Cell and Developmental Biology*, 8, 1886.

Zou, Z., **Luo, X.**, Chen, Z., Zhang, Y. S., & Wen, C. (2022). Emerging microfluidics-enabled platforms for osteoarthritis management: from benchtop to bedside. Theranostics, 12(2), 891.

Poster Presentation

Luo, X., & Wen, C. (2020, November). Acetylcholinesterase in osteoclastogenesis and osteoporosis via ACh-independent pathway. In JOURNAL OF BONE AND MINERAL RESEARCH (Vol. 35, pp. 187-187). 111 RIVER ST, HOBOKEN 07030-5774, NJ USA: WILEY.

Acknowledgements

Firstly, I want to express a deep sense of thanks to my supervisor Dr. Chunyi Wen from the bottom of my heart. For four years of my Ph.D. study, he has always been nice and patient in inspiring me in research ideas, teaching me in advance methodologies and knowledge, guiding me in experiments conduction, encouraging me in hard work. He is always glad to give opportunities and challenges to his students in our own research interests and provide help on key points. Because of his trust and education, I gradually grew to become an independent researcher.

Secondly, my sincere thanks go to all the mentors helps me in the past few years. I would like to thank my co-supervisor Prof. Yongping Zheng for his great support. I also want to thank Prof. Mo Yang, Dr. Youhua Tan, Dr. Xin Zhao, and Dr. Sharon Ruan in PolyU BME for their education on me and for giving me access to their research facilities. I thank my undergraduate supervisor, Dr. Bin Tang, in SUSTech for introducing me to Dr. Wen's lab and letting me conduct part of my experiments in his lab.

Apart from my supervisors and mentors, I want to thank my lab mates Ms. Yuqi Zhang and Ms. Zhou Zou, for their kindly help in my animal experiments. And thanks to Dr. Tony Liu in HKU for his technical help in microCT and Mr. Ye Tian for his help in microfluidics. I also would like to thank Dr. Manting Au, my junior labmate and my sister in life, for her

experimental and technical support and her inspiration to me in life. My great thanks also go to Dr. Marianne Lauwers, Ms. Xiaoqing Kuang, Ms. Karen Ching, Ms. Junguo Ni, Mr. Jun Liu for the relaxing working and studying atmosphere they created. I thank all the technical staff in BME, HTI, ULS, and CAF in PolyU.

My thanks must go to my dear friends and family. For their encouragement and supports spiritually in those hard time. I want to thank my mom and dad for their unconditional love and support, thank them for always comforting me when I was upset.

Table of Contents

List of Figures

List of Tables

List of Abbreviations

OB	Osteoblast
OC	Osteoclast
MSC	Mesenchymal stem cell
BMP	Bone morphogenetic protein
FGF	Fibroblast growth factor
Hh	hedgehog
PTH	parathyroid hormone
TGF-β	transforming growth factor-β
RunX2	runt-related transcription factor 2
SATB2	special AT-rich sequence-binding protein 2
ECM	extracellular matrix
ALP	alkaline phosphatase
COL1A1	collagen type 1 alpha 1 chain
ATF4	activating transcription factor 4
BSP	bone sialoprotein
OCN	osteocalcin
OPN	osteopontin
TNF	tumor necrosis factor
RANK	receptor activator of NF-κB
RANKL	RANK ligand
OPG	osteoprotegerin
ICAM-1	intercellular adhesion molecule 1
MMP-9	matrix metalloproteinases 9

CtsK	cathepsin K
CFU-GM	granulocyte-macrophage colony forming unit
M-CSF	macrophage colony stimulating factor
MITF	microphthalmia-associated transcription factor
TRAP	Tartrate resistance acid phosphatase
TNFR	tumor necrosis factor receptor
TRAF6	TNF receptor-associated factor 6
JNK	janus like kinase
NFATc1	nuclear factor of activated T cells, calcineurin-dependent 1
S1P	sphingosine 1-phosphate
MCP-1	monocyte chemotactic protein 1
Atp6v0d2	d2 isoform of vacuolar ATPase Vo domain
DC-STAMP	dendritic cell-specific transmembrane protein
OC-STAMP	osteoclast-stimulatory transmembrane protein
RGD	arginine-glycine-aspartic acid
BMU	basic multicellular units
ACh	acetylcholine
ChAT	choline acetyltransferase
VAChT	vesicular acetylcholine transporter
AChE	acetylcholinesterase
BChE	butyrylcholinesterase
AChR	Acetylcholine receptor
NNCS	non-neuronal cholinergic system
OVX	ovariectomy
IL-1	Interleukin 1

IL-6	Interleukin 6
TNF-α	tumour necrosis factor alpha
RT-PCR	transcription-polymerase chain reaction
AFM	Atomic force microscope
AD	Alzheimer’s disease
BBB	blood–brain barrier

Chapter 1 Introduction – Literature Review

1.1 Bone system

Bone is a complex but organized system which have multiple irreplaceable functions[1]. Bone is responsible for protecting the inner organs, supporting the body structure, and motivating the movement. For its vital functions in reserving the minerals, housing the formation of white and red blood cells, bone plays an important role in maintaining the homeostasis of human function. Recently, it is reported that bone have more new functions for its secreting cytokines involving in regulating kidney [2, 3]and brain function [4, 5].

Bone is a complex hard connective tissue composed of collagenous extracellular matrix, calcium phosphate minerals and various types of cells: osteoblast, osteoclasts, osteocytes, bone lining cells and their precursors[6, 7]. Among all these cells, the bone-forming cell family and the bone-resorbing cell family are the most important. These cells cooperate with each other under the regulation of multiple signaling factors to maintain bone homeostasis.

1.1.1 Bone structure

Bones can be divided into long bones, short bones, flat bones, irregulate bones,

and sesamoid bones based on their shapes. Long bones are found in arms and legs as well as in fingers. Short bones are carpals and tarsals existing in the wrist ankles with cube-like shapes. Flat bones include the cranial bone, the scapulae bone, the sternum, and the ribs. Irregulate bones, just as the name, have more complex structures that cannot be easily described as any simple shape, the typical examples of irregulate bones are vertebrae and many facial bones. Sesamoid bones are sesame-seed-like bones always found in tendons connected to the limbs[8, 9]. The anatomy of a representative long bone[9] is shown in Fig 1.1, a long bone can be mainly divided into three parts: proximal epiphysis, diaphysis, and distal epiphysis. The two expanded ends of the long bone are the epiphysis, whose internal is filled with spongy bone (also called trabecular bone) and red bone marrow. The structure in between the proximal epiphysis and the distal epiphysis is a long, hollow tubular shaft called the diaphysis. The walls of diaphysis are consisting of rigid compact bone (also called cortical bone). The compact bone encloses the medullary cavity, which is filled with yellow bone marrow storing bone marrow cells to produce chondrocytes, osteoblasts, and adipocytes. The field where every epiphysis connects to diaphysis is metaphysis. During growth, the cartilaginous epiphyseal plates located in the metaphysis act as the original site of new bone formation. After the bone growth stopped, these epiphyseal plates turn out into the epiphyseal line shown in Fig 1.1.

Flat bones, for example, those cranial bones, have a three-layer sandwich structure that can strongly protect the organ inside. For the sandwich structure, the inner layer is composed of spongy bone called *diploë,* the upper layer and downer layer are both consisting of compact bone, and their inner is filled with red bone marrow. This composite structure can provide sufficient mechanical properties with minimal mass.

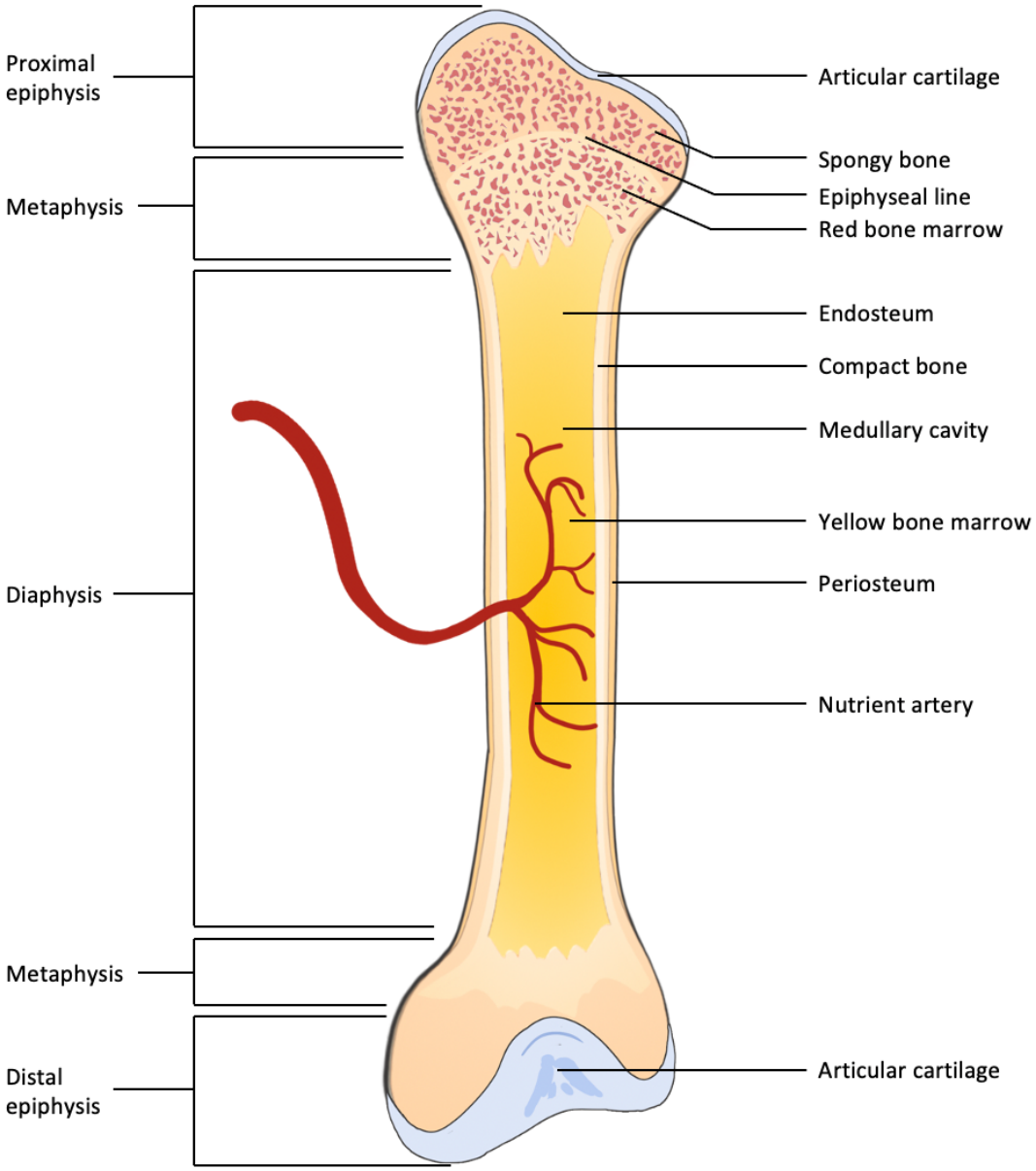

Fig 1.1 The structure of a typical long bone. A schematic diagram showing the structure of compact bone, spongy bone, articular cartilage, and other components of a long bone.

The outermost part of compact bone is enveloped with a bilayer structure called periosteum. (Shown in Fig 1.2). The outer layer is a fibrous layer and inner layer is a cellular layer which contribute to the bone growth, repair, and remodeling. Periosteum provides the binding site to tendon attachment, the route of vesicular, nervous, and lymphatic supply and separate the bone system from other organs. Periosteum wraps the entire bone outer surface, apart from the surface of joints, which is covered by a layer of cartilage tissue.

A layer of bone cells found on the inner side of the compact bone, near the medullary cavity is called endosteum[10]. This single layer of cells forms a thin membrane to cover both endocortical and trabecular bone surfaces. The incomplete cell layer of the endosteum is composed of bone lining cells and osteoprogenitor cells. In the exposed active site, osteoclasts and osteoblasts appear to reconstruct the bone matrix.

The compact bone is composed of many osteons, the basic functional units of compact bone. In an osteon, osteocytes line regularly in collagen and calcified matrix to assembly concentric layers of lamellae, surrounding the central canal. Generally, one or two blood vessels are presented in a central canal and function to supply blood in and out of the osteons. Many osteons stand parallelly together to form the compact bone and the central canals occupy

inside. There are other channels called perforating canals that run perpendicular to the bone surface to carry blood to the osteons deep inside the bone and to the tissues in the medullary cavity. All osteons align together to the direction of the long axis of the long bone shaft, providing strong mechanical stress along the long axis which can withstand 10–15 times the body's weight.

In spongy bones, the arrangement of lamellae is irregular. The spongy bone matrix is composed of a 3D bony fibrous open network known as trabeculae[11]. Red blood marrow filled in between the trabeculae supporting blood cells formation and trabecular bone cell metabolism. The osteocytes in trabeculae exchange wastes and nutrients by diffusion through the canaliculi which open on the surface of trabeculae. This kind of network structure provides spongy bone the capability to resist mechanical loading from different directions, also makes it easier for muscles to move bones for their lighter weight.

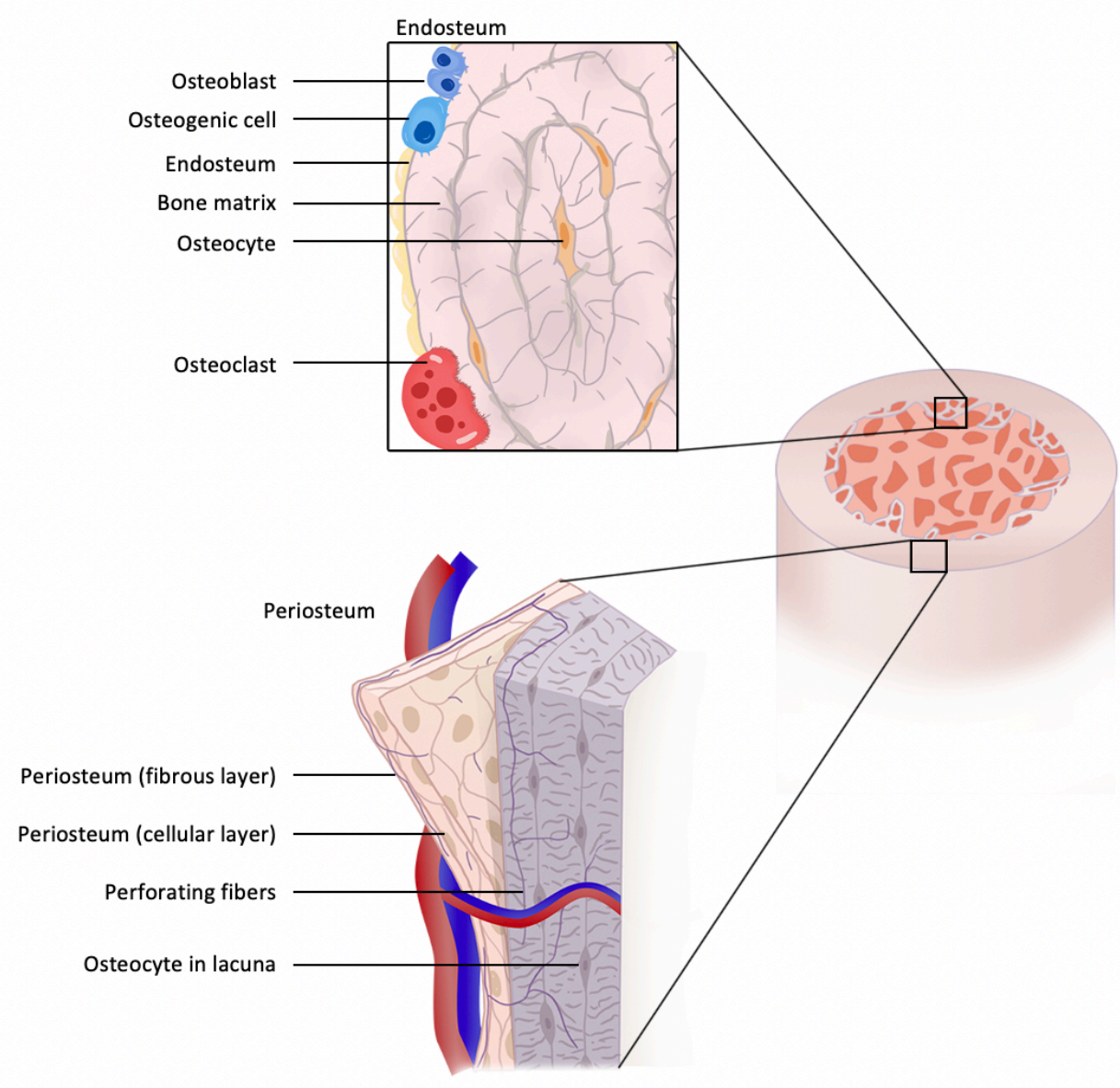

Fig 1.2 The Periosteum and the endosteum.

1.1.2 Blood supply to bone

During bone development and mature bone homeostasis, the bone system requires extensive oxygen, nutrients, and regulation factors supply. Therefore, there are abundant blood vessels to form a complex vascular network in bone tissue. Blood vessels formation is highly coupled with bone ossification. Studies from animals to human reported that the bone system demanded about 5-15% of cardiac output, which indicated the importance of blood vessels to skeleton development and homeostasis[12-15].

There are three typical types of blood vessels in the bone system: the nutrient artery and vein, metaphyseal and epiphyseal vessels, and periosteal vessels. The nutrient arteries and veins are large vessels located in the central diaphysis and branch into smaller arteries and veins which reach the metaphysis and endosteum[15]. The principal nutrient arteries pass through the cortical bone and then enter the medullary cavity via the foramen and then leave the inner diaphysis through Volkmann's arteries and Haversian arteries, and finally connected with the periosteal vessels in the super layer of the bone[12]. The periosteal system is a low-pressure system that supports the blood supply of the outer cortical bone. Instead of connecting to the medullary vessels, the epiphyseal vessels circulate as a separate system when the bone is still in youth, as the growth plate is avascular. So the epiphyseal vessels are vital for epiphysis development[16].

After the closure of the epiphyseal growth plate, these three systems of blood vessels are highly linked together via numerous capillaries. There are two subtypes of capillaries in bone, type H and type L. Type H capillaries are found in the metaphyseal area and region near the endosteum, which is identified to express a high level of junctional protein CD31 and the sialoglycoprotein endomucin. Type L capillaries, which indicated a low level of these two markers, are located in the medullary cavity. Type H capillaries show column-like structures while type L capillaries are extensively branched. The blood in arteries flow in the type H capillaries and then type L capillaries and drain into veins[17].

The vascular system is critical for the regulation of bone growth and repair, as it supports the metabolic activity of the bone. As age increases, oxygen consumption decreased in the human body. Studies also reported that the volume and speed of blood in the bone system declined with aging. Meanwhile, the number of type H capillaries and arteries is reduced in aged bones[12, 14-16]. Aging, vascular dysfunction, and bone loss are closely associated[18, 19].

1.1.3 Nerves and the neuronal regulation in bone

Rich nerves networks have been identified in the bone system over the past 170 years[20]. Although myelinated axons are also found in bone tissue, most of the nerves in bone are unmyelinated. The nerves in the bone are distributed in the bone marrow, periosteum, and epiphyseal plate, which are always accompanied by blood vessels[21]. There are sensory neurons and autonomic neurons in the bone system, including both cholinergic and adrenergic neurons[22, 23]. Peripheral nerves in bone are involved in the regulation of bone homeostasis via neurotransmitters, neuropeptides, and other signaling factors. Histological and transcription-polymerase chain reaction (RT-PCR) results proved the expression of adrenergic receptors in osteoblastic and osteoclastic cells. Activation of $\alpha 1$ and $\beta 2$ adrenergic receptors on osteoblastic cells indicated the anabolic effects in the aspects of promoting alkaline phosphatase (ALP) activity and DNA synthesis[24]. Meanwhile, stimulation of β adrenergic receptors also enhanced bone resorption in osteoclastic cells[24, 25]. For cholinergic regulation, both nicotinic acetylcholine receptors and muscarinic acetylcholine receptors were reported to be expressed on osteoblastic cells and osteoclastic cells. The increased cholinergic activity was associated with accelerated bone formation and inhibited bone resorption[23].

1.1.4 Bone cells

Bone is a complex hard connective tissue composed of collagenous extracellular matrix, calcium phosphate minerals and various types of cells: osteoblast (OBs), osteoclasts (OCs), osteocytes, bone lining cells and their precursors[6, 7]. Among all these cells, the bone-forming cell family and the bone-resorbing cell family have the most critical functions to maintain the bone homeostasis. These cells cooperate with each other under the regulation of multiple signaling factors to maintain bone homeostasis.

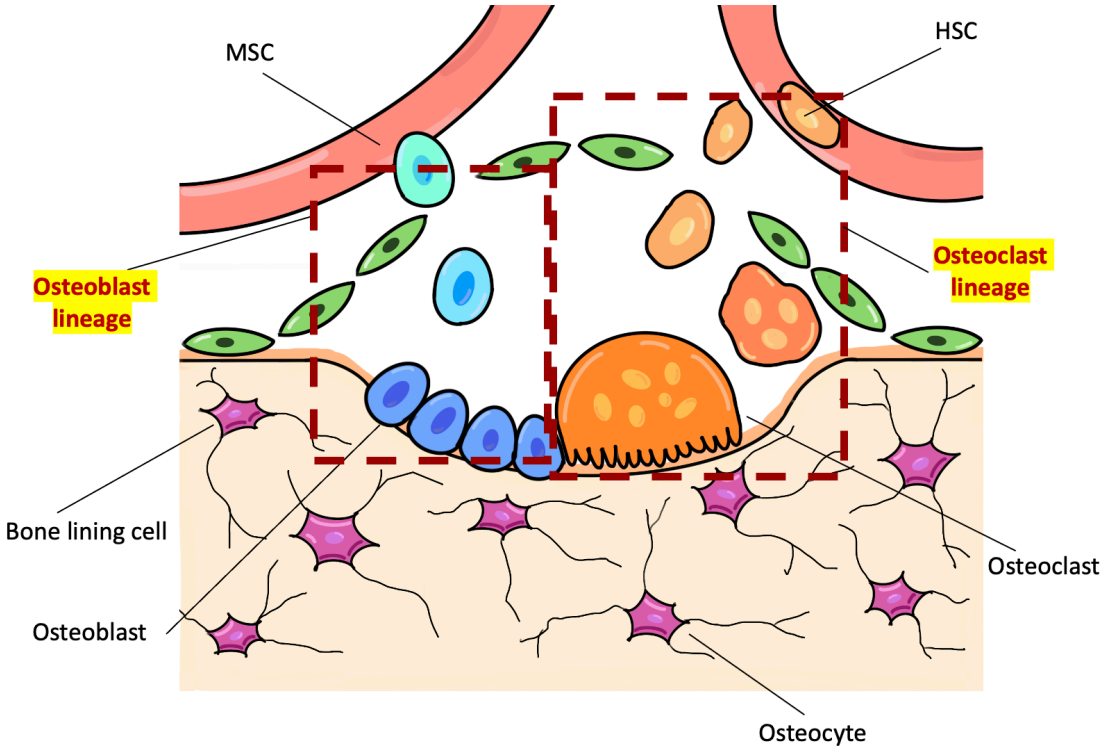

Fig 1.3 Bone cells.A schematic diagram showing the bone cells, including osteoblastic cells derived from mesenchymal stem cells and osteoclastic cells derived from hematopoietic stem cells.

Osteoblasts

Osteoblasts (OBs) are mononucleated fibroblast-like cells derived from mesenchymal stem cells. Osteoblasts in the active phase are a group of aligned cuboidal cells found on the bone surface, they adhere to each other by tight junctions and gap junctions[26, 27]. Osteoblasts display features of protein-synthesizing cells, containing a sufficient amount of endoplasmic reticulum, Golgi apparatus, and mitochondria[28, 29]. In the bone system, osteoblasts are responsible for new bone formation, which secret highly cross-linked collagen type I and other proteins to form an organic matrix and help concentrate surrounding calcium phosphate to induce inorganic components deposition to the bone matrix.

Early Stage of osteoblast differentiation

Osteoblasts are derived from bone marrow pluripotent mesenchymal stem cells (MSCs), which have multiple potentials to differentiate into several types of cells, such as osteoblasts, chondrocytes, and adipocytes[30]. Osteoblast differentiation is regulated by a lot of signaling molecules[31]. Under the regulation of the Wnt family[32], bone morphogenetic proteins (BMPs)[33], fibroblast growth factor (FGF)[34], hedgehog (Hh)[35], parathyroid hormone (PTH)[36] and transforming growth factor-β (TGF-β)[33], the mesenchymal stem cells begin to differentiate to osteoblasts, the expressions of transcription

factors runt-related transcription factor 2 (RunX2), special AT-rich sequence-binding protein 2 (SATB2) increase; therefore, the proliferation of pre-osteoblasts (pre-OBs) is activated and pre-OBs secret collagen, fibronectin, and TGF-β receptor 1 to synthesize the extracellular matrix (ECM). For the transcription factor, RunX2 and Osterix are upregulated, the pre-OB also expresses a low level of alkaline phosphatase (ALP) and collagen type 1 alpha 1 chain (COL1A1)[37].

Matrix maturation of osteoblasts

In the next step, still under the same signals stimulation, the proliferation of the immature osteoblasts decreases, and the transcription factors RunX2, SATB2, Osterix, and activating transcription factor 4 (ATF4) are highly expressed. The immature osteoblasts differentiate to mature osteoblasts and secret a large amount of COL1A1 (the major abundant fibrous protein of ECM), ALP and bone sialoprotein (BSP) to mature the matrix.

Matrix mineralization of osteoblasts

Once the stage of matrix maturation is finished, the mature osteoblasts express osteocalcin (OCN), osteopontin (OPN), and BSP to mineralize the ECM[38]. The OCN binds to calcium directly and therefore contributes to the mineral deposition in the bone matrix. The OPN regulates the balance of bone formation and mineralization. The BSP modulates the crystallization of

hydroxyapatite in the bone matrix. At the same time, the COLA1 and ALP are continuously produced by the mature osteoblasts. Finally, the mature osteoblasts are trapped in the bone matrix to become osteocytes or directly undergo apoptosis or become bone lining cells.

Apoptosis of osteoblasts

The balance of cell proliferation, differentiation, and apoptosis is critical for the number of osteoblasts, which is important for bone homeostasis. Apoptosis refers to the programmed death of cells and is essential for bone development and regeneration. There are two widely accepted cell apoptosis signaling pathways: the mitochondrial activated pathway[39] and the activation of the tumor necrosis factor (TNF) receptor family[40]. Apoptotic stimuli trigger mitochondria to secret cytochrome c to the cytosol or activate the death receptors of the TNF receptor family on the cell membrane, which both lead to the initiation of several initiator caspases, finally inducing cell apoptosis. BMPs family is documented as key regulators in interdigital apoptosis for limb development. FGF-2 and the FGF-2 receptor are reported to control the survival and apoptosis of osteoblast during bone remodeling. As the receptor activator of NF-κB (RANK), RANK ligand (RANKL), and osteoprotegerin (OPG) belong to the TNF receptor family, RANK/RANKL/OPG system are also under investigation for their relationship to apoptosis[41].

Osteocytes

Osteocytes are mature bone cells and are the most abundant cells in bone tissue as they occupy 90-95% of the bone cells. The end osteogenic stage of MSCs is osteocytes. The mature osteoblasts are trapped in the mineralized matrix and highly polarized to become osteocytes[42, 43]. In bone tissue, each osteocyte occupies one single small cavity named lacuna, which is enveloped in the layer structure called lamellae. There are small channels named canaliculi within the lamellae, which allow the exchange of nutrients and wastes. Osteocytes are able to extend their cytoplasm through the canaliculi to connect and communicate with other osteocytes via gap junctions. Osteocytes maintain the protein and mineral components of the surrounding matrix environment. Under specific conditions, osteocytes might be released from the lacuna to convert to osteoblasts or precursors to help to repair the damaged bone tissue.

Bone lining cells

The osteoblasts that neither go apoptosis nor differentiate into osteocytes refer to bone lining cells, the bone lining cells line the surface of the bone matrix just as suggested by their name. Compared with osteoblasts, bone lining cells have a more stretched and flatter morphology[44]. For their differences in proteins expression, both osteoblasts and bone lining cells express alkaline phosphatase and collagen type I. Bone lining cells secret intercellular adhesion molecule 1 (ICAM-1) but not osteocalcin, however, osteoblasts have a high

expression of osteocalcin but not ICAM-1[45]. Bone lining cells can be considered as an inactive phage of osteoblasts, while they still have the potential to convert to osteoblasts. Bone lining cells are also believed to be involved in the initiation of bone remodeling and participated in the regulation of osteoclastogenesis[46].

Osteoclasts

Osteoclasts are giant cells with multiple nuclear (up to 100 or more nuclear) responsible for digesting bone matrix and removing bone. These bone-resorbing cells are fused from the monocyte/macrophage precursor cells which belong to the hematopoietic lineage[47]. Apart from multinuclear, to support their resorbing function, osteoclasts have plenty of mitochondria, many layers of Golgi membranes to package functional proteins, and a large number of vacuoles and lysosomes. The mature osteoclasts are extremely heterogeneous cells with ruffled borders and sealing zones. The ruffled border is a structure with highly folded plasm membranes covering the damaged, old, or unwanted bone surface. Circling the ruffled border, there is a relatively smoother area of plasma membrane tightly attached to the bone matrix surface called the sealing zone. The sealing zones help osteoclast adhere to the targeting bone surface and isolation for the resorbing-needed area from the unresorbed bone area[48]. Active osteoclasts secret ATP6i complex related hydrogen ions to dissolve mineral hydroxyapatite, and proteolytic enzymes such as matrix

metalloproteinases 9 (MMP-9) and cathepsin K (CtsK) to degrade organic phage of bone matrix[49].

Origin of osteoclasts

The granulocyte-macrophage colony-forming unit (CFU-GM) is identified as the earliest hematopoietic progenitors that have the capability to differentiate to osteoclasts. Under the regulation of macrophage colony stimulating factor (M-CSF), the hematopoietic lineage myeloblasts show an upregulated expression of transcription factor PU.1 and turn to be CFU-GM. PU.1 belongs to the ETS family of transcription factors, the deficiency of PU.1 in mice hindered the differentiation of both macrophages and osteoclasts[50].

Proliferation of monocytic precursors

With the continuous stimulation of M-CSF, the monocytic precursors express higher levels of transcription factors PU.1and MITF (microphthalmia-associated transcription factor) and develop into pre-osteoclasts. The receptor of M-CSF is encoded by c-FMS, while its transcription is dependent on PU.1. Therefore, an autocrine loop forms and amplifies the M-CSF signaling pathway. M-CSF stimulating c-FMS are essential for the proliferation and survival of monocyte/osteoclasts precursors. Both gene mutation in M-CSF and blockage of CSF-1 receptor lead to a dramatical decrease in the number of macrophages and osteoclasts[51], indicating the significance of M-CSF and its

receptor in the development of osteoclastogenesis.

Differentiation of pre-osteoclasts

In this stage, under the stimulation of M-CSF, the pre-osteoclasts proliferate to a certain amount. The RANK on the membrane of the pre-osteoclasts is activated by RANKL, which induces pre-OCs to differentiate to TRAP (Tartrate resistance acid phosphatase) positive mononuclear osteoclasts[52]. RANK is a transmembrane protein expressed by the osteoclastic cells. RANK belongs to the tumor necrosis factor receptor (TNFR) molecular sub-family and is the receptor of RANKL. RANKL is generally expressed by bone marrow stromal cells and osteoblastic cells, however, under the inflammatory condition, it can also be expressed by T-lymphocytes[53] in a soluble form (sRANKL). RANKL or sRANKL binds to the extracellular domain of RANK and therefore triggers the cytoplasmatic domain of RANK to interact with an adaptor molecule TNF receptor-associated factor 6 (TRAF6). The activation of TRAF6 induces the translocation of downstream transcriptional factors of NF-κB, JNK (janus like kinase), AP-1, and NFATc1 (nuclear factor of activated T cells, calcineurin-dependent 1), which provokes the expression of osteoclastic genes such as TRAP.

Cell enlargement, recruitment, and cell-cell fusion of mononuclear osteoclasts

The mononuclear osteoclasts are not efficient enough to resorb larger areas of

bone tissues, so the strategy for osteoclasts to solve this problem is cell fusion[54]. As mentioned before, osteoclasts degrade bone matrix by entirely covering the surface and creating a closed chamber, and large cells with multinuclear enable them to cover a large component at once, thereby increasing the resorption efficiency. One of the most critical points of cell-cell fusion is the density of cells (to ensure cell contact). To increase the cell density on the bone surface, cytoplasm growth, proliferation, and recruitment are essential. The growth and proliferation of pre-osteoclasts are guaranteed by the unceasing signaling of M-CSF. For the recruitment, pre-osteoclasts and osteoclasts are able to secret sphingosine 1-phosphate (S1P) protein to attract the migration of other precursors via binding to SIP receptor 1[55]. RANKL/RANK signaling initiates the expressions of some chemokines like monocyte chemotactic protein 1 (MCP-1) and RANTES as chemotactic signals to recruit monocytic TRAP+ osteoclast to the bone-resorbing site. After cell recruitment, the activation of transcription factor NFATc1 via the RANK pathway induces the expression of Atp6v0d2 (d2 isoform of vacuolar ATPase Vo domain) and DC-STAMP (dendritic cell-specific transmembrane protein) to mediate cell-cell fusion of osteoclasts[56]. Atp6v0d2$^{-/-}$ mice showed a significant increase in bone mass and reduced number of osteoclasts, Atp6v0d2$^{-/-}$ bone marrow cells suggested an impaired osteoclasts fusion *ex vivo*[57]. DC-STAMP is a putative seven-transmembrane protein highly expressed by osteoclasts; reduction of cell fusion was also observed in DC-

STAMP deficient mice[58]. One DC-STAMP positive monocytic osteoclast acting as the leader contacts with a DC-STAMP negative cell as the follower to fuse together, the fused binucleated osteoclast will fuse with the next DC-STAMP negative follower and finally forms a giant polykaryon[59]. Another protein named osteoclast-stimulatory transmembrane protein (OC-STAMP) is also critical for monocytes fusion. Silence of mRNA expression of OC-STAMP in monocyte cell line RAW264.7 cell and mouse bone marrow cells blocked the cell-cell fusion and osteoclastogenesis *in vitro*[60].

Activation of fused polykaryon to resorbing multinucleated osteoclasts

The fused polykaryon needs to undergo polarization to adapt to the functional requirement of resorption. To form the resorption specific structures ruffled border and sealing zone, the αvβ3 integrin anchored to the fused polykaryon membrane recognizes the RGD (arginine-glycine-aspartic acid) peptide motif in osteopontin and bone sialoprotein[61, 62]. This recognition triggers the cytoplasmic domain of αvβ3 integrin linking to intracellular cytoskeletal complexes and bundles of actin filaments, activates the Rho GTPases to induce cytoskeletal reorganization[63]. Therefore, the mature multinuclear osteoclasts with resorbing ability form on the targeting bone surface.

1.1.5 Bone development

Intramembranous ossification and endochondral ossification are the two major processes being responsible for bone formation during skeleton development. In intramembranous ossification, bones are formed from the direct differentiation of mesenchymal stem cells. While in endochondral ossification, templates of chondrocytes first form and are replaced by osteoblasts differentiated from mesenchymal stem cells.

Intramembranous ossification

During intramembranous ossification, the embryo mesenchyme tissues directly undergo osteogenesis to form osteoblasts. In the human body, cranial bones, parts of the mandible, and the clavicle are developed from intramembranous ossification. In short, embryonic mesenchymal progenitor cells are attracted and gathered, so the ossification center is formed at the programmed site, and these stem cells in the ossification center begin to release the organic components of the bone matrix. With the interference of the enzyme alkaline phosphatase, the matrix is mineralized via the crystallization of calcium salts, the mesenchymal stem cells differentiate into osteoblasts during this process. In the initiation stage, the ossification centers are scattered in the bone-forming area, growing bone tissues develop outwards from these centers and form organized structures called spicules. Blood vessels develop along the spicules to supply nutrients and take away the wastes. As the bone grows and spicules

fuse together, some of these blood vessels are trapped in the bone. The early differentiated osteoblasts buried in the bone matrix become osteocytes, and following mesenchymal cells keep developing into new osteoblasts. In the early stage, the intramembranous bones are all spongy bones, with vascular penetration, the monocytic precursors come and differentiate into osteoclasts that couple with existing osteoblasts to undergo bone remodeling to form compact bone.

Endochondral ossification

Most of the bones, long bones, for instance, are developed from endochondral ossification. Generally, in endochondral ossification, the calcified bone structures are formed by replacing previously formed cartilage. To start, the mesenchymal stem cells are recruited and clustered to undergo chondrogenesis. The differentiated chondrocytes developed a cartilage template composed of hyaluronic acid, chondroitin sulfate, and collagen proteins for the formation of the future bone. Under the regulation of a series of bone developmental factors, the cartilage grows and the chondrocytes in the center of the shaft become hypertrophic, meanwhile, the matrix comes to be a series of struts and starts to calcify. As there is no blood vessel inside the calcified cartilage, and diffusion is blocked, without nutrients supply and with the accumulation of metabolic wastes, the chondrocytes gradually die and disintegrate. The outer surface of hyaline cartilage is covered by a bi-layer structure named perichondrium. In

the next stage, blood vessels grow into the perichondrium, and the cellular layer of the perichondrium converts to osteoblasts starting secreting proteins and minerals to form a thin layer of bone tissue. Therefore, the perichondrium is replaced by the periosteum. As the inner chondrocytes die and leave some cavities, these cavities allow blood vessels to penetrate and bring osteoblasts in, releasing minerals to create spongy bone at a primary ossification center. The bone grows from the primary ossification center to the two ends. Further vascular penetration also lets osteoclasts in to create bone marrow and remodel the bone structure to generate a medullary cavity. Osteoblasts and osteoclasts communicate persistently to increase the length and size of the bone. At a certain time point, the hyaline cartilage in the center of epiphyses also begins to calcify, with the same process, blood vessels, osteoblasts, and osteoclasts come into these areas to form secondary ossification centers. Spongy bones fill in the secondary ossification centers and thin layers of cartilage at the edges of the end are still left which prevent abrasion between bones. In between the diaphysis and epiphysis, the thin plates of hyaline cartilage are remained, which will exist throughout childhood and adolescence, known as the growth or epiphyseal plate [64].

1.1.6 Bone homeostasis

Even after the skeleton is mature, bone is constantly resorbed and replaced

with new bone in a process known as bone remodeling. Bone undergoes the remodeling process in response to mechanical stimuli in daily life. This requires the orchestration of the bone formation and the bone resorption process, which is tightly controlled by bone-forming cells-osteoblasts and bone-resorbing cells-osteoclasts. Physiological bone remodeling is necessary to repair damaged bone and to maintain mineral homeostasis. However, once the activity of osteoblasts-mediated bone formation is stronger than that of osteoclasts-mediated bone resorption, or the bone resorptive activity overwhelms bone formation, an imbalance, or says uncoupling occurs. This imbalance between bone formation and bone resorption leads to the appearance of bone diseases like osteoporosis [65].

Bone remodeling occurs in “basic multicellular units” (BMUs), which couples several types of cells with multiple factors and cytokines [66, 67]. BMUs are covered by a canopy of cells believed to be bone-lining cells or osteomacs [68]. The bone remodeling process that occurs in a BMU is highly collaborative and orderly. Most of the time, these canopy cells are in a dormant status, and the mature osteoblasts, T cells and B cells derived from bone marrow continuously inhibit osteoclastogenesis by releasing osteoprotegerin [69]. However, after receiving bone remodeling initiation signals, e.g., structural damages caused by mechanical strain or hormone changes as a result of the systemic calcium homeostasis regulation, the BMU becomes active.

Structural damage will attribute to osteocytes apoptosis, which leads to a decreased local level of transforming growth factor beta which will reduce the control of osteoclastogenesis. Moreover, reduced serum calcium levels lead to the release of humoral factor parathyroid hormone, therefore stimulating the parathyroid hormone receptor on preosteoblasts. Consequently, the osteoblasts start to secret monocyte chemoattractant protein-1 and assemble osteoclasts precursors from the capillary blood vessels or nearby macrophage progenitors to the bone surface[70]. Additionally, a reduced osteoprotegerin expression and increased level of macrophage colony-stimulating factor and receptor activator of NF-kB ligand (RANKL) [71] in osteoblasts promote osteoclast proliferation and differentiation. Mature osteoclasts land in the damaged site and form the Howship's lacunae. In this sealed space, osteoclasts release hydrogen ions and proteolytic enzymes, like cathepsin K, to degrade the mineralized bone matrix. Later, the exposed demineralized collagen is removed by unknown phenotype reversal cells, which activate the bone formation signal. Osteocytes, receiving humoral and mechanical signals, decrease sclerostin expression resulting in Wnt-induced bone formation. When a sclerostin expression returns to the original level, bone formation stops, and minerals deposit [72]. The whole BMU goes back to the resting phase. This process occurs throughout the bone and maintains bone homeostasis. Apart from these well-known bone-regulating factors, evidence indicates that cholinergic components also play a role in the regulation of bone homeostasis.

1.2 Bone degeneration and osteoporosis (OP)

1.2.1 Aging and the prevalence of osteoporosis

Currently, Hong Kong and mainland China are facing the challenge of a rapidly aging population. In 2014, about 14.7% of people in Hong Kong were over 65 years old, and this ratio was said to increase to 31.5% in 2015 [73]. This situation may cause a huge economic and social burden to society. A huge budget for medical and care services will be spent on age-related diseases, such as osteoporosis.

Osteoporosis is a condition that the systemic skeletal strength weakness increases to a critical level that bone fractures occur under a minimum loading or trauma, sometimes bone breaks even in routine daily life activities[74]. This skeletal disorder is associated with lower bone mass and abnormal bone microstructures, which is considered caused by the imbalance between bone formation and bone resorption, more specifically the imbalance between the osteoblasts and osteoclasts. It occurs more in females than in males [75]. Osteoporosis affected more than 69.44 million people over 50 years old in China [76]; About 15% of white people in their 50s and 70% of those over 80 years of age had osteoporosis[77]. Osteoporosis greatly threatens the elderly, it carries an enormous and ongoing pain on patients and greatly impairs their

daily life function, providing unmeasurable mental and physical damage.

1.2.2 Current preventions or treatments of osteoporosis

Current preventions/treatments of bone loss mainly include anabolic approaches and anti-resorption approaches[78]. As we mentioned, studies show that bone loss is due to declined bone formation and enhanced bone resorption. The anabolic agents aim to enhance the activity of osteocytes and osteoblasts, upregulate the number of osteoblasts precursors and promote the maturation of osteoblasts. In contrast, the antiresorptive agents target to induce apoptosis in the osteoclast precursors. Calcium and vitamin D supplement are commonly used for the prevention and treatment of primary osteoporosis in the past few decades[79]. However, the outcomes of these supplements are controversial. Some observational studies claimed that calcium and vitamin D supplements may provide a little improvement in hip bone density and no obvious benefits to bone fracture[79]. However, other studies even suggested that calcium and vitamin D supplements may increase the risks of myocardial infarctions, kidney stones, and stomach problems[78]. Bisphosphonates are commonly used FDA-approved antiresorptive drugs in the long-term treatment of osteoporosis. Studies have shown that bisphosphonates are beneficial in reducing the risk of another fracture followed by previous bone broken due to bone loss[80]. Evidence indicates that this strategy is not able to lower the risk

of the first fracture caused by osteoporosis[81]. Also, as the duration of taking bisphosphonates generally lasts for 3 to 4 years, it may lead to serious side effects such as severe bone joint or muscle pain and even the occurrence of atypical femoral fractures[82]. Parathyroid hormone, a hormone secreted by the parathyroid gland, has been reported to have an anabolic effect on bone formation in the animal model and humans [83]. In 2002, a Recombinant DNA form of parathyroid hormone (1-34) was approved by FDA for the treatment of osteoporosis. PTH can improve the microarchitecture and strength of bone by modulating the cAMP concentrations and cAMP-dependent protein kinase A to stimulate the PTH receptors on the surface of osteoblasts, bone lining cells, and bone marrow stromal cells. Meanwhile, PTH can activate the calcium protein kinase C pathway to promote the proliferation of cells in the osteoblast lineage[84]. However, PTH is highly expensive and may increase the risk of osteosarcoma[85]. Although several FDA-approved drugs are available, osteoporotic fractures remain an unresolved problem[86].

1.3 The cholinergic system

The cholinergic family, including neurotransmitter acetylcholine as well as enzymes for its synthesis, hydrolysis, transportation, and its receptors, is found in the brain and peripheral nervous system[87, 88], especially in the parasympathetic nervous system. The parasympathetic division of the

autonomic nervous system is activated during rest and can be seen as the brake and play important roles in regulating visceral functions[89] of learning, memory, sleeping, and stress regulation.

1.3.1 The neuronal cholinergic system

Acetylcholine (ACh), mainly known for its neurotransmission function in the nervous system, was first discovered in 1921 by Otto Loewi [90]. The acetylcholine is formed from acetyl coenzyme A and choline under the catalysis of choline acetyltransferase (ChAT) [91]. After synthesized in the neurons, ACh is transferred via cytoplasm to the synaptic vesicles of neurons by VAChT (vesicular acetylcholine transporter) [92, 93]. During neurotransmission, the action potential reaches the end of the presynaptic axon, which causes depolarization and fusion of the vesicles with the cell membrane. This will cause the release of acetylcholine into the synaptic cleft, which subsequently activates the postsynaptic acetylcholine receptors. Two types of acetylcholine receptors are identified: the nicotinic and muscarinic receptors. Nicotinic acetylcholine receptors are pentameric ligand-gated ion channels [94]. So far ten subtypes have been identified. These subtypes can be assembled homomerically (e.g., the pentameric α7 receptor) or heteromerically (e.g., the pentameric α4β2 receptor) using the following five subunits: $\alpha, \beta, \gamma, \delta, \varepsilon$. They are present on the post-junctional membrane and are instantly

activated by acetylcholine for signal transmission. The signal mediates the fast depolarization and excitation of the target cell by allowing the entry of Ca^{2+} [95, 96]. The muscarinic acetylcholine receptors can be activated by muscarine or acetylcholine. They are G-coupled protein receptor complexes that are generally responsible for the slow recovery of target cells after stimulation. Five subtypes (M1-5) of the muscarinic acetylcholine receptor are identified, each of them with a slightly different function [97]. Acetylcholinesterase (AChE) is a well-known enzyme that catalyzes the hydrolysis of choline esters, such as acetylcholine. After hydrolysis of acetylcholine, choline and acetic acid are formed [93, 98]. AChE functions rapidly and efficiently in the neuromuscular synapses: 50% of acetylcholine molecules are hydrolyzed by AChE before they reach the postsynaptic receptor sites, and the other acetylcholine molecules are broken down by AChE after they activate the acetylcholine receptors [93]. AChE has thus an important suppressive role in cholinergic regulation by terminating the action of acetylcholine.

Next to AChE, another cholinesterase can also degrade acetylcholine and other esters. This enzyme is called butyrylcholinesterase (BChE) as it can quickly hydrolyze butyrylcholine. The tissues expressing AChE also always express BChE[99-101]. Although BChE is the dominant cholinesterase in plasma and liver, the expression and/or the activity of AChE is higher than that of BChE in the skeleton, muscle, brain, heart, and placenta[102]. Moreover, human

individuals with the hereditary complete absence of BChE activity are healthy and fertile[103]. Additionally, BChE knock-out mice are fertile and have a normal phenotype unless challenged with drugs [104].In contrast, total inhibition of AChE leads to death due to respiratory failure. AChE nullizygous mice are only able to live up to 21 days after birth with delayed physical development[105].

1.3.2 The non-neuronal cholinergic system

The cholinergic components not only exist in neural tissues but are also widely distributed in many non-neural tissues[106-109]. The non-neuronal expressed cholinergic components are denominated as the non-neuronal cholinergic system (NNCS). The presence of the non-neuronal cholinergic system is implied when acetylcholine is present or thus when cells have the capability of synthesizing acetylcholine and releasing it. The expression of acetylcholine receptors or acetylcholinesterase alone does not represent the NNCS. The NNCS is for example reported in human epithelial cells[110] and immune cells [111] as acetylcholine, its synthesizing enzyme ChAT, and its receptors are reported to be expressed in these cell types.

1.3.3 Non-neuronal cholinergic components expression in bone system

The NNCS in bone health and disease has gained increasing interest as mounting evidence indicates its presence. This is summarized in **Table 1-1.** The mRNA of ChAT and VAChT is reported to be expressed in differentiated murine primary osteoblasts and MC3T3-E1 cells[112]. The non-classical acetylcholine synthesizing enzyme carnitine acetyltransferase (CarAT) is identified in human SAOS-2 cells and mouse MC3T3-E1 cells[113]. Osteoclasts differentiated from murine bone marrow-derived macrophages also express ChAT [114]. At the tissue level, ChAT has been identified in chicken embryo limbs[115] and the mRNA expression of CarAT and VAChT has been confirmed in rat maxilla[116]. The expression of ChAT or CarAT by osteoblastic and osteoclastic cells strongly suggests the local production of acetylcholine and thus the presence of the NNCS. Moreover, also the nicotinic and muscarinic acetylcholine receptors are expressed in osteoblasts, osteoclasts, and bone tissues [112, 113, 117-121]. The acetylcholine-hydrolyzing enzyme AChE is identified in mouse, rat, and human primary osteoblasts[112, 122], and both murine and human osteoblastic cell lines [122, 123]. AChE is also detected in osteoclasts differentiated from murine bone marrow macrophages[124]. Next to the expression in cells, a protein level of AChE is also expressed in rat maxilla, calvaria, femur, ulnae, and chicken embryo limbs.

Expression of cholinergic components in bone cells or tissues	Study Model	Expression level	References
Osteoblastic lineage			
Carnitine acetyltransferase (CarAT)	human SAOS-2 cell line; mouse MC3T3-E1 cell line	mRNA	[113]
AChE, vesicular acetylcholine transporter (VAChT), choline acetyltransferase (ChAT)	Differentiated Murine primary osteoblasts and MC3T3-E1 cells	mRNA	[112]
AChE	mouse MC3T3-E1 cell line	mRNA	[113]
AChE	Human and rat primary osteoblasts, mouse MC3T3-E1 cell line, human MG63 cell line; human TE85 cell line	Protein	[122]
AChE	SAOS-2, MC3T3-E1, MG63, and TE85 cell line; Primary rat osteoblasts	mRNA	[123]
AChE	Primary cultured rat osteoblasts	Protein	[125]
Muscarinic acetylcholine receptors subtypes M1-5	Human osteosarcoma HOS cells	mRNA	[117]
Muscarinic acetylcholine receptors subtypes M4, M5	Human Reaming debris derived mesenchymal stem cells (RDMSC) and osteoblasts differentiated from RDMSC	mRNA	[118]
Muscarinic acetylcholine receptors subtypes M3, M5	human SAOS-2 cell line	mRNA	[113]
Muscarinic acetylcholine receptors subtypes M1, M2, M4	mouse MC3T3-E1 cell line	mRNA	[113]
Muscarinic acetylcholine receptors subtypes M1, M2, M4	Differentiated Murine primary osteoblasts and MC3T3-E1 cells	mRNA	[112]
Nicotinic acetylcholine receptors $\alpha1, \alpha6, \alpha7, \beta4, \delta, \varepsilon$	Differentiated Murine primary osteoblasts and MC3T3-E1 cell	mRNA	[112]

Nicotinic acetylcholine receptors $\alpha5, \alpha7, \alpha9$	Human Reaming debris derived mesenchymal stem cells (RDMSC) and osteoblasts differentiated from RDMSC	mRNA	[118]
Nicotinic acetylcholine receptor subunit $\alpha4$	human primary osteoblasts, MG63 osteoblastic cell line, human bone cores	mRNA	[126]
Nicotinic acetylcholine receptors $\alpha3, \alpha5, \alpha7, \alpha9, \alpha10, \beta2$	human SAOS-2 cell line	mRNA	[113]
Nicotinic acetylcholine receptors $\alpha2, \alpha5, \alpha9, \alpha10, \beta2$	mouse MC3T3-E1 cell line	mRNA	[113]
Osteoclastic lineage			
ChAT	Osteoclast differentiated from murine bone marrow-derived macrophages	Protein	[114]
AChE	murine bone marrow macrophages derived from tibia and osteoclasts differentiated from murine bone marrow macrophages	Protein	[124]
Muscarinic acetylcholine receptors subtypes M3	Osteoclast differentiated from human peripheral blood mononuclear cells	mRNA	[120]
Nicotinic acetylcholine receptors $\alpha2, \alpha7$	Osteoclast differentiated from human peripheral blood mononuclear cells	mRNA	[120]
Bone tissues			
ChAT	Chicken embryo limbs	mRNA	[115]
CarAT	Rat maxilla	mRNA	[116]
AChE	Rat calvarias and femurs	mRNA and Protein	[125]
VAChT and AChE	Rat maxilla	mRNA and Protein	[116]

AChE	Chicken embryo limbs	Protein	[115]
AChE	Rat ulnae	Protein	[122]
Muscarinic acetylcholine receptors subtypes M1-5 expressed in rat femur; M1, M4, M5 expressed in mouse femur	Rodents femur bone	mRNA	[117]
Muscarinic acetylcholine receptor subtypes M2, M3, and M4 were detected in bovine blade bone; subtypes M2 and M3 were detected in spongy bone; subtypes M2 and M4 were identified in periosteum	Bovine bone	mRNA	[117]
Muscarinic acetylcholine receptors subtypes M1-5	Human rib	mRNA	[117]
Muscarinic acetylcholine receptors subtypes M3, M5	Rat thoracic vertebra	mRNA	[119]
Muscarinic acetylcholine receptors subtypes M1, M2, M4, M5	Mouse tibia tissue	mRNA	[121]
Muscarinic acetylcholine receptors subtypes M1, M2, M3, M4, M5	Rat maxilla	mRNA	[116]
Nicotinic acetylcholine receptors$\alpha1$, $\alpha2$, $\alpha3$, $\alpha5$, $\alpha7$, $\alpha10$, $\beta1$, $\beta2$, $\beta4$, γ	Rat maxilla	mRNA	[116]

Table 1-1 Expression of cholinergic components in bone cells or tissues.

1.4 Acetylcholinesterase

As mentioned, the principal function of AChE is to catalyze the breakdown of choline esters, such as acetylcholine. AChE is believed to be the fastest, most sensitive, and most efficient enzyme known so far[127]. It is abundantly expressed in the nervous system and peripheral organs, playing an indispensable role in many aspects. So, it is important to discuss the structure and functions of AChE as well as their underlying relationship.

1.4.1 Structure-function relationships of AChE

The first crystal structure of AChE, *Torpedo californica* acetylcholinesterase, was identified in 1991[128]. Since then, researchers have gradually understood the structure of AChE monomers and oligomers from different species. The AChE monomer consists of 537 amino acids. It belongs to the α/β hydrolase family with 12-stranded β sheets and 14 α helices. This enzyme is ellipsoid with dimensions of 45 × 60 × 65 Å[127]. A narrow and deep gorge is hidden in the bottom of this protein, where located its active sites are to enable the interactions with ACh and other molecules like AChE inhibitors[129]. AChE is a multi-tasking protein with diverse active sites: the peripheral anionic site (PAS) and the catalytic site. The catalytic site in the gorge bottom includes two subsites: the esteratic subsite and the anionic subsite. And the peripheral anionic site is located at the opening of the gorge. The catalytic site is critical

for the principal function of AChE, breaking down acetylcholine. The PAS, however, is associated with many non-enzymatic functions[130].

The molecule forms of AChE vary from monomer, dimer, tetramer, to large collagen-tailed forms. In the physiological environment, AChE exists as a tetramer associated with either collagen-like Q subunit (ColQ) or proline-rich membrane-anchoring protein (PRiMA). Amphiphilic monomers and dimers of acetylcholinesterase (AChE) were also identified in human tissue[127, 131, 132].

1.4.2 Acetylcholinesterase inhibitors

Acetylcholinesterase inhibitors are chemical compounds that inhibit the enzyme AChE from hydrolyzing acetylcholine, therefore increasing the cholinergic activity. Generally, AChE inhibitors can be divided into reversible inhibitors and irreversible inhibitors[133]. The reversible inhibitors are always used for the treatment of cholinergic disorders, such as Alzheimer's disease[134]. The irreversible inhibitors, however, are also applied to many situations based on their toxicity.

The reversible AChE inhibitors

Commonly used reversible AChE inhibitors include donepezil, galantamine, rivastigmine, Huperzine A, tacrine, etc. Reversible AChE inhibitors are

important drugs in clinics to treat mild to severe Alzheimer's disease (AD) [135]. They are also involved in the therapy of other diseases, for example, myasthenia gravis.

Donepezil, one of the second-generation AChE inhibitors approved to treat Alzheimer's disease, is a selective piperidine-type cholinesterase inhibitor to AChE. Donepezil can bind to both the catalytic site (CAS) and the peripheral site (PAS) of AChE[136]. Donepezil is a potent and blood-brain barrier permeable inhibitor[137], its IC50 to AChE is 5.7 nM[138]. As the half-life time of donepezil is around 70 hours, it can be orally taken once a day at the dose of 5 and 10 mg/day with significant improvement of cognitive function in AD patients[139].

Galantamine is a tertiary alkaloid isolated from plants, it is also a selective inhibitor to AChE. Galantamine direct binds to the bottom of the active gorge[140]. In addition to its inhibition to AChE, galantamine is also an allosteric modulator interacting with the nicotinic receptor of acetylcholine[141]. Galantamine is a central-acting BBB permeable AChE inhibitor with good biosafety[142] with 7 hours half-life time. The IC50 of galantamine to AChE is 800 nM[143]. With the dosage of 16 or 24 mg/day, significant improvement in cognition can be reached.

Rivastigmine is a carbamate inhibitor that non-selectively inhibits both AChE and BChE. Rivastigmine covalently links to the catalytic site of AChE[144]. Rivastigmine is BBB permeable AChE inhibitor with selective inhibition in the hippocampus and cortex[145]. The IC50 of Rivastigmine to AChE is 4150 nM[146]. The therapy suggestion of rivastigmine is 6 to 12 mg/day.

Huperzine A is a nootropic alkaloid extracted from the Chinese herb *Huperzia serrata*. Huperzine A interacts with AChE in its catalytic triad through hydrogen bonds [147]. Huperzine A is also a selective BBB permeable AChE inhibitor. The IC50 of Huperzine A to AChE is 44.5 nM [148]. In China, Huperzine A has been approved for the treatment of age-related dementia[149].

Tacrine is one of the first-generation AChE inhibitors approved for the treatment of Alzheimer's disease. Due to its liver toxicity to the liver, however, tacrine was canceled for the clinic use of anti-dementia. Tacrine is derived from tetrahydroacridine and has an inhibitory effect on both AChE and BChE[150]. The IC50 of tacrine to AChE is 167 nM[151]. Tacrine also binds to the catalytic site of AChE[152].

Apart from their therapeutic applications in human diseases, reversible AChE inhibitors such as Aldicarb, Mancozeb, and Pebulate are also applied in agriculture, they are widely used as insecticides, herbicides, and

fungicides[133].

Compounds	Chemical structure	IC_{50} to AChE	BBB permeable?	Binding affinity	Application	Reference
Donepezil	Piperidine derivative	5.7nM	Yes	PAS CAS	Autism, AD	[137] [138]
Galantamine	Alkaloid	800nM	Yes	CAS	myasthenia gravis, myopathy, residual poliomyelitis paralysis syndromes, AD	[140] [141] [142]
Rivastigmine	Carbamate	4150 nM	Yes	CAS	AD, Parkinson's disease	[144] [145] [146]
Huperzine A	Alkaloid	44.5nM	Yes	CAS	AD	[147] [148] [149]
Tacrine	Acridine derivative	167 nM	Yes	CAS	AD	[150] [151] [152]
Ambenonium	Quaternary amines derivative	0.698nM	No	PAS CAS	myasthenia gravis	[153] [154] [155]
Physostigmine	Carbamate	27.9nM	Yes	CAS	myasthenia gravis, glaucoma, and delayed gastric emptying	[156] [153] [157]

Table 1-2 Typical reversible AChE inhibitors applied in human diseases and their basic information.

The irreversible AChE inhibitors

The irreversible AChE inhibitors refer to organophosphorus compounds. Due to their irreversible phosphorylation to esterases, they have acute toxic effects on the central nervous system. The toxic organophosphorus compounds such as malathion, diazinon, and dichlorvos are commonly used as nonspecific insecticides[133]. However, some organophosphorus compounds, for example, diisopropyl fluorophosphate and echothiophate, are used in ophthalmology to treat a chronic eye disease, glaucoma.

1.4.3 Classic enzymatic function of acetylcholinesterase in bone tissue

The functions of AChE were also observed outside the nervous system, for example, the bone tissue[158]. The classical functions of AChE in regulation bone systems were summarized in **Table 1-2**, which reflects the non-neural roles of AChE in embryo bone development and postnatal bone homeostasis.

Non-neuronal cholinergic role of AChE in bone development

Expression of AChE has been investigated in various animal models, including rat maxilla, which supported its formation is mainly through intramembranous ossification. For example, in rat calvaria, AChE activity and protein amount increase during the embryonic period to the 6th day after birth then decreases during postnatal bone development, i.e. till two months after birth [159].

However, among the currently available studies on non-neuronal cholinergic regulation of bone development, the role of AChE during intramembranous ossification has not been fully understood [116]. All the findings now propose a prospective regulative role of AChE in the process of intramembranous ossification.

ChAT, being a protein responsible for the production of AChE, is equally important as AChE during endochondral ossification, the expression of the two proteins has been well acknowledged, especially during the early stages of embryonic bone development in chicken and rodent models [115, 159, 160]. Hyaline cartilage is generally considered as the main expression site of AChE at the onset of early limb development, while it increases in apoptotic regions in the later stage. The study targeted chicken embryos indicated a reduction of AChE expression when it comes to bone mineralization. The temporal difference in expression between AChE and ChAT – with AChE expression being the preceding event in bone development in limbs, shows the leading role of AChE in endochondral ossification. Nonetheless, the presence of ChAT also implies local acetylcholine production during embryonic bone development. By implanting acetylcholine- and ChAT-soaked beads in chicken embryonic limbs, a beneficial effect on bone mineralization was observed [115]. In murine fetuses which AChE, BChE, or both were deleted (called here A^-B^+, A^+B^-, A^-B^-, respectively), accelerated bone growth and remodeling were

observed. The source of acetylcholine was not directly studied; however, the researchers suggested a possibility of ACh expression by mesenchymal stem cells in the early endochondral ossification stage [160]. Pharmaceutical inhibition of AChE by BW284c51 *in vitro* using micromass culture of mesenchymal cells extracted from embryonic chick wing buds further confirmed the role of AChE in cartilage degeneration and accelerated mineralization. Taken together, AChE plays an important role by maintaining ACh concentration at an optimal level to decelerate bone growth, as well as favoring cartilage apoptosis and hampering bone mineralization.

Non-neuronal cholinergic role of AChE in postnatal bone homeostasis

AChE regulates postnatal bone homeostasis via its classic enzymatic role. Reduction of the relative number of osteoclasts was observed in sixteen-week-old Ache+/- mice with 50% lower brain AChE activity compared to their wildtype littermates [161]. Genetic knock-out of AChE affects the systemic chondrogenic system, yet the possible non-neuronal function cannot be overlooked. An animal study in which mice were treated with pharmaceutical inhibitors of AChE showed a higher BV/TV ratio compared to phosphate-buffered saline control further confirms the beneficial effect of AChE suppression on bone formation. In addition, AChE inhibitor donepezil could rescue RANKL-induced bone loss.

The roles of AChE on bone formation and resorption have also been proven in various *in vitro* studies. Upregulation of AChE expression was observed in osteoclastogenesis of bone marrow macrophages, while genetic knockdown of AChE using siRNA suppressed RANKL-induced osteoclast differentiation. Osteoclast formation could be promoted by treatment of recombinant AChE in bone marrow macrophages through the upregulation of RANK, the receptor of RANKL. Oppositely, donepezil, an AChE inhibitor, could mitigate osteoclastogenesis *in vitro*. Overall, the reduction of AChE, which in turn leads to increased acetylcholine activity [124], drives an increase in bone formation and a decrease in bone resorption.

Stage	Discovery	Study Model	Enzymatic/Non-enzymatic	Source of Acetylcholine	References
Intramembranous ossification	mRNA expression of acetylcholine, VAChT, AChE, nicotinic receptors and muscarinic receptors is identified in rat maxilla.	Rat	Enzymatic	Mesenchymal stem cells, bone matrix and bone marrow cells	[116]
	the AChE activity and protein amount first increases during embryonic period to the 6th days after birth and then decreases to a stale level in 2 months after birth in rat calvarias.	Rat	Enzymatic	N/A	[125]
Endochondral ossification	the AChE activity and protein amount first increases during embryonic period to the 6th days after birth and then decreases to a stale level in 2 months after birth in rat femurs.	Rat	Enzymatic	N/A	[125]
	the AChE activity first increases when hyaline cartilage forming and peaks at cartilage apoptosis stage, AChE activity decreases when the development direction shifts to bone mineralization. Implantation of acetylcholine- and ChAT-soaked beads benefits bone	Chicken embryo	Enzymatic	Expression of ChAT indicates possible local production of acetylcholine	[115]

	mineralization.				
	Genetic knockout of AChE, or BChE, or both of them accelerates cartilage remodeling into mineralizing bone.	Mouse	Enzymatic	N/A	[160]
Postnatal bone homeostasis	16-week-old *Ache*$^{+/-}$ mice exhibited a reduction of the relative number of osteoclasts.	Mouse	Enzymatic	N/A	[161]
	Pharmaceutical suppression of AChE suggests a higher BV/TV ratio compare to control treatment of phosphate-buffered saline. AChE expression upregulates during osteoclastogenesis.	Mouse	Enzymatic	N/A	[124]
	Matrix coating with AChE promote osteoblastic cells attachment.	Rat; MC3T3-E1, MG63, and TE85 cell lines	Non-enzymatic	N/A	[123]
	Pharmaceutical suppression of AChE decreases the adhesion ability of osteoblastic cells without interfering their cell viability.	Human and rat primary osteoblasts, mouse MC3T3-E1 cell line, human MG63 cell line; human TE85 cell line	Non-enzymatic	N/A	[122]

Table 1-3 Function of AChE during bone development and homeostasis.

1.4.4 An emerging non-neuronal and non-enzymatic role of AChE in bone homeostasis

AChE is a multi-tasking protein with two different binding sites for acetylcholine: a catalytic site and a peripheral anionic site. The latter is recently studied for its non-enzymatic function. More specifically, it is hypothesized that the peripheral anionic site can make heterologous protein associations that play a role in cell recognition and adhesion [162]. This function was already demonstrated in neurogenesis and hematopoiesis. Studies exploring the role of AChE in neurite growth demonstrated that purified AChE could promote neurite growth from cultured chick nerve cells, while no influence was observed after adding inhibitors targeting the catalytic site. This suggests a non-enzymatic role of AChE [163, 164]. Moreover, AChE expressed in blood cell progenitors, can regulate lymphocyte activation via its enzymatic and non-enzymatic function [111, 165, 166].

Non-enzymatic function of AChE in postnatal bone homeostasis

The non-enzymatic function of AChE in postnatal bone growth was first assumed after the discovery of a new class of proteins i.e., the cholinesterase-like adhesion proteins, for example, neurotactin, neuroligin, and thyroglobulin. Although these proteins lack catalytic activity, their cholinesterase-like part can act as a protein-protein interaction domain. This domain, located extracellularly, can form cellular junctions through binding with other

extracellular elements. The existence and function of these proteins form the foundation of the assumption that AChE itself can also act in protein-protein interactions [167, 168].

To validate this hypothesis, it is essential to determine possible interaction partners for AChE. Laminin-1 or more specifically the globular domain IV of the beta-1 chain of laminin-1 was the first interaction partner identified, followed by collagen IV. This protein-protein interaction is possible through the binding of the extracellular matrix components to the peripheral anionic site. This theory is justified as inhibitors of the peripheral anionic site (fasciculin, propidium, and gallamine) interrupt this binding. The binding is characterized as electrostatic, as it is influenced by ionic strength and pH [169-171].

The protein-protein interaction between the extracellular matrix components and AChE facilitates cell-cell recognition and cell signaling via membrane receptors. This suggests that AChE and its non-enzymatic function can influence bone homeostasis [169-171]. Moreover, the transcription of AChE mRNA variant 3' terminated with exon 6 that encodes for the catalytically and morphologically E6-AChE expression, can be modulated by the osteogenic markers Wnt-3a and RunX-2 [159, 172].

Literature on the non-enzymatic function of AChE in bone mainly focusses on its role in the osteoblastic lineage. Evidence indicates that AChE presents in osteoblasts as membrane protein and bone matrix protein[123]. As bone matrix protein, AChE needs to be excreted in its glycosylated form via the ER/Golgi apparatus pathway. The major detection sites of AChE include the sites of bone formation, along cement lines, and in osteoid seams. The formation of AChE-rich cement lines can be explained by the secretion of AChE at newly resorbed surfaces by differentiated osteoblasts. The interaction between osteoblasts and AChE will help them attach. This is confirmed by the reduction of cell adhesion after addition of AChE inhibitors. As the bone formation advances, it will trap AChE into the osteoid. Later in the bone development process, the differentiated osteoblast will no longer secrete AChE and more non-secreted glycosylated AChE was formed. This will assist in bone matrix mineralization [122, 123, 173].

Few studies investigate the non-enzymatic function of AChE in the osteoclastic lineage. One study treated bone marrow macrophages with heat-inactivated recombinant AChE. The researchers identified a larger number of TRAP-positive cells in the treatment group, although the difference was not statistically significant [124]. Therefore, the emphasis of future studies should be on the non-enzymatic role of AChE in osteoclastic lineage.

1.5 Research gap

AChE and other cholinergic components have been reported to be identified in the bone system and involved in the process of bone development. Its roles in bone degeneration, especially in osteoblast senescence and osteoclastogenesis, however, remain unknown. Also, whether the pharmaceutical inhibition of AChE can rescue bone loss is still poorly investigated.

1.6 Objectives of the study

This study aims to determine the role of AChE and its inhibitors in bone homeostasis and disease, i.e., in the context of OP.

1. To investigate the role of AChE in regulating osteoblast senescence
2. To investigate the non-neuronal functions of AChE during osteoclastogenesis (non-cholinergic and non-enzymatic)
3. To investigate the role of AChE on OB-OC crosstalk via a microfluidic co-culture system.
4. To investigate the role of AChE during osteoporosis development and the effects of AChE inhibitors on the rescue of OVX-induced bone loss (central acting or peripheral acting).

Chapter 2 Osteoblast senescence induces upregulated expression level of non-neuronal acetylcholinesterase *in vitro*: a vicious circle

2.1 Introduction

Aging and cell senescence

Aging is a common risk factor for many chronic diseases such as Alzheimer's disease, cardiovascular diseases, cancers, osteoarthritis, osteoporosis, etc.[174]. These age-related diseases bring a huge healthy and economic burden to the global society. It is urgent for researchers to understand the processes of aging.

The age-related diseases are generally associated with functional aging, which have the following features: i) low-grade inflammation[175], ii) DNA damage[176], shorten of telomere length[177], mitochondrial dysfunction[178], misfolded proteins[179], etc., iii) declined differentiation ability of stem cells[180], iv) cell senescence[181]. By targeting these features, researchers are trying to solve the problem of age-related diseases and therefore extend the health span of human beings[182].

Cell senescence is when cells enter a state in which they permanently stop cell division but are still alive. Cell senescence is thought to be a protective mechanism that prevents damaged or unwanted cells from developing into malignant tumors. Senescent cells could be found in anytime, however, their accumulation is the major contributor to aging and age-related diseases[183].

Cellular senescence is triggered by DNA damage responses induced by stress such as ROS and telomere shortening[184, 185]. The characteristics of senescent cells include cell hypertrophy, increased expression of p21 and $p16^{Ink4a}$, and elevated activity of Senescence-Associated Beta-Galactosidase (SA-β-GAL)[183]. Both p21 and $p16^{Ink4a}$ are cyclin-dependent kinase inhibitors, the upregulation of p21 is earlier than the expression of $p16^{Ink4a}$, p21 is considered the early marker of cell senescence, while the increase of $p16^{Ink4a}$ reflects the full stage of cell senescence[181].

Osteoblast senescence and osteoporosis

As mentioned, the overall aging process is in the majority part the result of senescent cell accumulation. In the bone system, age-related bone loss is associated with senescence-resulted osteoblast dysfunction. Similar to the cellular senescence of other cell types, the senescence of osteoblasts is induced by several intrinsic factors such as shortening of telomere, excessive oxidative stress, and DNA damage [186]. Senescent osteoblastic cells reflected attenuated cell proliferation ability, shorter functional lifespan, impaired differentiation capability of progenitor cells, and weaker responses to growth factors[187]. In a previous study, the osteoblast progenitors, osteoblasts, and osteocytes were isolated through a magnetic-activated cell sorting (MACS) method in both 6-month-old (young) and 24-month-old mice (old). Compared to the young mice, the older mice showed a significantly higher expression of senescence marker $p16^{INK4a}$ and telomere dysfunction-induced foci in isolated osteoblastic cells[188]. Clearance of senescent cells, especially of

osteocytes in aged mice (a relative reduction of 46%) resulted in a high ratio of BV/TV in spine, femur, and tibia trabecular bone[189]. An accelerated senescent mice model was established by a double mutation in genome repair molecules TERC (Telomerase RNA component) and WRN (Werner syndrome helicase). In these $Wrn^{-/-}$ $Terc^{-/-}$ mutant mice, the researchers found that the differentiation potential of osteoblast progenitors was inhibited, while the osteoclastogenesis was not affected. The bone loss phenotype was also observed in the mutant mice. These studies pointed out a critical role of senescent osteoblastic cells in osteoporosis.

2.2 Rationale

AChE is a multifunctional protein with multiple active sites which can combine enzymatic and non-enzymatic functions within one molecule[190]. Acting enzymatically, AChE hydrolyses acetylcholine to hinder osteoblast lineage activity. Acetylcholine would activate both nicotinic and muscarinic receptors on osteoblasts. By binding to nicotinic receptors, acetylcholine increases the expression level of Cyclin D1, promoting the cell proliferation of osteoblasts[112]. Via stimulating muscarinic receptors, calcium signaling in osteoblasts was activated, accelerating osteoblasts proliferation[117]. The involvement of AChE in skeletogenesis has been reported in both mouse and chick embryos[160, 191]. Endochondral ossification is accelerated in the embryo of *Ache*$^{-/-}$ mice[160]. AChE inhibitors like donepezil favor postnatal bone growth in mice[192, 193]. Acting non-enzymatically, osteoblasts-derived AChE was shown to modulate their interaction with bone extracellular matrix[122,

123]. All the evidence points to an emerging role of AChE in osteogenesis and osteoblasts in the bone development stage. Yet, the role of AChE in osteoblastic lineage at the degeneration stage was poorly investigated.

2.3 Materials and methods

Reagents

Fetal bovine serum, Minimum Essential Medium α, trypsin–EDTA reagent, Penicillin-Streptomycin, RevertAid First Strand cDNA Synthesis Kit, NucBlue reagent (Thermo Fisher Scientific, Waltham, USA, #10270-106 & #12561-056 & #25300-062 & #15140-122 & #K1622 & #R37605); Donepezil HCl (Aladdin, Shanghai, China, # 120011-70-3); Galantamine Hydrobromide (Sigma-Aldrich, St. Louis, USA, PHR1623-500MG); Cell Proliferation Kit 1 (MTT) (Roche, Penzberg, German, #11465007001); E.Z.N.A.® Total RNA Kit I (Omega Bio-tek, Norcross, USA, #R6834-02); QuantiNova SYBR Green PCR Kit (Qiagen, Hilden, German, #208056); Recombinant Mouse Acetylcholinesterase (AChE) Protein, (USA, # 5518-CE-010); Anti-Acetylcholinesterase antibody, Anti-CDKN2A/p16INK4a antibody, secondary Goat Anti-Mouse IgG (H&L) antibody (Alexa Fluor® 647), Donkey anti-Rabbit IgG H&L (DyLight® 488) secondary antibody (Abcam, UK, #ab2803 & #ab189034 & #ab150115 & #ab98488); Senescence β-Galactosidase Staining Kit (Cell signaling technology, Danvers, USA, #9860), Hydrogen Peroxide 30% (Merck, Kenilworth, USA, # 1.07298.0250).

Animals

For the natural aged mice, 3-month-old, 6-month-old, 9-month-old, 16-month-old and 18-month-old mice (every time point 3 mice) were obtained from PolyU CAF under a license (20-129) in DH/HT&A/8/2/4/ Pt.2 issued by the Department of Health, Hong Kong. The bone samples of all mice were collected and fixed. The samples were then decalcified, dehydrated, embedded, and sectioned to slides. Slides were deparaffinized and rehydrated for routine H&E staining, TRAP staining, and immune-histochemical staining.

Histochemistry

Spine tissues were dissected from mice and fixed immediately in 4% PFA solution overnight, then decalcified in 10% EDTA for 2 weeks. After decalcification, the samples were dehydrated in an alcohol gradient ranging from 70% to 100% and were embedded in paraffin following the standard protocols. Samples will be cut into 5um sections using the microtome. Slides were deparaffinized and rehydrated for routine H&E staining, tartrate resistance acid phosphatase (TRAP) staining (Sigma-Aldrich) and AChE immunofluorescence (Anti-Acetylcholinesterase antibody (Abcam, ab2803)).

Cell culture of osteoblastic MC3T3-E1 cells

The murine osteoblastic MC3T3-E1 Subclone 4 cell line was obtained from the American Type Culture Collection (ATCC CRL-2593, Manassas, VA, USA) and was cultured in αMEM medium supplemented with 10% Fetal Bovine Serum and 1% penicillin/streptomycin (Growth medium). When reaching the 50–60 % confluency, MC3T3-

E1 cells were treated with 100μM or 200μM H2O2 for senescence induction. For treatment of AChE inhibitors, the cells were treated with 1μM donepezil or galantamine in senescence induction medium after reaching the 50–60 % confluency. The concentration and treatment time of donepezil and galantamine were determined by a Cell Proliferation Kit I with MTT (Roche, Switzerland). In some experiments, mouse recombinant AChE protein or heat-inactivated AChE protein was added to medium with cultured MC3T3-E1 cells for 3 days in the concentration of 200ng/ml. "Heat-inactivated" AChE was prepared by heating the protein for 3 min at 100°C. All cells were incubated in a humidified atmosphere with 5% CO2 at 37 °C and medium was replaced every two days.

MTT assay

The cell proliferation assay will be performed using the Cell Counting Kit-8 (CCK- 8, Dojindo, Kumamoto, Japan). MC3T3-E1 cell suspension (100 μL, 1×10^4 per well) will be dispensed into 96-well plates and incubated for 24 h, then changed for the fresh media containing different concentrations of donepezil and galantamine (0.01 /0.05 /0.1 /0.5 /1 /5 /10 /50 /100μM) and incubated for another day. Finally, 10 μL of CCK-8 solution will be added into each well and incubated for 4 h, after the absorbance will be measured at 570 nm using a BioTek microplate reader (Winooski, VT, USA).

SA-βgal Staining

SA-βgal was conducted to verify whether the cell was in the status of senescence. The sample cells were stained with beta-galactosidase in the procedure adapted from a well-

established protocol (Dimri et al., 1995). In brief, cells were first washed with PBS once and submerged in fixative solution for 10 minutes at room temperature. Afterward, the fixed cells were then washed twice with PBS and exposed to the staining solution. During the process of staining, cells submerging under staining solution was incubated at 37°C without the supply of CO2 overnight. Stained cells were observed under the bright field of a microscope.

qRT-PCR

MC3T3-E1 cell samples were lysed with a TRK Lysis to extract Total RNA (with proteins and other organic matters). Total RNA was further extracted and purified by using E.Z.N.A.® Total RNA Kit I (Omega, R6834-01) according to the manufacturer's protocol. RNA concentrations were measured by Nano-drop (ND-1000 spectrophotometer). Extracted RNA of each sample ($1\mu g$) was reverse transcribed into cDNA with Revert Aid First Strand cDNA Synthesis Kit (Thermo fisher). qRT-PCR then was carried out on BIO- RAD CFX96 Touch™ Real-Time PCR Detection System with primers of specific genes (Table 4-1 for *Ache* targeting senescence related genes) and Quanti Nova SYBR Green PCR Kit (Qiagen).

Gene	**Forward Primer**	**Reverse Primer**
GAPDH	AGGTCGGTGTGAACGGATTTG	GGGGTCGTTGATGGCAACA
AChE	AGGTCGGTGTGAACGGATTTG	GGGGTCGTTGATGGCAACA
P16^{INK4a}	GCTTCTCACCTCGCTTGTCA	GTGACCAAGAACCTGCGAC
P21	GAGAGGAGAGGCCACCATTT	CACTATCCTGGGCATTTCGGT

Table 2-1 Primer sequence of *Ache* targeting senescence related genes used in qPCR.

Cell immunofluorescence

MC3T3-E1 cells were seeded with a density of 1000 cells/well in 12-well plates on circle cover slips. Subsequently the cells were fixed in 4% paraformaldehyde for 10 min, permeabilized in 0.1% Triton-X 100 for 30 min, blocked with 5% BSA for 30 min. AChE was visualized using the Anti-Acetylcholinesterase antibody (Abcam, ab2803) as well as Anti- CDKN2A/p16INK4a antibody (1:200; Abcam, ab189034) in combination with the secondary Goat Anti-Mouse IgG (H&L) antibody (Alexa Fluor® 647), Donkey anti-Rabbit IgG H&L (DyLight® 488) secondary antibody (Abcam, ab150115 & ab98488) for detection. Nuclei were visualized by NucBlue reagent (Life Technologies, R37605). Cells were imaged on an Olympus BX61 inverted microscope system.

Statistical Analysis

All statistical results were presented as mean $\pm$ standard error of the mean (SEM). The comparison between multiple groups was quantitatively analyzed using one-way ANOVA. Post-hoc tests were performed following statistically significant results. A significant difference was indicated when $P<0.05$.

2.4 Results

AChE protein accumulated in aged mice bone in vivo and senescent osteoblasts in vitro

To investigate the expression pattern of AChE during the aging process, we checked the AChE expression and the number of osteoclasts in bone sections of 3-month-old, 6-month-

old, 9-month-old, 16-month-old, and 18-month-old mice via IHC staining. As shown in Fig 2.1A, obvious bone loss was indicated in the bone sections of 18-month-old mice. In Fig.2.1C, we observed a darker brown signal in the bone surface of 18-month-old mice femur section. Meanwhile, more TRAP+ signals were found in bone sections of both 16-month-old and 18-month-old mice. These results suggested that increased AChE expression was associated with age-related bone loss. To investigate the relationship between AChE and osteoblast senescence, we identified the AChE expression in an H2O2 induced senescent model *in vitro*. Much more SA-βgal positive cells were found in the H2O2 treated group (Figure 2.1E), which confirmed the validation of the cell senescent model. After treatment of H2O2, both the mRNA and protein level of senescent marker $p^{16INK4a}$ increased (Fig 2.1F, G), the mRNA level of early senescent marker p21 also increased, associated with the elevated expression of AChE, the results showed a dose-dependent effect.

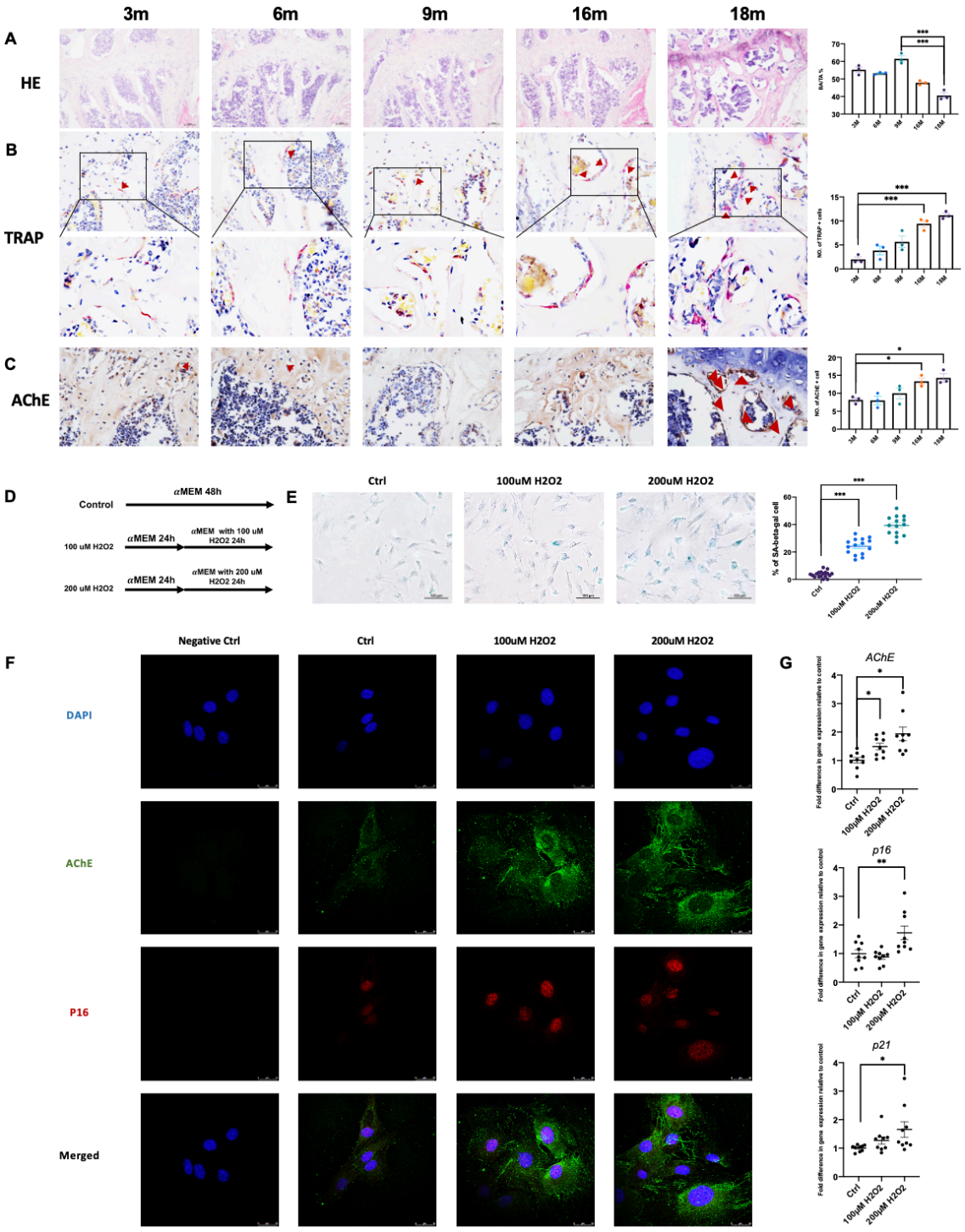

Fig 2.1 AChE expression and bone loss observed with natural aging process in mice. AChE expression increased during senescence induction via H2O2 treatment in MC3T3 cells *in vitro*. (A, B, C) Representative images quantitative results of H&E staining, TRAP staining, and DAB staining for AChE (brown) from 3-month-old mice (n=3), 6-month-old mice (n=3), 9-month-old mice (n=3), 16-month-old mice (n=3), and 18-month-old mice (n=3) bone samples. Scale bar, 100 μm, 100 μm, 50 μm, respectively. Positive signals were indicated with red arrows. (D) *In vitro* Experiment design and (E)representative images of SA-βgal staining when cells were treated with 100 μM or 200 μM of H2O2. Scale bar, 50 μm. (F) Representative immunofluorescence staining images of $p16^{INK4a}$ (red) and AChE(green) with different concentrations of H2O2 induction. Scale bar,

25 μm. Cells were counter-stained with DAPI (blue). (G) Relative mRNA expression of *AChE*, senescent markers (*p16*^{INK4a} and *p21*) under the treatments of (D)(n=9). Cells were pretreated with blockers for 30 minutes before H_2O_2 stimulation. All data are expressed as means ± SEM. One-way ANOVA with Post-hoc tests were performed following statistically significant results. * $p<0.05$; ** $p<0.005$; *** $p<0.001$.

Both recombinant AChE protein and heat-inactivated AChE initiated the senescence of osteoblasts in vitro

To distinguish the enzymatic function and non-enzymatic function of AChE on osteoclastogenesis, we incubated cells with AChE and Heat-inactivated AChE. Heat treatment will irreversibly inactivate the catalytic function of AChE [194]. As shown in Fig 2.2, we used both intact AChE protein and heat-inactivated AChE protein to treat the osteoblastic MC3T3-E1 cells. We found that the incubation of AChE/HAChE resulted in a higher percentage of SA-βgal positive cells with a statistically significant difference. While in the mRNA level, both the AChE and HAChE treatment groups indicated a higher expression of senescent markers P21 with a statistically significant difference.

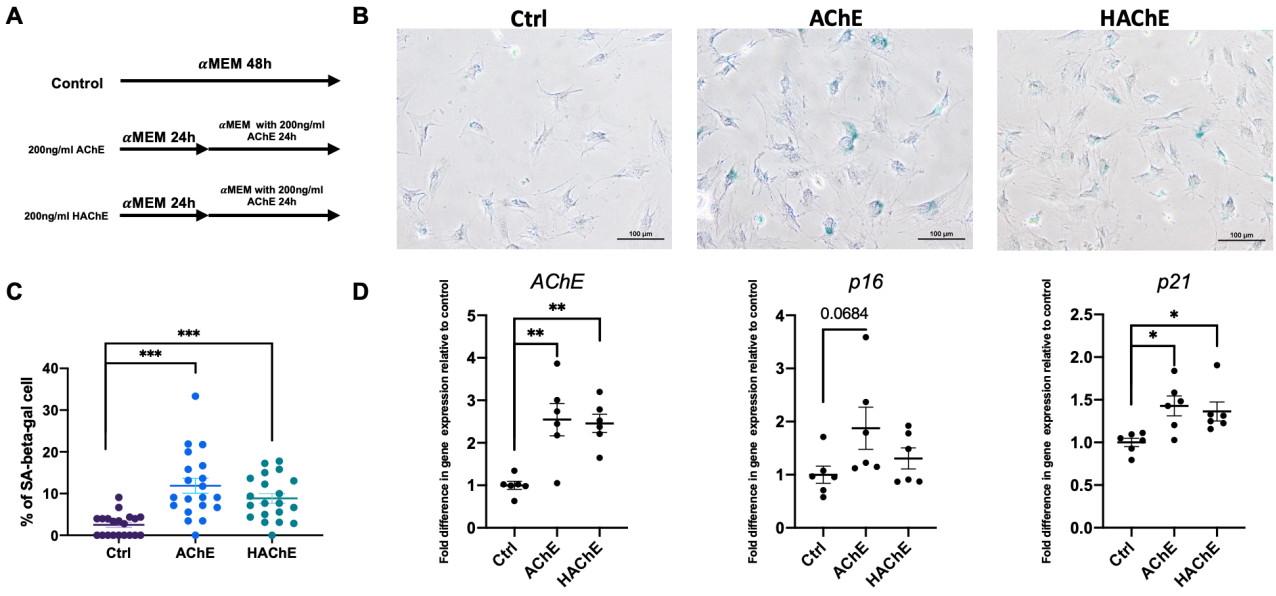

Fig 2.2 Treatments of both mouse recombinant AChE and heat-inactivated AChE initiate osteoblast senescence in MC3T3 cells. (A)experiment design. (B) Representative images of SA-βgal staining (blue) when cells were treated with were treated with recombinant AChE (200ng/mL) and heat inactivated AChE (200ng/mL) (24h). Scale bar, 100 µm. (C)Quantification results of percentages of SA-βgal positive cells under conditions of (B) (n=20). (D) expression of *AChE*, senescent markers ($p16^{INK4a}$ and *p21*) under the treatments of (B) (n=6). All data are expressed as means ± SEM. One-way ANOVA with Post-hoc tests were performed following statistically significant results. * $p<0.05$; ** $p<0.005$; *** $p<0.001$.

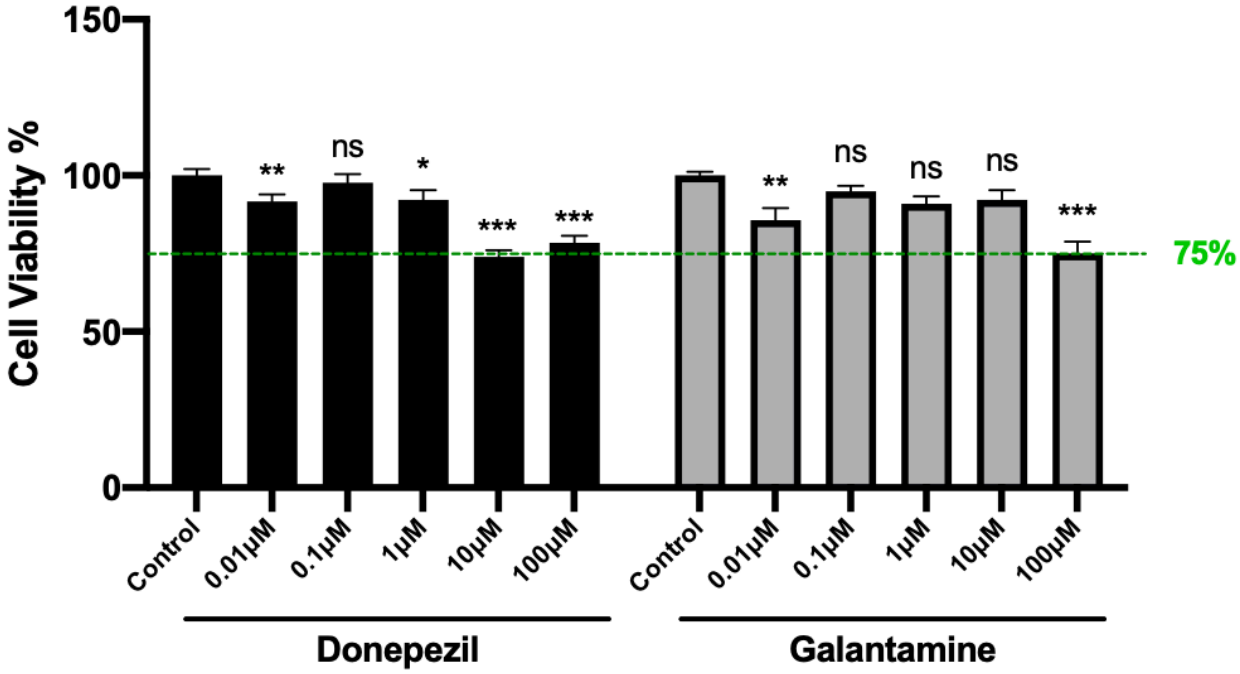

Fig 2.3 Cell viability of MC3T3 with increasing concentrations of one day treatments of donepezil and galantamine, respectively. Both donepezil and galantamine treatment for 24h showed a concentration-dependent reduction of cell viability. Set 75% viability as a threshold, 1μM was the maximum tested safe concentration for both donepezil and galantamine. All data are expressed as means ± SEM. All data are expressed as means ± SEM. One-way ANOVA with Post-hoc tests were performed following statistically significant results. * $p<0.05$; ** $p<0.005$; *** $p<0.001$.

Dual-binding AChE inhibitor donepezil but not galantamine could rescue the effect of H2O2 induced senescence in vitro.

To further identify the non-enzymatic function of AChE, AChE inhibitors with different binding affinities were used to treat senescent osteoblasts. We used two ACHE inhibitors to treat the cells, donepezil, and galantamine. As mentioned before, donepezil and galantamine show controversial results in preventing bone loss. As shown in Figure 2E-H, after treatment of AChE inhibitors, the H2O2 induced senescence was hindered in the donepezil treated group but there was no significant difference. Our results showed that treatment of donepezil could suppress the level of p16 and p21in both mRNA levels and protein levels.

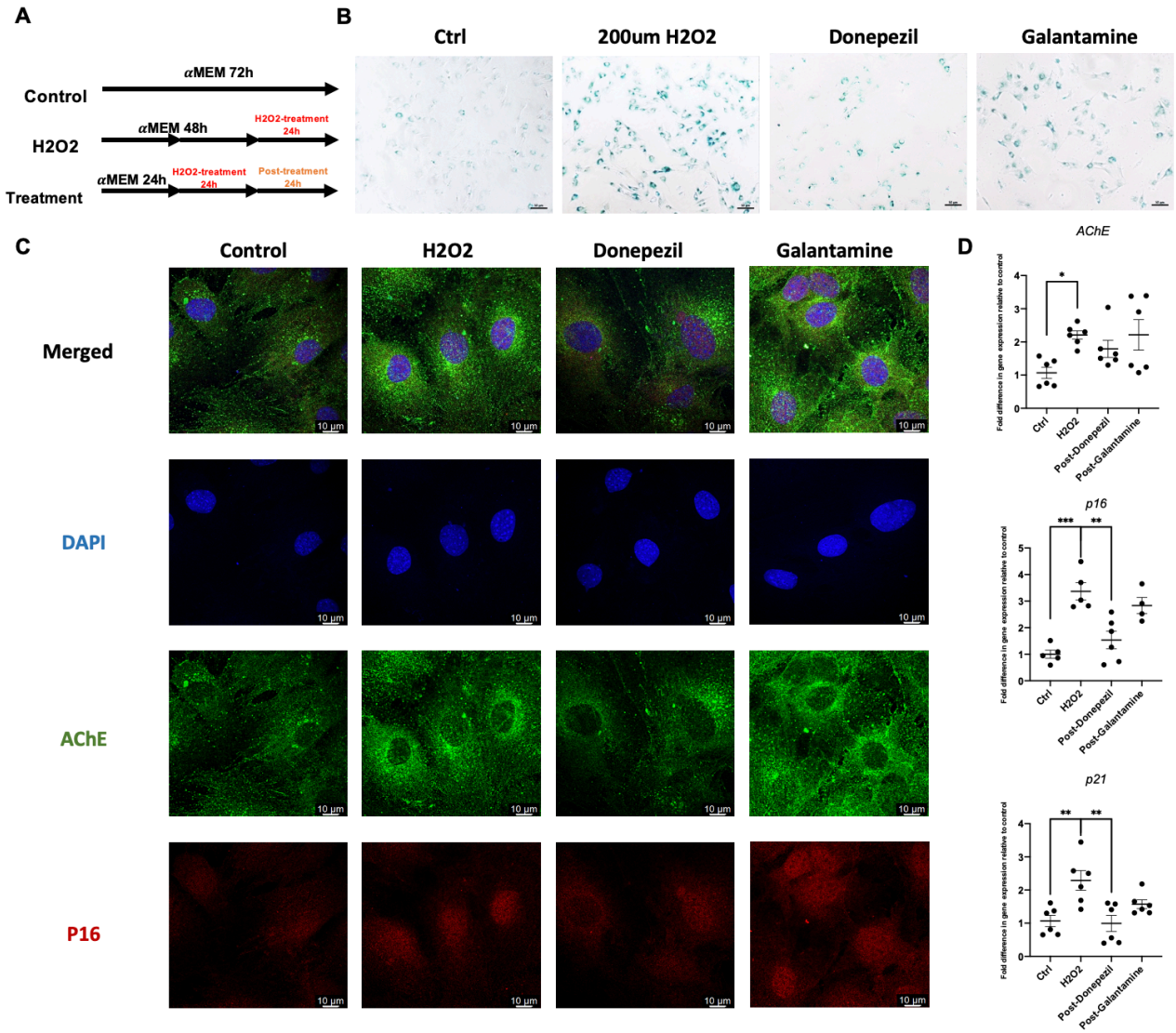

Fig 2.4 Treatment of donepezil to senescent osteoblastic MC3T3 reduced the expression of AChE and p16^{INK4a} *in vitro*. (A) Experiment design. (B) Representative images of SA-βgal staining when cells were treated with of H2O2 and post-treatments of donepezil and galantamine. Scale bar, 50 μm. (C) Representative immunofluorescence staining images of p16^{INK4a} (red) and AChE(green) with different concentrations of H2O2 induction. Scale bar, 10 μm. Cells were counter-stained with DAPI (blue). Cells were pretreated with blockers for 30 minutes before H_2O_2 stimulation. (D) Relative mRNA expression of *AChE*, senescent markers (*p16^{INK4a}* and *p21*) under the treatments of (B)(n=6). All data are expressed as means ± SEM. One-way ANOVA with Post-hoc tests were performed following statistically significant results. * $p<0.05$; ** $p<0.005$; *** $p<0.001$.

2.5 Discussion

Previously studies on AChE and osteoblasts all focused on the role of AChE in cell proliferation and osteogenesis in the bone development period [112, 117, 122, 123, 160, 191]. Our study was the first time that demonstrated the regulative effect of AChE in osteoblast senescence. We first found that AChE expression increased during the natural aging process in the mice model. Moreover, H2O2 induced senescence of osteoblastic cells was associated with upregulated expression of AChE. Our results also supported that both AChE and heat-inactivated AChE led to the early senescence of osteoblastic cells. In addition, the AChE inhibitor, donepezil but not galantamine could attenuate the senescence of osteoblastic cells. We concluded that the senescent osteoblasts secreted AChE to the bone matrix, the secreted AChE triggered active osteoblasts to undergo senescence, and a vicious cycle formed.

However, further studies should be performed to explore the underlying mechanism. As mentioned, osteoblast senescence was caused by the shortening of telomere, excessive oxidative stress, and DNA damage. The association between AChE and these factors should be further investigated. We should notice two interesting results: First, a higher percentage of SA-β gal positive cells was observed in heat-inactivated AChE treated MC3T3-E1 cells, both recombinant AChE and heat-inactivated AChE treatment groups show higher expression of early senescent marker P21; Second, the AChE inhibitor donepezil is a dual-binding inhibitor, which binds to both the catalytic site and the peripheral anionic site of acetylcholine, while galantamine only binds to the catalytic site, our results suggested that

only the donepezil treatment showed the inhibition of senescence in osteoblastic cells. So, the presenting data indicated the possible non-enzymatic regulation function of AChE in osteoblast senescence.

Several studies illustrated that the increased intrinsic cell stiffness was associated with cellular senescence[195, 196]. MSCs isolated from Hutchinson–Gilford Progeria Syndrome phenotype showed increased cell stiffness compared to the cells in the WT phenotype[195]. The senescent human trabecular meshwork cells in the eyes reflected a 1.88±0.14 or 2.57±0.14 folds (with/without serum) increase in stiffness compared to the control cells[196]. AChE was reported to perform structural functions on adherent chicken retinal cells non-enzymatically[197]. Basically, the researchers transfected rabbit AChE cDNA vector to chicken retinal cells, these transfected cells expressed more heterologous AChE protein but no more activity. A high level of cytoskeleton protein vimentin was expressed in the transfected cells, for which the authors claimed that the AChE could affect the cytoskeleton of retinal cells independent of its enzymatic function. So, AChE might also interfere with the cytoskeleton structure of osteoblastic cells and consequently affect the process of osteoblastic senescence, further studies which investigate the cell stiffness and cytoskeleton proteins of AChE and HAChE treated osteoblastic cells should be conducted.

Chapter 3 Acetylcholinesterase promote osteoclastogenesis via acetylcholine-independent pathway *in vitro*

3.1 Introduction

Role of integrins in osteoclast adhesion and migration

The adhesion and migration processes are essential for the differentiation of osteoclasts. Integrins are a group of heterodimeric transmembrane receptors expressed by all multicellular animals[198]. Different subunits α and β, both are class-I transmembrane proteins, assemble by non-covalent interactions to form an integrin, among different species, there are 25 different receptors[198, 199]. It was reported that $\alpha_v\beta_3$, $\alpha_2\beta_1$, $\alpha_v\beta_1$ integrins were expressed in human osteoclasts, among them, $\alpha_v\beta_3$ integrin was the dominant one[200-202]. The integrins are vital for the adhesion and migration of osteoclasts precursors. The extracellular domain of $\alpha_v\beta_3$ integrin on osteoclasts was suggested to bind to many ECM proteins containing RGD-motif, such as osteopontin, bone sialoprotein, and vitronectin, therefore sustaining the adhesion of osteoclast precursors and osteoclasts[203]. Moreover, researchers found that treatment of echistatin, an RGD-containing integrin antagonist, could inhibit the migration and cell distribution of osteoclast precursors. Additionally, they noticed that $\alpha_v\beta_3$ integrins were identified in podosomes at the migrative edges of osteoclasts in normal OC culture, however, with the treatment of echistatin, the integrins were randomly spreading on the adhesion surfaces. These results indicated that $\alpha_v\beta_3$ integrins also played an important role in osteoclasts migration[204].

RANKL/RANK/OPG signaling pathway in bone remodeling

The RANKL/RANK/OPG signaling pathway is a classic and critical pathway for the crosstalk of bone cells, more specifically, the crosstalk between osteoblastic cells and osteoclastic cells. RANK, receptor activator of nuclear factor kappa B, is a receptor expressed on the membrane of osteoclast precursors that triggers the process of osteoclastogenesis. RANKL is the membrane ligand to RANK which is expressed by osteoblastic cells, and some of RANKL can be released to the bone microenvironment as a soluble form. OPG, osteoprotegerin, a decoy receptor for RANKL, is also released by osteoblastic cells and binds to RANKL to prevent excessive bone resorption. The RANKL/OPG ratio is a critical regulator for bone remodeling[205, 206].

Overview of microfluidics

Microfluidics refers to the precise observation, control, and manipulation of working fluids in channels with dimensions of tens to hundreds of micrometers[207]. Due to their low cost, small size, versatility, operating flexibility, high resolution, and sensitivity in a minute quantity of samples, as well as a short time in analysis, microfluidic devices quickly prevail in the biological fields of genome sequencing, proteomics, cell biology, and medical diagnostics[208]. The first batch of researchers in the 1990s [209, 210] used photolithography techniques to fabricate microfluidic devices, which gained high resolution but were expensive and inconvenient. After a new flexible method, soft lithography was

invented in 2001[211], microfluidics has been prosperous in bioengineering labs all over the world.

As mentioned above, in the beginning, the method to fabricate microfluidic devices was photolithography and etching, which was adapted from the microelectronics industry, was precise but costly, laborious, and inflexible. Later in 2001, soft lithography techniques were applied to microfluidics. This method needs only one mask being fabricated in photolithography, and the following finished devices can be made in open lab environments, which greatly increased the efficiency of processing progress and bring it out of a clean room[211]. The material used in soft lithography, elastomer poly(dimethylsiloxane) (PDMS) is inexpensive and easy to mold. More importantly, this material is optically clear, bio-inert, non-toxic, and non-flammable.

3.2 Rationale

The enzymatic function of AChE may play a dominant role in bone formation[192, 193]. Yet the role of AChE, either its enzymatic or non-enzymatic function, in bone resorption is relatively less understood.

Although is also evidence that indicates a potential effect of AChE in the process of osteoclastic lineage, the mechanism still needs to be explored. A remarkable decrease in the number of osteoclasts was reported in lumbar vertebrae of the heterozygous

acetylcholinesterase-knockout mice[212]. Meanwhile, AChE could also directly stimulate the respiratory burst in peritoneal macrophages[213], and enhance osteoclast differentiation of bone marrow monocytes, which is independent of its enzymatic function[214]. Another study showed that AChE inhibitor donepezil could suppress osteoclastogenesis in cell cultures of murine bone marrow-derived macrophages [124]. However, a recent study claimed that other AChE inhibitors, Galantamine and Pyridostigmine had no direct effects *in vitro* on the survival and differentiation of osteoclast progenitors[215]. These controversial results need to be further confirmed with mechanism detection.

Under the regulation of many cytokines, the osteoclasts precursors are recruited to proliferate and become preosteoclasts and attach to the bone resorption site. With continuous signaling of M-CSF and RANKL, the pre-osteoclasts differentiate from mononuclear osteoclasts and at the same time migrate and adhere to fuse together. And finally became activated multinuclear osteoclasts. So, we investigate the role of AChE in osteoclast precursors adhesion, migration, and fusion.

3.3 Materials and methods

Reagents

Fetal bovine serum (FBS), Dulbecco's Modified Eagle Medium(high-glucose) (DMEM), Minimum Essential Medium α (αMEM), trypsin–EDTA reagent, Penicillin-Streptomycin (P/S), RevertAid First Strand cDNA Synthesis Kit (Thermo Fisher Scientific, Waltham,

USA, #10270-106 & #11965-092 & #12561-056 & #25300-062 & #15140-122 & #K1622); Soluble RANKL (Sigma-Aldrich, St. Louis, USA, #R0525-10UG); Donepezil HCl (Aladdin, Shanghai, China, # 120011-70-3); Galantamine Hydrobromide (Sigma-Aldrich, St. Louis, USA, PHR1623-500MG); Cell Proliferation Kit 1 (MTT) (Roche, Penzberg, German, #11465007001); E.Z.N.A.® Total RNA Kit I (Omega Bio-tek, Norcross, USA, #R6834-02); QuantiNova SYBR Green PCR Kit (Qiagen, Hilden, German, #208056); Recombinant Mouse Acetylcholinesterase (AChE) Protein, Recombinant Mouse M-CSF Protein (R&D Systems, Inc, Minneapolis, USA, # 5518-CE-010 & # 416-ML-500).

Cell culture and osteoclast in vitro differentiation of RAW 264.7 cells

The murine macrophage RAW 264.7 cell line was obtained from the American Type Culture Collection (ATCC TIB-71, Manassas, VA, USA) and was cultured in DMEM medium supplemented with 10% Fetal Bovine Serum and 1% penicillin/streptomycin (Growth medium). When reaching the 50–60 % confluency, RAW 264.7 cells were cultured with growth medium containing 15ng/mL soluble RANKL (RANK Ligand from mouse, R0525, sigma) for 3-7 days to differentiate to osteoclasts. For treatment of AChE inhibitors, the RAW 264.7 cells were treated with 1μM donepezil or galantamine in differentiation induction medium after reaching the 50–60 % confluency. The concentration and treatment time of donepezil and galantamine were determined by a Cell Proliferation Kit I with MTT (Roche, Switzerland). In some experiments, mouse recombinant AChE protein or heat-inactivated AChE protein was added to the differentiation medium with cultured RAW 264.7 cells for 3 days in the concentration of 200ng/mL. "Heat-inactivated" AChE was prepared by

heating the protein for 3 min at 100°C. All cells were incubated in a humidified atmosphere with 5% CO2 at 37 °C and medium was replaced every day.

Fabrication of microfluidic device

The microfluidic chip was fabricated by the soft lithography method. In brief, the silicon wafer was firstly washed under a standard wash process and blown dry the wafer with nitrogen. After baking on the hot plate at 180°C for 30min, the wafer was placed on the ultra-clean wiper to cool down the wafer. Then, the wafer was coated with SU-8 3010 at 3000rpm for the 30s to get a 10 μm photoresist layer. After 3min soft baking at 95°C, the coated wafer was put in the UV aligner and covered with the designed photomask for exposure with the exposure energy at 210 mJ/cm^2. It should be noted that the practical exposure parameters were fixed according to the equipment condition duly to avoid the prism effect and standing wave effect. Then, the SU-8 mold was obtained after a 3min post-baking process (1min at 65°C and 2min at 95°C), and a 3min development process. The wafer was cleaned by the nitrogen flow after every operation.

Before processing the demolding process, the fabricated silicon wafer was coated with 1H,1H,2H,2H-perfluorodecyltriethoxysilane (FDTS) for a hydrophobic layer. Then, the mixture of PDMS (10:1) was poured onto the mold after a thoroughly stirring process. The mold with PDMS was put in the vacuum for 30min to bleed the air in the mixture. After that, put the mold in the oven overnight at 70°C to get the PDMS mold. Then, tearing off the PDMS mold and cut it to get the single mold. The ports of medium and cell were punched by

a sharp puncher. Tapes were used to clean the surface of the PDMS and glass coverslip. Then, the chip was obtained by bonding PDMS and coverslip after oxygen plasma treatment. After washing with deionized water and 70% ethanol, the chip was ready for use. Chips were cleaned with sterile PBS solution and exposed to UV light to be sterilized for 30 minutes. Then the channels of the chip were coated with 50μg/ml of collagen I solution for 1 hour and then washed with PBS.

Live cell imaging

To investigate how AChE and HAChE proteins affect the cell adhesion of osteoclasts precursors, we observed the cell adhesion behaviors under the AChE/ HAChE coating conditions via the live cell imaging microscope (Nikon Eclipse Ti2). Basically, the petri dish was coated with a layer of collagen I (50μg/ml) or collagen I (50μg/ml) with ACHE (200ng/ml) or HAChE (200ng/ml). Osteoclast precursors were seeded at the density of 0.3 X 10^6 per well in each petri dish. And then they were stable incubated for 2 hours (in a humidified atmosphere with 5% CO2 at 37 °C). The petri dishes were shaken every 3 minutes for 40 hours. Live cell imaging microscope to monitor the adhesion behaviors of cells in each petri dish. Adhesion index (A) was introduced to quantify the degree of cell adhesion (0-20%: A=1; 21-40%: A=2; 41-60%: A=3; 61-80%: A=4; 81-100%: A=5).

To characterize osteoblastic cells and osteoclasts cells in the microfluidic device, the cells were alive and stained by different fluorescent cell membrane labeling dyes. The osteoblastic cells were stained with a green-fluorescent dye (Sigma-Aldrich, St. Louis, USA,

#PKH67GL) and the osteoclasts were stained with red-fluorescent dye (Sigma-Aldrich, St. Louis, USA, #PKH26GL). Senescence of osteoblastic cells was induced by 200μM H2O2 for 24 hours. Live cell imaging microscope to monitor the migration behaviors of cells in the microfluidic device.

Isolation of primary cultured osteoclasts form mice long bones in vitro and differentiation induction

The mouse primary cultured bone marrow cells and osteoclast precursors were isolated based on an established protocol[216]. Briefly, four balb/c mice were sacrificed with an overdosed anesthetic cocktail [ketamine (100mg/mL): Xylazine (20mg/mL): saline = 5:2.5:2.5], and the limb bones were collected and rinsed with ice PBS. After all samples were dissected, the bones with PBS were transferred to a biosafety cabinet. The bones were then placed in ice PBS with 1% P/S. The end of the 200 μL pipette tips were cut so that they could be put in the 1.5mL centrifuge tubes. Small incisions (approximately 1 to 2 mm) at both ends of the bones were made and the cut bone were transferred to the cut tips in the centrifuge tubes. 100μL of αMEM supplemented with 10% FBS and 1% P/S were added to each centrifuge tubes with inserts. The tubes with bone were centrifuged at 10,000 x g for 15 s at room temperature to flush and pellet the bone marrow. The inserts of hollow bones were removed and the medium with bone marrow were collected. For every 500 μL of samples, 10ml of growth medium was added. The mix cells were allowed to attach for 48h. After 48 hours, the non-adherent cells were collected, these were the targeted osteoclastic progenitors.

For the osteoclastogenetic induction of primary cultured osteoclastic progenitors, 25ng/mL RANKL and 15ng/mL M-CSF were added to the culture medium (differentiation medium). The differentiation medium was replaced every other day for 4 days. Multinucleated cells were observed to form from the third day of induction. For treatment of AChE inhibitors, the primary cultured osteoclastic progenitors were treated with 1μM donepezil or galantamine in differentiation induction medium after reaching the 50–60 % confluency. The concentration and treatment time of donepezil and galantamine were determined by a Cell Proliferation Kit I with MTT (Roche, Switzerland). In some experiments, mouse recombinant AChE protein or heat-inactivated AChE protein was added to the differentiation medium with cultured cells for 3 days in the concentration of 200ng/mL. "Heat-inactivated" AChE was prepared by heating the protein for 3 min at 100°C. All cells were incubated in a humidified atmosphere with 5% CO2 at 37 °C and medium was replaced every two days.

MTT assay

The cell proliferation assay will be performed using the Cell Counting Kit-8 (CCK- 8, Dojindo, Kumamoto, Japan). RAW 264.7 cell suspension (100 μL, 1×10^4 per well) will be dispensed into 96-well plates and incubated for 24 h, then changed for the fresh media containing different concentrations of donepezil and galantamine (0.01 /0.05 /0.1 /0.5 /1 /5 /10 /50 /100μM) and incubated for another day. Finally, 10 μL of CCK-8 solution will be added into each well and incubated for 4 h, after the absorbance will be measured at 570 nm using a BioTek microplate reader (Winooski, VT, USA).

TRAP staining

Cultured osteoclast-like cells were fixed in 4% paraformaldehyde solution for 15min at room temperature and stained with the leukocyte acid phosphatase kit (387A, Sigma-Aldrich) according to the protocol of the manufacturer. Briefly, deionized fast garnet GBC solution, naphthol AS-BI phosphate solution, acetate solution, tartrate solution and deionized warm water were mixed together according to the manufacturer instructions at 37 °C, cells were stained with the mixed solution for 1h at 37 °C in dark environment. After staining the cells were rinsed with deionized water 3 times. Images of cells were collected with a Nikon microscope. TRAP positive multinucleated cells (nuclear numbers > 3) were counted using the image J software.

Cell immunofluorescence

RAW 264.7 cells or primary cultured osteoclasts were seeded with a density of 1000 cells/well in 12-well plates on circle cover slips. Subsequently the cells were fixed in 4% paraformaldehyde for 15 min, permeabilized in 0.1% Triton-X 100 for 30 min, blocked with 5% BSA for 30 min. AChE was visualized using an Anti-Acetylcholinesterase antibody (Abcam, ab2803) in combination with the secondary Goat Anti-Mouse IgG (H&L) antibody (Alexa Fluor® 647) (Abcam, ab150115) for detection. Nuclei were visualized by NucBlue reagent (Life Technologies, R37605). Cells were imaged on an Olympus BX61 inverted microscope system.

Total RNA Extraction

Total RNA from cells was collected using E.Z.N.A.® Total RNA Kit I (Omega Bio-tek) according to the manufacturer's instructions. Briefly, cells were lysed directly on a culture plate with lysis buffer. 1 volume of 70% ethanol was added and mixed with the lysate, followed by centrifugation at 10000 for 1min in a spin column. The supernatants were removed, and the samples trapped in the column filter were washed with wash buffer I and wash buffer II for several times. 20 μL of RNase/DNase-free water was added to the filter membrane to dissolved RNA. The concentration of total RNA was measured by NanoDrop One (Nanodrop Technologies). Only samples with A260/280 > 1.7 were used for reverse transcription. Isolated total RNA was stored at -80 °C

Reverse transcription of total RNA to cDNA

The extracted total RNA was reverse transcribed to cDNA via a RevertAid First Strand cDNA Synthesis Kit (Thermofisher) according to manufacturer's protocol. Briefly, 1000ng of total RNA was mixed with appropriate amount of water, making up total volume of 11 μL, and added with 1 μL of Oligo(dT)$_{18}$ primer. The 12μL of mixture was incubated at 65 °C for 5 minutes and chill on ice immediately for 1 minute. Later, for every sample, 1μL of RiboLock RNase Inhibitor, 1μL of RevertAid RT, 2μL of 10 mM dNTP Mix and 4μL of 5X Reaction Buffer were added to the sample to make a final volume of 20μL mixture. The 20μL of mixture was incubated at 42 °C for 60 minutes and followed by an incubation at 25 °C for 5 minutes.

Quantitative Polymerase Chain Reaction (qPCR)

Quantitative real-time polymerase chain reaction was then performed by BIO- RAD CFX96 Touch™ Real-Time PCR Detection System using primers of specific genes (See Table 1) and QuantiNova SYBR Green PCR Kit (Qiagen). 25 μg of cDNA was used in each reaction. All the mRNA expression levels were normalized using the endogenous control, *Gapdh*. Melt curve analysis was conducted.

Gene	Forward Primer	Reverse Primer
GAPDH	AGGTCGGTGTGAACGGATTTG	GGGGTCGTTGATGGCAACA
Integrin $\beta 1$	GGAAACTCTAGTAATGTGATCCAGC	CACTTGGGACTGGCTGGGATGCCATG
Integrin αv	CTGGCCTTGAAGTGTACCCTAGCAT	TGCTTGAGTTTATCCAGTAGAAGCT
Integrin $\beta 3$	TGACTCGGACTGGACTGGCTA	CACTCAGGCTCTTCCACCACA

Table 3-1 Primer sequence of targeted integrin genes used in qPCR.

Gene	Forward Primer	Reverse Primer
TRAP	CTGCTGGGCCTACAAATCAT	GGTAGTAAGGGCTGGGGAAG
RANK	AAACCTTGGACCAACTGCAC	ACCATCTTCTCCTCCCGAGT
CtsK	AGCACCCTTAGTCTTCCGCT	TTTCCTCCGGAGACAGAGCA
MMP9	CGTCGTGATCCCCACTTACT	AGAGTACTGCTTGCCCAGGA
DC-Stamp	GTGCTTTGTGCTTGTGGAGG	ACAGAAGAGAGCAGGGCAAC
OC-Stamp	CATCCGCTGCCTATTTGTGC	CACGCACATTGCCTAAGACG

Table 3-2 Primer sequence of targeted osteoclastogenic genes used in qPCR.

Gene	Forward Primer	Reverse Primer

AChE	AGGTCGGTGTGAACGGATTTG	GGGGTCGTTGATGGCAACA
ChAT	TTGGGTCTCTGAATACTGGCT	CTGCAAACCTTAGCTGGTCAT

Table 3-3 Table 2 Primer sequence of targeted cholinergic genes used in qPCR.

siRNA transfection

The target sequence for mouse AChE siRNA was 5′-CGACUUAUGAAAUACUGGA -3′ (Genebank accession number NM_009599.4 and NM_001290010.1). The target siRNA and control siRNA (no silencing) were synthesized by Thermo Fisher. One day before transfection, RAW264.7 cells or primary cultured OCs were plated onto six-well plates with growth medium without antibiotics at a density of 1×10^6 cells/well. When cells grew to a confluency of 40 on the second day, transfection was performed by using Opti-MEM media, lipofectamine2000 and AChE siRNA according to manufacturer's recommendations. The final concentration of AChE siRNA was 100 nM. After 24 hours, the media was replaced with growth media without antibiotics and cells were treated with 15 ng/ml RANKL for 3-7 days (RAW264.7 cell) or 25ng/ml RANKL and 15ng/ml M-CSF (primary cultured OCs) for 1-4days. The control cells were transfected with lipofectamine2000.

Protein extraction and Western blotting

For protein extraction, cells were suspended in SDS lysis buffer and boiled. Then, the lysate was centrifuged at 12,000 × g for 2 min and the supernatant was collected. For Western blotting, protein samples were separated on SDS-polyacrylamide gels, transferred to PVDF membranes (Millipore, USA), blocked with 5% non-fat milk and incubated with the primary

antibody of AChE (A-11) (Santa Cruz, sc-373901) in combination with the secondary Goat Anti-Mouse IgG H&L (HRP) antibody (Abcam, ab97040). Images were acquired on a Bio-Rad system.

Statistical Analysis

All statistical results were presented as mean ± standard error of the mean (SEM). The comparison between multiple groups was quantitatively analyzed using one-way ANOVA. Post-hoc tests were performed following statistically significant results. A significant difference was indicated when $P<0.05$.

3.4 Results

Coating of AChE and HAChE promotes the cell adhesion of RAW264.7 cells associated with increased expression of beta 3 integrin

The AChE TRAP co-staining results suggested that the TRAP-positive cells adhered to the AChE protein. We further investigated this phenomenon in vitro. So, basically, the petri dish was coated with a layer of collagen 1 or collagen 1 with ACHE or HAChE. Osteoclast precursors were seeded in each petri dish. And stable incubated for 2 hours. The petri dishes were shaken every 3 minutes for 40 hours. The results indicated that (Fig.3.1), in the Ctrl group, Cells were floating from the start to the finish. However, in both AChE and HAChE coated groups. The cells were attached to the petri dish tightly. These results suggested that Both AChE and HAChE coating could promote the adhesion of osteoclast precursors. To

further confirm the adhesion function of AChE protein, we checked the expression of integrin subunit proteins in the treatment of AChE and HAChE groups. Integrins are transmembrane receptors that facilitate cell-cell and cell-extracellular matrix (ECM) adhesion. We found that, after treatment of AChE and HAChE, the $\beta 3$ integrin subunit expression in both groups was strongly increased. These results further suggested the link between AChE and osteoclast precursor adhesion.

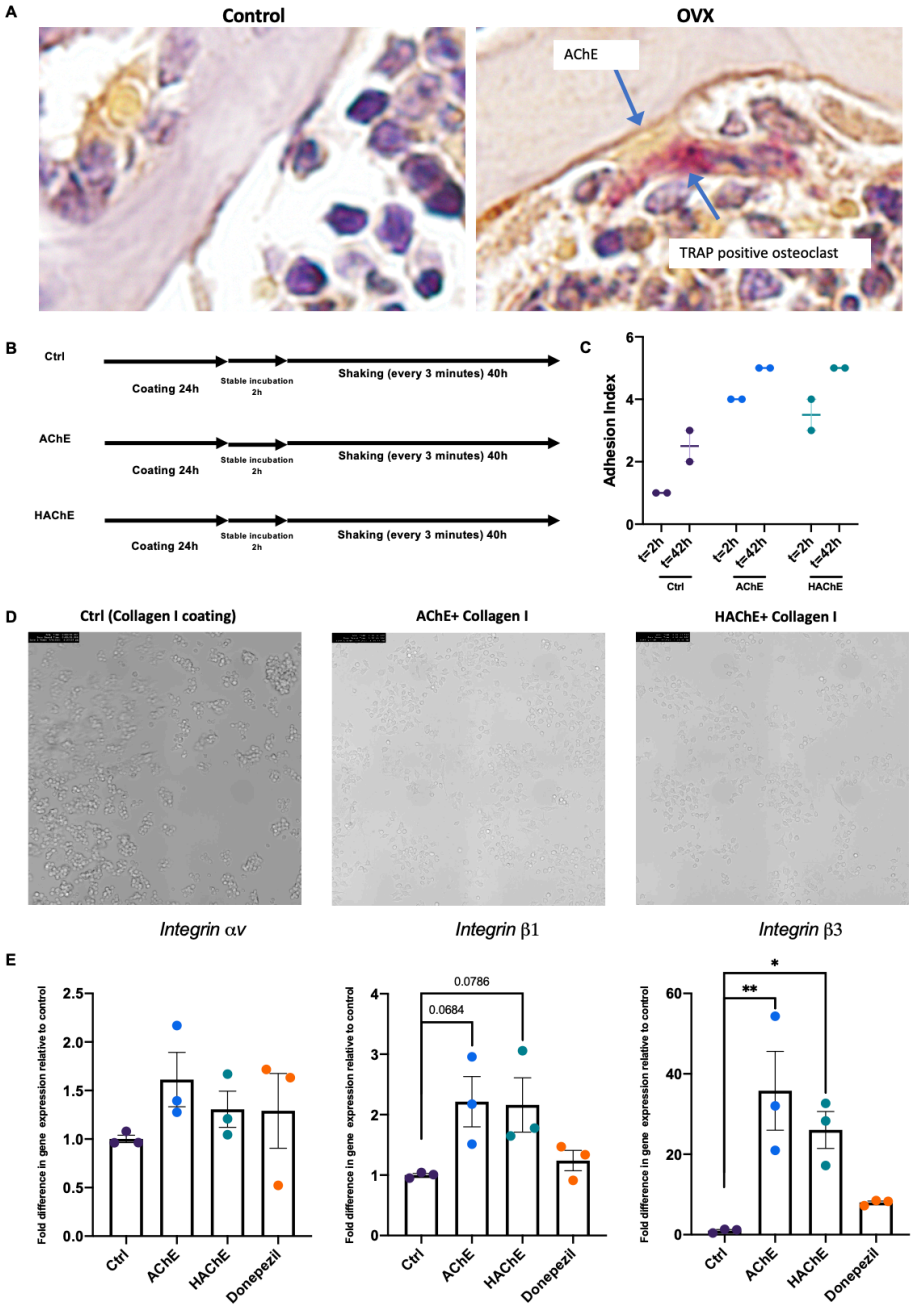

Fig 3.1 Both coating of AChE/HAChE proteins promoted the adhesion of RAW 264.7 cells *in vitro*. (A) Representative images of DAB AChE/ TRAP co-staining of bone sections of Ctrl and OVX-induced osteoporosis mice. (B) Experiment design. (C) Quantification results of Adhesion Index for different coating groups. (D) Representative images of live cell imaging coated with a layer of collagen I (50μg/ml) or collagen I (50μg/ml) with ACHE (200ng/ml) or HAChE (200ng/ml). (E) Relative mRNA expression of different integrin subunits (*Integrin* β1, *Integrin* αv, *Integrin* β3) under the treatments of (B) (n=3). All data are expressed as means ± SEM. One-way ANOVA with Post-hoc tests were performed following statistically significant results. * $p<0.05$; ** $p<0.005$; *** $p<0.001$.

Osteoclast precursors showed the tendency of migrating to the side of senescent osteoblastic cells which secreted AChE

H2O2 treated osteoblasts secret AChE. However, the OPG/RANKL signaling pathway could also affect the migration of osteoclast precursors. In order to exclude the influence of donepezil on OPG/RANKL. We checked OPG/RANKL mRNA levels before and after donepezil treatment. The results showed no difference, which means the different result in the donepezil treatment group was caused by inhibition of AChE. The MC3T3-el cells were stained with a green-fluorescent dye (green cells in Fig.3.2F) and the RAW264.7 cells were stained with red-fluorescent dye (orange cells in Fig.3.2F). From the image and quantitative results, we found that compared to the Ctrl group, the osteoclasts co-cultured with senescent osteoblasts tended to migrate to the osteoblast chamber. However, after treatment of donepezil, this migration tendency disappeared.

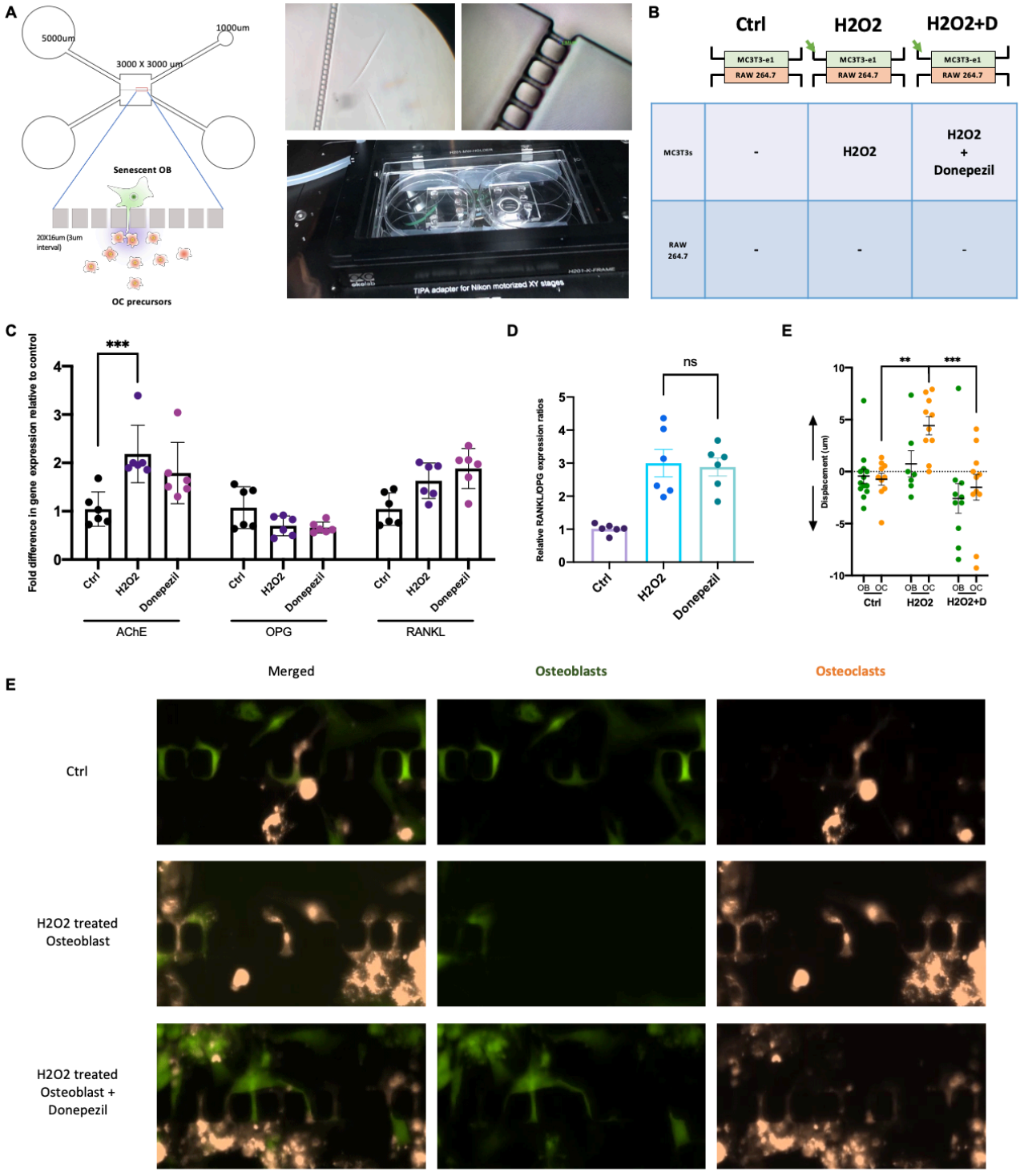

Fig 3.2 RAW 264.7 cells showed the tendency of migrating to the side of senescent osteoblastic cells which secreted AChE *in vitro*. (A) Schematic and real images of the microfluidic device. (B) Experiment design. (C)Relative mRNA expression of *AChE, OPG, RANKL* under the treatments of (B) (n=6). (D) Relative mRNA expression ratio of *RANKL/OPG* (n=6). (E) Representative images of migration of cells under the treatments of (B) (RAW264.7 cells: orange, MC3T3-e1 cells: green). All data are expressed as means ± SEM. One-way ANOVA with Post-hoc tests were performed following statistically significant results. * $p<0.05$; ** $p<0.005$; *** $p<0.001$.

Treatments of both mouse recombinant AChE and heat-inactivated AChE promoted osteoclastogenesis by regulating cell-cell fusion

To explore whether AChE and HAChE protein could promote cell fusion of osteoclasts precursors. We incubated both RAW264.7 cells and primary cultured osteoclastic cells with AChE protein or HAChE protein. After incubation, osteoclasts ((Fig.3.3, RAW264.7 cells; Fig.3.4, Primary cultured osteoclastic cells) with larger size and more nuclei were observed in 200ng/ml AChE-treated group compared to RANKL induction group in both RAW264.7 cell and primary cultured osteoclasts. Surprisingly, heat-inactivated AChE treatment was also able to promote osteoclastogenesis. As cell-cell fusion is a key step for osteoclast to enlarge their size and gather more nuclei, the mRNA expression level of two osteoclastic fusion markers, DC-STAMP and OC-STAMP was investigated. qRT-PCR analysis showed that both AChE and heat-inactivated AChE treatments were associated with upregulated DC-STAMP and OC-STAMP in a dose-dependent manner.

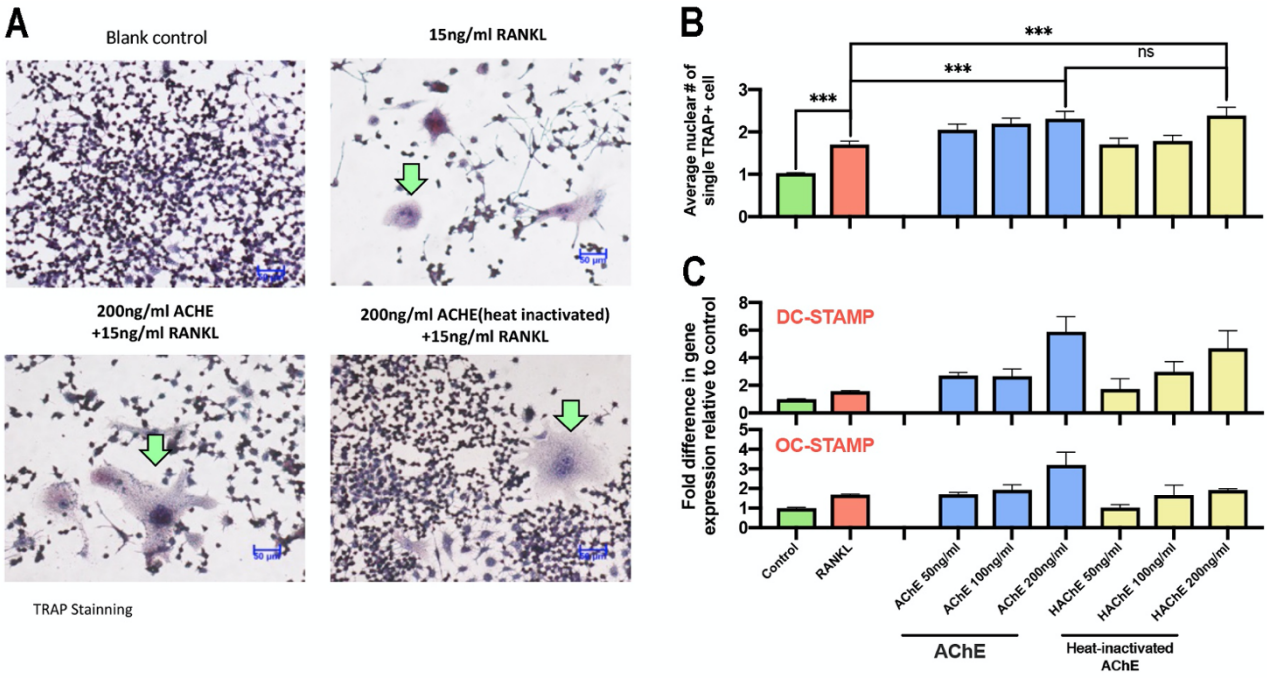

Fig 3.3 Treatments of both mouse recombinant AChE and heat-inactivated AChE promoted osteoclastogenesis by regulating cell-cell fusion in RAW264.7 cells. (A)Representative images of TRAP staining when cells were treated with RANKL, RANKL + recombinant AChE (200ng/mL), RANKL + heat inactivated AChE (200ng/mL). (48h) TRAP+ multinuclear cells were indicated by green arrows. Scale bar, 50 μm. (B)Quantification results of average nuclear numbers of single cell when cells under conditions of (A) (n=6). (C) Relative mRNA expression of cell-cell fusion markers (*DC-STAMP* and *PC-STAMP*) before and after treatments of different concentration of AChE and heat-inactivated AChE (n=6). All data are expressed as means ± SEM. One-way ANOVA with Post-hoc tests were performed following statistically significant results. * $p<0.05$; ** $p<0.005$; *** $p<0.001$.

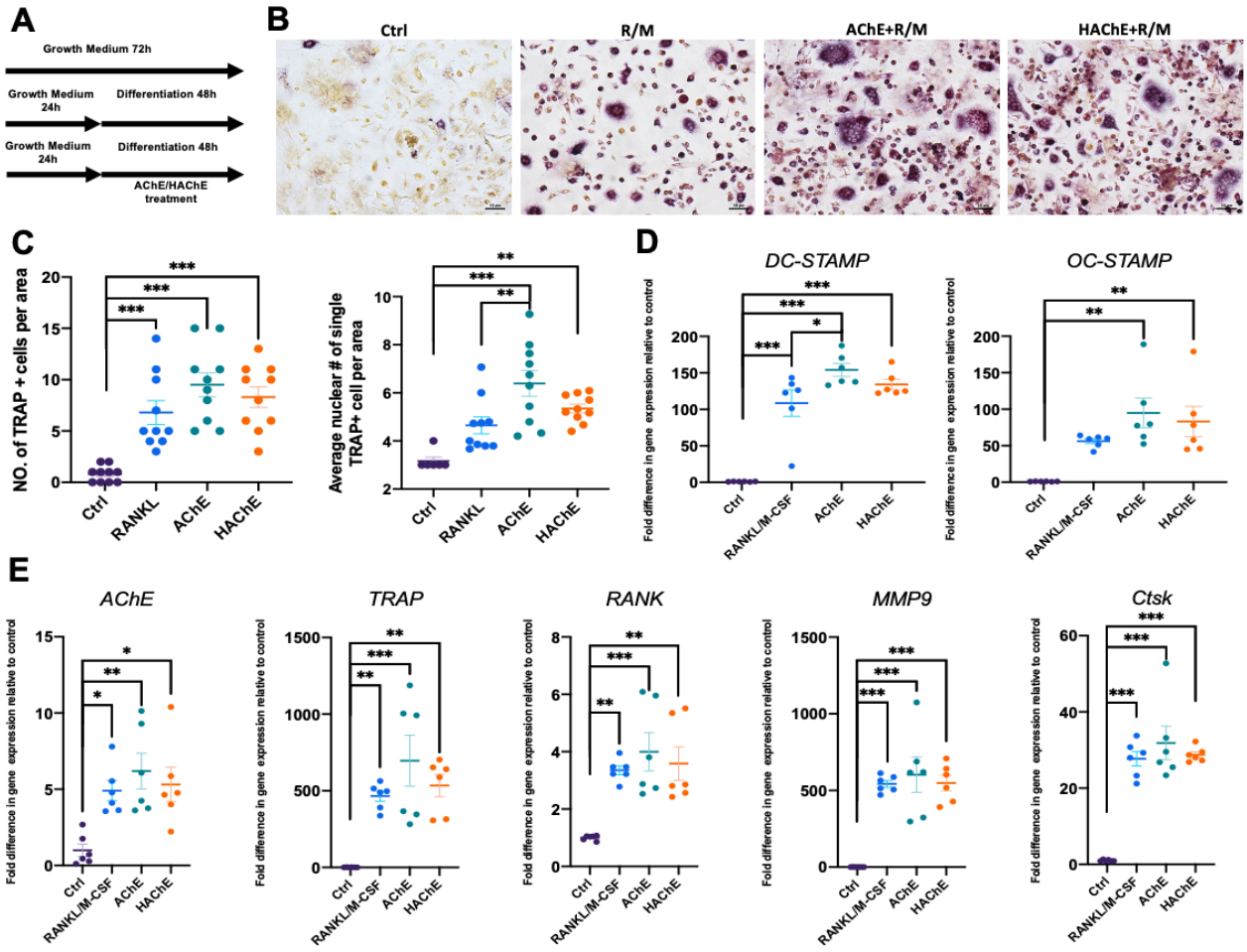

Fig 3.4 Treatments of both mouse recombinant AChE and heat-inactivated AChE promoted osteoclastogenesis by regulating cell-cell fusion in primary cultured OCs.(A) Experiment design. (B) Representative images of TRAP staining when cells were treated with R/M (25ng/ml RANKL and 15ng/ml M-CSF), R/M + recombinant AChE (200ng/mL), R/M + heat inactivated AChE (200ng/mL). Scale bar, 50 µm. (C) Quantification results of NO. of TARP+ multinuclear cells per area (0.314mm^2) and average nuclear numbers of single cell when cells under conditions of (B) (n=10). (D) Relative mRNA expression of cell-cell fusion markers (*DC-STAMP* and *PC-STAMP*) under the treatments of R/M (25ng/ml RANKL and 15ng/ml M-CSF), R/M + recombinant AChE (200ng/mL), R/M + heat inactivated AChE (200ng/mL) (n=6). (E) Relative mRNA expression of *AChE* and osteoclastic markers (*TRAP*, *CtsK*, *MMP9* and *RANK*) under the treatments of (B) (n=6). All data are expressed as means ± SEM. One-way ANOVA with Post-hoc tests were performed following statistically significant results. * p<0.05; ** p<0.005; *** p<0.001.

AChE expression increased during osteoclastogenesis *in vitro* in both RAW 264.7 cells and primary culture of OCs

To explore the role of AChE during osteoclastogenesis, the AChE expression pattern *in vitro* was investigated. First, the establishment of an *in vitro* osteoclastogenesis model based on the differentiation of the RAW 264.7 cell line and primary cultured osteoclasts were confirmed visually as TRAP-positive large multinuclear osteoclasts via RANKL induction (Fig 3.5A, Fig 3.6A). Next, the expression of AChE was investigated during differentiation. The mRNA expression level of AChE increased after osteoclastogenetic induction in both RAW 264.7 cell lines and primary cultured osteoclasts. The same increasing trends were observed in the protein expression level of AChE by immunofluorescence staining (Fig 3.5C, Fig.3.6C) and western blot (Fig.3.5D). The mRNA expression of osteoclastogenic markers TRAP, MMP9, and CtsK was upregulated after osteoclastogenetic induction in both RAW 264.7 cell line and primary cultured osteoclasts, which was positively associated with the AChE mRNA expression.

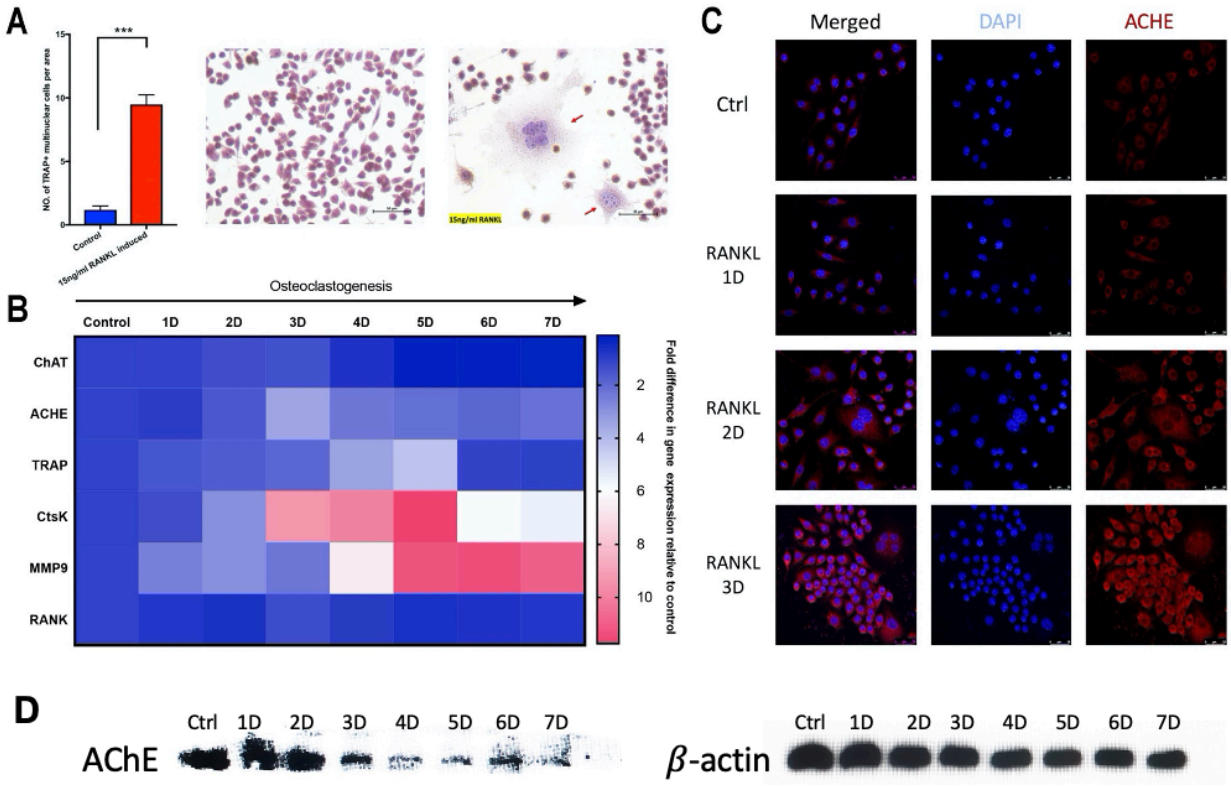

Fig 3.5 AChE expression increased during osteoclastogenesis in RAW 264.7 cells *in vitro*. (A) Validation of osteoclastogenesis induction of RAW264.7 cells, multinuclear TRAP positive cells were observed after 15ng/ml RANKL induction for 4 days (NO. of TRAP+ multinuclear cells were quantified and present as means ± SEM. Unpaired T test was used for statistical analysis. * $p<0.05$; ** $p<0.005$; *** $p<0.001$. (B) qPCR results showed the expression pattern of *AChE*, *ChAT* and osteoclastic markers (*TRAP, CtsK, MMP9* and *RANK*) during osteoclastogenesis, from blue to red, the relatively expressed fold of mRNA increased from low to high. (C) Representative immunofluorescence staining images of AChE(red) at different time-points with osteoclastogenesis induction. Scale bar, 25 μm. Cells were counter-stained with DAPI (blue). Cells were pre-treated with blockers for 30 minutes before H_2O_2 stimulation. (D) Examples of actual Western blot analyses of AChE protein during osteoclastogenesis in RAW 264.7 cells.

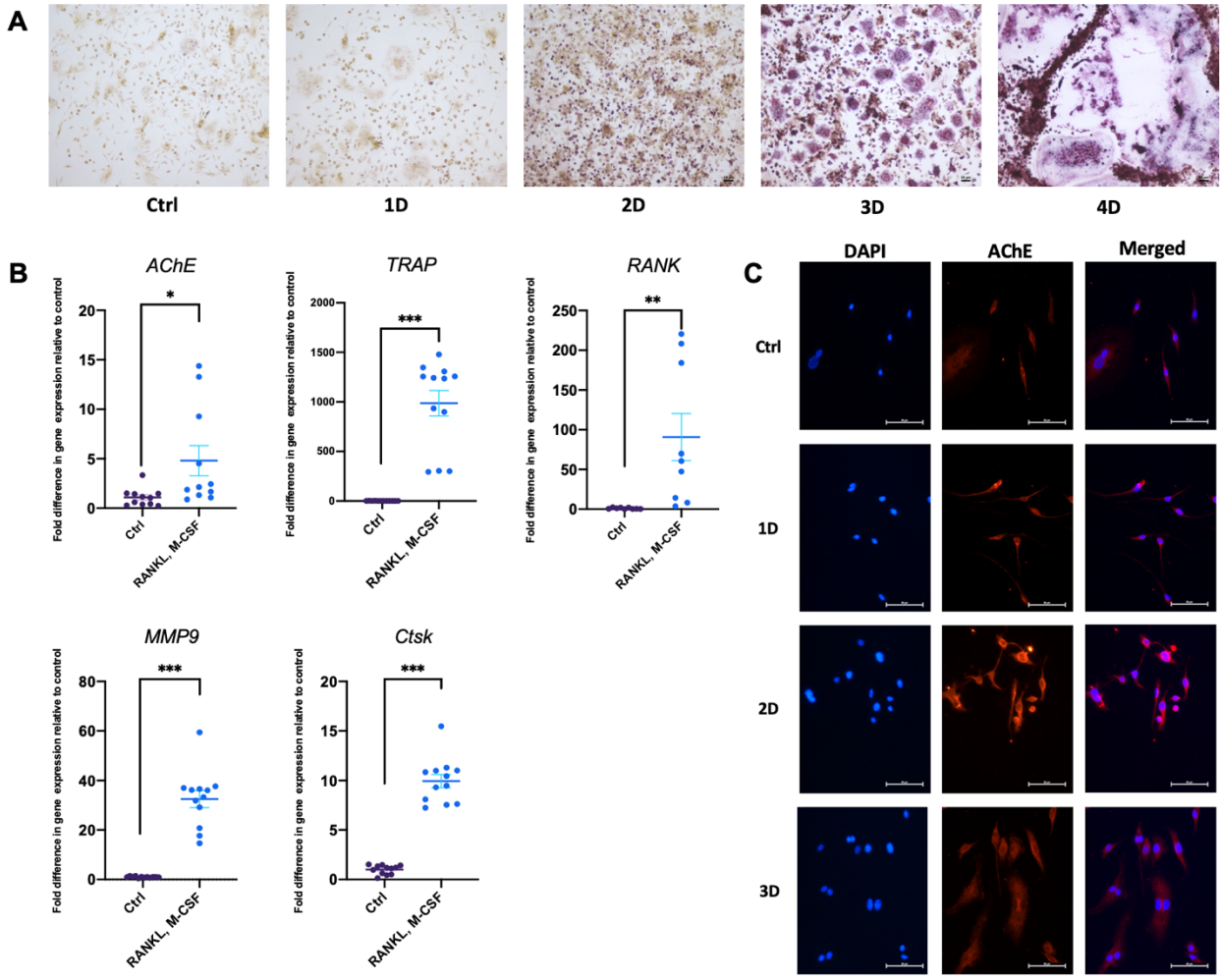

Fig 3.6 AChE expression increased during osteoclastogenesis in primary cultured osteoclasts *in vitro*. Osteoclastogenesis of primary cultured OCs was induced via 25ng/ml RANKL and 15ng/ml M-CSF for 4 days. (A) Representative images of TRAP staining at different time points during osteoclast differentiation. (purple). (C) Relative mRNA expression of *AChE* and osteoclastic markers (*TRAP*, *CtsK*, *MMP9* and *RANK*) before and after osteoclastogenesis induction (n=6). All data are expressed as means ± SEM. Unpaired T test was used for statistical analysis. * $p<0.05$; ** $p<0.005$; *** $p<0.001$. (D) Representative immunofluorescence staining images of AChE(red) at different time-points with osteoclastogenesis induction. Scale bar, 50 μm. Cells were counter-stained with DAPI (blue). Cells were pretreated with blockers for 30 minutes before H_2O_2 stimulation.

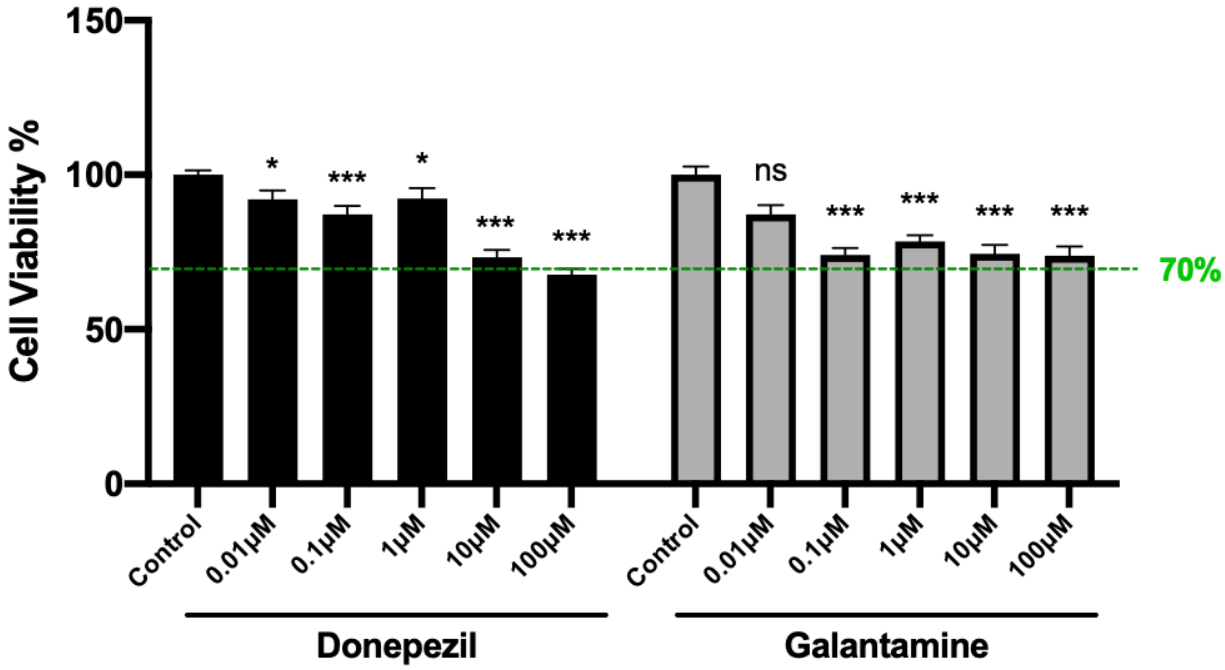

Fig 3.7 Cell viability of RAW 264.7 with increasing concentration of one day treatments of donepezil and galantamine, respectively. Both donepezil and galantamine treatment for 24h showed a concentration-dependent reduction of cell viability. Set 70% viability as a threshold, 10μM was the maximum tested safe concentration for both donepezil and galantamine. All data are expressed as means ± SEM. One-way ANOVA with Post-hoc tests were performed following statistically significant results. * $p<0.05$; ** $p<0.005$; *** $p<0.001$.

Silencing of AChE Gene by siRNA suppressed osteoclastogenesis *in vitro*

To further confirm the role of AChE during osteoclast differentiation, AChE siRNA was used to inhibit AChE expression in a genetic manner. First, AChE siRNA was validated by using qRT-PCR (Fig 3.8B, Fig 3.9). After 24 h transfection of siRNA, the mRNA expression levels of AChE were suppressed in both RAW 264.7 cell line and primary cultured osteoclasts. As shown in Fig.3.8C, RAW 264.7 cells with inhibited expression of AChE hardly differentiated to osteoclasts compared to the normal RANKL-induced group as barely TRAP+ cells were detected in the siRNA treated group. Results from qRT-PCR also supported this conclusion as the expression of osteoclastogenic markers decreased in siRNA treated cells. A similar phenomenon was observed in primary cultured osteoclastic cells.

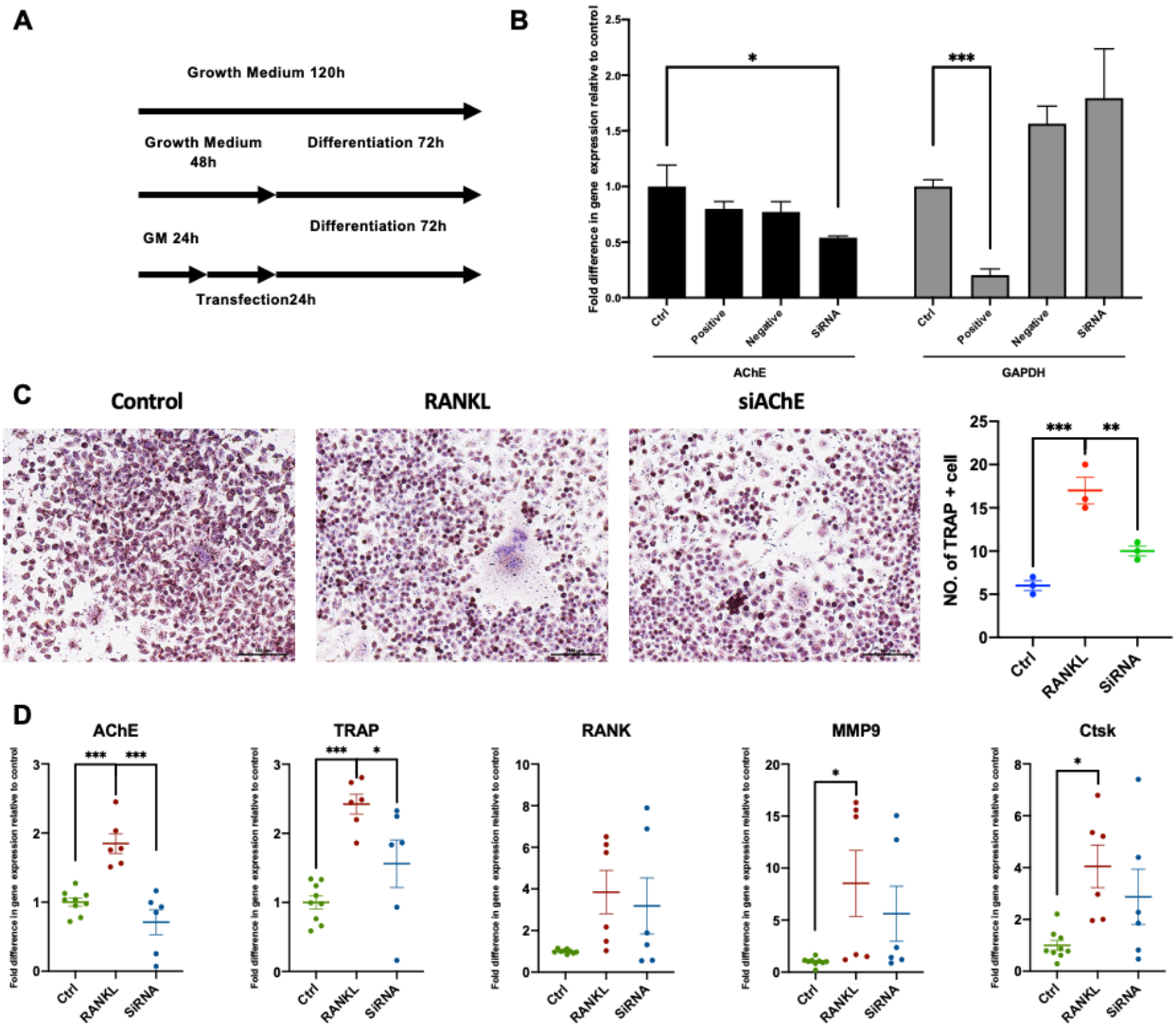

Fig 3.8 Transfection of AChE siRNA suppressed osteoclastogenesis in RAW264.7 cells.(A) Experiment design. (B) Validation of AChE siRNA by qPCR tests. (n=3). (C) Representative images of TRAP staining when cells were treated with 15ng/ml RANKL and siAChE and the quantification results of TARP+ multinuclear cells per area (2.512mm^2). Scale bar, 100 μm. (D) Relative mRNA expression of *AChE* and osteoclastic markers (*TRAP*, *CtsK*, *MMP9* and *RANK*) under the treatments of (C) (n=6). All data are expressed as means ± SEM. All data are expressed as means ± SEM. One-way ANOVA with Post-hoc tests were performed following statistically significant results. * $p<0.05$; ** $p<0.005$; *** $p<0.001$.

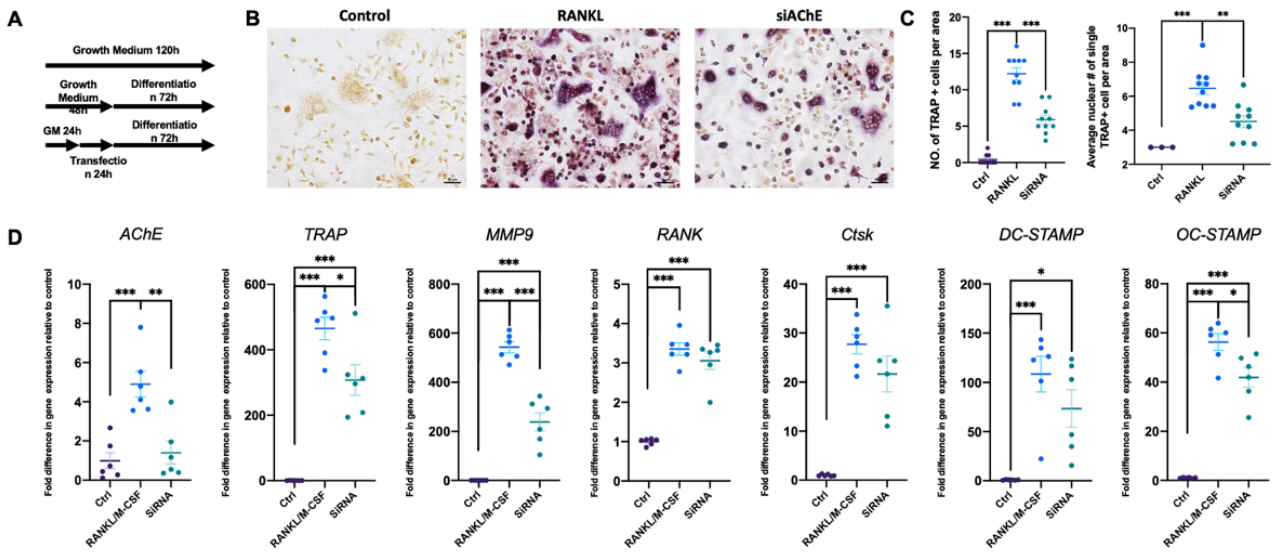

Fig 3.9 Silencing of AChE gene via siRNA suppressed osteoclastogenesis in primary culture OCs.(A) Experiment design. (B) Representative images of TRAP staining when cells were treated with 15ng/ml RANKL and siAChE; the quantification results of number of TARP+ multinuclear cells per area (2.512mm^2) and average nuclear numbers of single cell (n=10). Scale bar, 50 μm. (D) Relative mRNA expression of *AChE*, osteoclastic markers (*TRAP*, *CtsK*, *MMP9* and *RANK*) and cell-cell fusion markers (*DC-STAMP* and *PC-STAMP*) under the treatments of (C) (n=6). All data are expressed as means ± SEM. One-way ANOVA with Post-hoc tests were performed following statistically significant results. * $p<0.05$; ** $p<0.005$; *** $p<0.001$.

Dual-binding AChE inhibitor Donepezil suppressed osteoclastogenesis and cell-cell fusion, but Galantamine had no effect on osteoclastogenesis *in vitro*

To identify the non-enzymatic function of AChE, AChE inhibitors with different binding affinities were used to treat RAW 264.7 cells during osteoclastogenesis. Donepezil and galantamine are anti-dementia treatments that limit the AChE activity in the brain. Donepezil was reported to bind both the peripheral and catalytic site of AChE, whereas galantamine only binds the catalytic site as it is too short to bind the peripheral site (Fig3.10B). The RAW 264.7 cells were treated with the AChE inhibitors by adding them to the differentiation medium at a concentration of 1μM for 4 days to evaluate their effects on osteoclastogenesis. After treatment, a large reduction in multinuclear TRAP+ cells were detected in the donepezil treatment group (Fig 3.8C), whereas no difference was observed in the Galantamine group. Subsequently, Donepezil was administered for 2 days to RAW 264.7 cells 2-days before RANKL induction (pre-treatment) or 2-days after the 3-days RANKL induction (post-treatment). We found that both the donepezil pre- and post- treatment groups showed fewer multinuclear cells. The fluorescent intensity of the AChE signal (red) was not decreased in the donepezil pre- and post- treatment group, however, the microstructure of the cytoskeleton (F-actin, green) changed compared to the RANKL induced group.

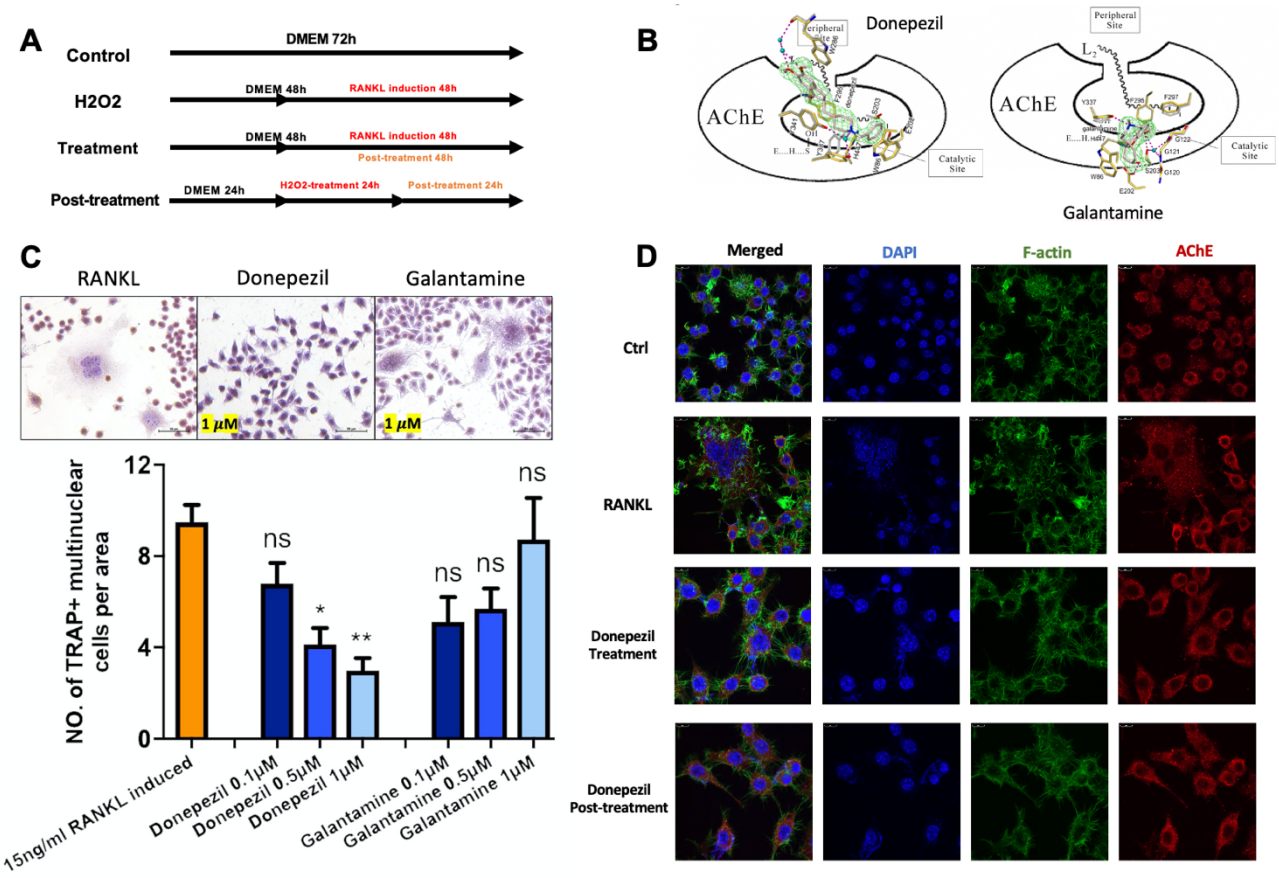

Fig 3.10 Dual-binding AChE inhibitor Donepezil suppressed osteoclastogenesis and cell-cell fusion, but Galantamine had no effect on osteoclastogenesis *in vitro*.(A) Experiment design. (B) the schematic diagram showing the binding affinities of donepezil and galantamine to AChE. Representative images of TRAP staining when cells were treated with 15ng/ml RANKL, 1μM of donepezil and galantamine, respectively; the quantification results of number of TARP+ multinuclear cells per area (2.512mm^2) under different concentration of donepezil and galantamine (n=10). Scale bar, 50 μm. (D) Representative immunofluorescence staining images of AChE (red), F-actin (green) under treatment or post-treatment of 1μM donepezil with osteoclastogenesis induction. Scale bar, 25 μm. Cells were counter-stained with DAPI (blue). Cells were pre-treated with blockers for 30 minutes before H_2O_2 stimulation. All data are expressed as means ± SEM. One-way ANOVA with Post-hoc tests were performed following statistically significant results. * $p<0.05$; ** $p<0.005$; *** $p<0.001$.

3.5 Discussion

In this chapter, by using microfluidic technics and live cell imaging, we confirmed that H2O2 induced senescence of osteoblastic cells expressed a higher level of AChE, which triggered the migration of osteoclast precursors. We also reported that the coating of Both AChE and HAChE promoted the adhesion of osteoclast precursors with increased expression of adhesion-associated integrins. Moreover, our results indicated that both AChE and HAChE treatments accelerated the process of osteoclast precursors fusion. Reversely, we found that genetic silence of AChE led to a lower differentiation ratio of osteoclasts, donepezil but not galantamine could inhibit the osteoclastic differentiation. These results suggested that the non-enzymatic function and peripheral anionic site of AChE got involved in the regulation of osteoclasts.

Our results first illustrated that both AChE and HAChE proteins promoted the adhesion and migration of osteoclast precursors, however, the underlying mechanism was not clear. Our data only suggested the association between mRNA levels of integrin subunits and AChE protein. To further investigate how AChE protein, especially its non-enzymatic peripheral site, affects the adhesion of osteoclasts, we may explore the mechanical interaction between integrins and AChE/HAChE proteins directly. The atomic force microscope (AFM), a super-high resolution scanning probe microscope probing the samples by sensing micro- to nanoscales of mechanical interactions, is widely used in studying cell mechanics such as cell adhesion[217-221]. In the future study, the AFM technology could be used to analyze the cell adhesive interactions between osteoclasts precursors and AChE proteins.

In our study, it was demonstrated that the AChE expression level increased during osteoclastogenesis in both RAW 264.7 cell and primary culture osteoclasts. This result is consistent with a prior study of the osteoclastogenetic process of bone marrow-derived macrophages [124]. In their study, they indicated that RANKL treatment upregulated AChE expression in both mRNA and protein levels. To further investigate if AChE is essential for the regulation of osteoclast differentiation, the AChE gene expression in osteoclast precursor cells was knocked down by siRNA. A lower expression of AChE hindered the following differentiation of osteoclasts. This is supported by an *in vivo* study using AChE knock-out mice [212], in which a strikingly decrease in the number of osteoclasts per perimeter was detected in the lumbar vertebra. The researchers attributed this phenotype to acetylcholine accumulation resulted from the inhibition of AChE catalytic function. It can be suspected based on these data that AChE plays an important role in osteoclast differentiation, no matter by its enzymatic function or non-enzymatic function.

To determine whether AChE regulates osteoclastogenesis by enzymatic or non-enzymatic effect, both recombinant AChE protein and heat-inactivated AChE were added to the osteoclast precursors culture system. Our results demonstrated that both AChE and heat-inactivated AChE promoted osteoclastogenesis. In contrast, the Sato et al study claimed that heat-inactivated AChE did not promote RANKL-induced osteoclast differentiation. However, their results showed a promotive trend of heat-inactivated AChE in osteoclastogenesis although no significant differences could be observed. The precursor cells of osteoclasts are monocytes or macrophages, given that a previous study indicated that

AChE could activate a "respiratory burst" in macrophages, moreover, heat inactivation of enzymatic activity or application of BW284C51 at a concentration that totally blocks the catalytic activity of AChE did not eliminate the effect [213], we conclude that non-enzymatic function of AChE played an role in osteoclastogenesis.

Our results demonstrated that pharmaceutical inhibition of AChE by donepezil also hindered the process of osteoclastogenesis. This is a noticeable difference from prior studies [215] in pharmaceutical inhibition, which claimed that AChE inhibitors had no direct effect on the survival and differentiation of osteoclast progenitors *in vitro*. It is important to point out that the inhibition drugs used were galantamine and pyridostigmine. Based on the molecular structure of AChE, there are two active sites presented in AChE: the catalytic site and a peripheral anionic site. Galantamine is a single binding AChE inhibitor that only binds to the catalytic site of AChE due to its short length[140, 142]. Our results also suggested that galantamine did not affect osteoclastogenesis by both TRAP stain and qPCR analysis. However, our data indicated that the dual binding AChE inhibitor, donepezil [222], did have significant inhibition effects on the differentiation of osteoclasts *in vitro*. The binding affinity of pyridostigmine to the AChE peripheral binding site has not been clearly investigated. Therefore, further determination of this binding should be performed to completely explain the difference in results. The osteoclastogenic inhibition effect of donepezil was also confirmed in an OVX mice model.

Combined together, these result points to the involvement of the non-enzymatic function of AChE in osteoclastogenesis. It was shown here that the AChE proteins can act as a bridge, binding to specific proteins on the cell membrane or extracellular matrix. This was proven by the up-regulation at mRNA level of cell-cell fusion markers DC-STAMP and OC-STAMP after stimulation with both AChE and heat-inactivated AChE. The adhesion function of AChE was previously reported in osteoblasts [122, 123] and neurite growth[169, 170]. The specific molecular pathway of how AChE promotes cell-cell fusion still needs to be explored.

This chapter showed that (1) heat-inactivated AChE can promote osteoclastogenesis, (2) dual-binding AChE inhibitor Donepezil suppresses osteoclastogenesis and cell-cell fusion, and (3) the catalytic inhibitor Galantamine had no effect on osteoclastogenesis. Our findings confirm the non-enzymatic function of AChE in regulating osteoclasts via cell-cell fusion. Therefore, it warrants further investigation into the PAS site of AChE in the pathogenesis and management of osteoporosis.

In the bone system, osteoblasts and osteoclasts couple together and cooperate in harmony to maintain bone homeostasis[66]. As mentioned before, in osteoblast lineage, AChE was identified as a bone matrix protein to promote osteoblast-ECM adhesion[122, 123]. Studies showed that AChE was dominated expressed by osteoblasts[122, 159], our data in chapter 2 showed that AChE expression in osteoblasts strikingly increased after senescent induction. When we added exogenous AChE to RAW 264.7 cells during osteoclastogenesis, their

differentiation process was accelerated, and the increased expression of AChE by osteoblasts due to aging might be the possible cause of age-related osteoporosis. The specific interaction between osteoblasts and osteoclasts needs to be further explored.

In summary, it was demonstrated that during osteoclastogenesis, AChE expression showed a similar tendency to the osteoclast's differentiation markers on both mRNA and protein levels *in vitro*. Moreover, genetic inhibition of AChE suppressed osteoclastogenesis *in vitro* while AChE and non-enzymatic aspects of AChE could promote this process. Dual-binding AChE inhibitor donepezil hindered osteoclastogenesis while single catalytic-binding inhibitor Galantamine have no effect on it. All this evidence supports that AChE plays a vital role in osteoclastogenesis and that this role is at least partly mediated via its non-enzymatic function.

Chapter 4 Acetylcholinesterase expression increased in age-related and postmenopausal osteoporosis, peripheral acting AChE inhibitor rescues bone loss in mouse OVX animal models

4.1 Introduction

Alzheimer's disease, aging and osteoporosis

Osteoporosis is a common bone disorder in which bone mass is reduced and bone microarchitecture changes, which makes bone fragile and is associated with an increased risk of fractures. The risk of osteoporotic fracture is exponentially correlated with the increase in age[223]. Research focusing on the mechanical properties of bone indicated that the fracture toughness of cortical bone decreased 7-12% every 10 years during aging[224]. For the organic matrix of bone, studies[225, 226] showed that the denaturation degree and nonenzymatic glycation of the collagen network were highly correlated with age. And the bone minerals were believed to form larger and denser crystals in the bone matrix with increasing age, which was associated with reduced fracture toughness[227, 228]. All this evidence points to the close relationship between osteoporosis and aging from a macro perspective.

Alzheimer's disease (AD) is the most common form of the chronic neurodegenerative disease characterized by plaques and tangles in the brain as well as cognitive function declining, which contributes to 60% - 70% of cases of dementia worldwide. According to World Health Organization, the global population of people with dementia in 2010 is

estimated at 35.6 million and this number will double in 20 years[229]. Dementia, or more specifically, Alzheimer's disease is highly associated with aging, 3% - 6% of people aged 60 and over worldwide are estimated affected by Alzheimer's disease[229]. Its negative consequences strikingly impact the health, life quality, and independence of old people and it's also devastating the caregivers.

The co-occurrence of osteoporosis and Alzheimer's disease was documented a lot previously. It was reported that osteoporosis patients had a 2-fold increased risk of Alzheimer's disease conversion compared with the controls in both men and sexes in the Chinese cohort [230]. A community-based prospective cohort study was performed on 987 subjects, finding that subjects with low bone mineral density were related to a higher incidence of AD and all-cause dementia in women but not in men[231]. Consistently, Alzheimer's disease also increases the risk of bone loss. Investigation results indicated that older Australians (≥60 years) with dementia had a 6.3-fold (95% CI 5.1–7.1) risk of hip fracture[232].

Central cholinergic activity and acetylcholinesterase during aging process

The cholinergic activity in the brain system is closely related to Alzheimer's disease development and aging[233-235]. The activity of choline acetyltransferase, the enzyme catalyzing the synthesis of ACh, is significantly reduced in the brain of Alzheimer's disease patients [236, 237]. Moreover, the decrease in ChAT was correlated with the severity of dementia[238]. In a rat animal model, it was reported that acetylcholine release in the

cortical brain increased first after birth and reached the peak in the 30-day-old rats, this evoked release of ACh declined during the later brain development. The level of ACh was reduced to the same level of newborn rats in 24-month-old aged rats[239]. For the activity of AChE in the brain, it was demonstrated that the AChE activity in the brain was decreased in aged rats[240]. While in the human brain, the AChE activity was reported to remain unchanged[241, 242]. Therefore, as the synthesis of ACh declined, however, the AChE activity remains unchanged, and the relative cholinergic activity significantly reduced during aging.

Postmenopausal osteoporosis and acetylcholinesterase

Osteoporosis occurs more in elderly women than in men [75], especially the postmenopausal women. The bone loss of postmenopausal osteoporosis involves two stages: The first is the initial stage lasting for 3-5 years with rapid bone loss in trabecular bone, this stage is menopause related. The followed stage is a slower age-related bone loss lasting for 10-20 years affecting both trabecular bone and cortical bone[243]. The reduced ovarian production of estrogen led to a higher expression of IL-1(interleukin-6), IL-6 (interleukin-6), TNF-α, M-CSF, and GM-CSF by monocytes in the bone microenvironment. These cytokines, on the one hand, promoted the osteoclastogenesis of monocytes, on the other hand, they also triggered pre-osteoblasts to secret more IL-6, and finally contributed to the imbalance between bone resorption and bone formation[244].

Estrogen-cholinergic interaction has been widely studied in cognitive decline with aging[245]. As reported, brain AChE increased after ovariectomy[246], and donepezil could improve memory performance in ovariectomized rats[247]. The anabolic effect of donepezil has been reported in an ovine ovariectomy-induced osteoporosis model[248].

Ovariectomy models (OVX) of Osteoporosis

The initial reason for postmenopausal osteoporosis is the deficiency of estrogen. To establish an animal model to mimic this pathologic progress, ovariectomy is performed on rodents. Although there is no menopause in rodents, it is clear that the sex hormone estrogen decreases with increased age-related bone loss, deficiency of estrogen could accelerate the bone loss process in rodents[249]. The ovariectomy refers to removing ovaries surgically, ovariectomized rodents share many similar features to postmenopausal humans: The OVX rodents also show a rapid short bone loss phase followed by a longer phase with slower bone mass reduction; the bone loss is also much stronger in trabecular bone compared to that in cortical bone; the OVX model indicates a similar physiological response to current osteoporosis treatments such as estrogen, bisphosphates and parathyroid hormone[250].

4.2 Rationale

Osteoporosis and associated fragility fractures are actually not simply a problem of bone, but also involve a complex neuromusculoskeletal multisystem dysfunction. It is not uncommon that osteoporosis is closely associated with a plethora of other age-related disorders such as

Alzheimer's disease[251, 252]. However, current osteoporosis treatment is limited to balancing bone resorption with the formation in one single system. Although several FDA-approved drugs are available, osteoporotic fractures remain an unresolved problem[86].

Both Alzheimer's disease and osteoporosis are the most prevalent chronic disorders, they affect enormous older people worldwide and give huge societal burdens. Many researchers noticed the co-occurrence of Alzheimer's disease and osteoporosis as well as their sharing risk factors like aging, hypertension, alcohol, and smoking[253]. Interestingly, recent clinical reports showed that the use of donepezil, has been associated with decreased risk of hip fracture, enhanced osteoporotic fracture healing, and reduced overall mortality in older adults[254-258]. This observation has been recapitulated in a RANKL-induced bone loss rodent model, in which donepezil not only can mitigate RANKL-induced osteoclastogenesis and subsequent bone loss but also favor bone mass accrual[124]. These findings suggested a possible role of AChE in age-related bone disorders. As documented in Chapter 1, AChE got involved in the regulation of bone development. Yet bone AChE remains poorly understood in bone degeneration, both age-related and postmenopausal.

In chapter 2, we demonstrated that AChE accumulated during the aging process in the mice model. In this chapter, we aim to investigate the AChE expression pattern in OVX-induced bone loss mice model *in vivo*. After that, we will discuss the bone loss rescue effects by pharmaceutical inhibition of AChE with both the treatments of BBB-permeable AChE inhibitor donepezil and BBB-impermeable inhibitor ambenonium.

4.3 Materials and methods

Reagents

Donepezil HCl (Aladdin, Shanghai, China, #120011-70-3); Ambenonium dichloride (Toronto Research Chemicals, North York, Canada, #A575875); Harris Hematoxylin solution, Eosin Y (yellowish), leukocyte acid phosphatase kit (Sigma-Aldrich, Massachusetts, United States, #HHS32 & #1159350100 & #387A); Anti-Acetylcholinesterase antibody [HR2], Anti-Acetylcholinesterase antibody, Anti-CDKN2A/p16INK4a antibody - N-terminal (Abcam, Cambridge, UK, #ab2803 & #ab97299 & #ab189034).

Animals grouping

For OVX-induced animal model, a total of 30 3-month-old female balb/C mice were obtained from PolyU CAF under a license (20-69) in DH/HT&A/8/2/4/ Pt.2 issued by the Department of Health, Hong Kong. The mice were randomly divided into 5 groups (n=6 for each group). They were kept on a normal laboratory diet in an environmentally controlled clean room. Four groups of mice received OVX surgery and on the last group of mice a SHAM operation (only performed skin and muscle incisions) was performed at week 0. Four weeks post-surgery, one OVX group and the SHAM group received placebo treatment (Saline), the other three OVX group received a low dose donepezil treatment (0.2mg/kg bodyweight per day) or a high dose donepezil treatment (2mg/kg bodyweight per day) or

ambenonium treatment (0.2mg/kg bodyweight per day) respectively for another 4 weeks. All treatments were administered I.P. and on mice of all groups micro-CT analysis was conducted at Week 0, Week 4, and Week 8. The experimental design was shown in Fig 2.1 below.

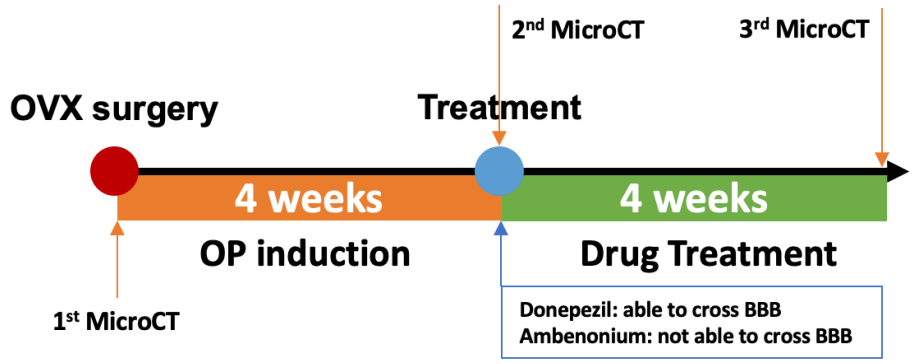

Fig 4.1 Schematic diagram of animal experiment. Before OVX surgery, all mice received the first microCT scanning to collect their bone mass baseline; After 4-weeks induction, the second microCT scanning was performed to confirm the OP model establishment; The third microCT scanning was conducted after 4 weeks of AChEIs treatment to evaluate their bone loss rescue effects.

Osteoporotic model establishment via OVX surgery

Mice were performed OVX surgery to establish osteoporosis[249]. Basically, all mice were anaesthetized by intraperitoneal injection of an anesthetic cocktail [ketamine (100mg/mL): Xylazine (20mg/ml): saline = 1:0.5:8.5]. The fur on the lower back of the mouse was gently removed, and the exposed skin was disinfected with iodine solution. the mice were placed back up, and a 1 cm skin incision as made on the dorsolateral surfaces of both sides to expose the dorsolateral abdominal muscles. The underlying muscles on both sides were cut to expose the ovaries with fat pad. The ovaries and associated ovarian fat pad were identified, separated, and ligated from the oviduct and part of the uterus. Sterile scissors were

used to remove the ovaries, the rest tissues were returned to the abdomen. The subcutaneous muscle layer and the skin were closed with suture. Normal food and drink supply was provided after surgery. The osteoporotic model establishment was last for 4 weeks and checked with microCT scanning.

In vivo intraperitoneal injection

After 4 weeks osteoporotic model establishment, Donepezil HCl (0.2mg/kg or 2mg/kg) or Ambenonium Dichloride (0.2 mg/kg), was injected intraperitoneally on a daily basis for another 4 weeks. Same amount of vehicle (Saline) was administered to control groups. The bodyweight of all mice was recorded every day to monitor their health conditions. Mice were sacrificed after 8 weeks of surgery, with bones of their lower limbs and other organs harvested for histological analysis.

Micro-computed tomography and analysis

Longitudinal monitoring of bone mass and microarchitecture was conducted in femurs of mice by a micro-CT system (Viva CT40, Scanco, Switzerland) at time zero, 1- and 2- month post-surgery. The resolution of images was 18 μm for femur. Isotropic voxel size for the scans was 10.5μm. X-ray voltage of 70kV and 1.0 filter were applied. After standardized reconstruction by a modified Feldkamp algorithm via SkyScan recon software, the data sets for each group were analyzed using SkyScan CT-analyzer software. The trabecular bone region undergrowth plate of the femur was chosen for micro-architectural analysis of trabecular thickness (Tb.Th), trabecular number (Tb.N) and trabecular spacing (Tb.Sp), bone

volume fraction (BV/TV). 301 slices covering the target region were used for analysis.

H&E staining

Femur tissues were dissected from mice and fixed immediately in 4% PFA solution overnight, then decalcified in 10% EDTA for 2 weeks. After decalcification, the samples were dehydrated in an alcohol gradient ranging from 70% to 100% and were embedded in paraffin following the standard protocols. Samples will be cut into 5um sections using the microtome. Slides were deparaffinized and rehydrated for routine H&E staining. Generally, the slides were stained with Harris hematoxylin for 3 mins, then differentiated with acid alcohol, and rinsed with Scott's tap water. The samples were stained with eosin for 2 mins and dehydrated and mounted. Images of slides were captured with the Olympus BX51W1 microscope.

Tartrate resistance acid phosphatase (TRAP) staining

Spine tissues were dissected from mice and fixed immediately in 4% PFA solution overnight, then decalcified in 10% EDTA for 2 weeks. After decalcification, the samples were dehydrated in an alcohol gradient ranging from 70% to 100% and were embedded in paraffin following the standard protocols. Samples will be cut into 5um sections using the microtome. Slides were deparaffinized and rehydrated and stained with the leukocyte acid phosphatase kit according to the protocol of the manufacturer. Briefly, deionized fast garnet GBC solution, naphthol AS-BI phosphate solution, acetate solution, tartrate solution and deionized warm water were mixed in a certain ratio at 37 °C, slides were stained with the

mixed solution for 1h at 37 °C in dark environment. After staining the slides were rinsed with deionized water 3 times. Nuclear in sections were stained with hematoxylin. Samples were dehydrated and mounted. Images of slides were captured with the Olympus BX51W1 microscope. TRAP positive multinucleated cells were counted with image J software.

Immunohistochemistry

Immunohistochemical staining was performed on tissue sections. Antigen retrieval was performed according to the manufacturer's instructions. Endogenous peroxidase activity was quenched using 3% (v/v) hydrogen peroxide in PBS for 10 minutes. Sections were blocked with 10% (v/v) normal horse serum for 1 hour. The sections were incubated with primary antibodies at 4°C overnight. Primary antibodies used: AChE (reacted with mouse samples) (1:1000; Abcam, ab2803), AChE (reacted with rat samples) (1:1000; Abcam, ab97299), CDKN2A/p16INK4a (1:200; Abcam, ab189034). For DAB staining, Vectastain ABC kit and DAB substrate kit for peroxidase (Vector Labs, USA) were used to stain targeted antigens followed by counterstaining using Harris Hematoxylin. The negative immune controls underwent the same procedure without adding primary antibody. All images were taken using a Olympus BX51W1 microscope.

Statistical analysis

All statistical results were presented as mean $\pm$ standard error of the mean (SEM). The comparison between multiple groups was quantitatively analyzed using one-way ANOVA. Post-hoc tests were performed following statistically significant results. A significant

difference was indicated when $P<0.05$.

4.4 Results

AChE expression and number of OCs increased after OVX osteoporotic induction and decreased with peripheral acting AChE inhibitor treatments *in vivo*

A previous study demonstrated a reduction in bone loss after treatment with donepezil using a RANKL-induced osteoporotic mouse model [124]. This model is not considered a well-established animal model to investigate the bone loss. Therefore, the well-established OVX mouse model was used here to investigate the effects of AChE on bone degeneration *in vivo*. Bone loss was confirmed by three-dimensional micro-computed tomography (μCT) analyses (Fig 4.2) after OVX induction. The increases in OC number and AChE expression were also identified in the mice OVX model (Fig 4.4). For the bone loss rescue effects of AChE inhibitors, both the BBB (blood-brain barrier)-impermeable AChE inhibitor ambenonium and BBB-permeable inhibitor donepezil were used to treat the OVX mice. As shown in Fig 4.3, there was no obvious bodyweight difference before or after both donepezil and ambenonium treatment, indicating that the two drugs were safe for animals. A significant increasing trend of BV/TV was observed in both the low and high-dose donepezil treatment groups as well as the ambenonium treatment group (Fig 4.2C). The rescue effect of ambenonium was comparable to that of donepezil under the same concentration. Meanwhile, after quantification, significant reductions in osteoclast number were observed in both low and high-dose donepezil treatment group and ambenonium via bone section TRAP staining (Fig 4.4). These results suggested the osteoprotective effect of AChE inhibitor via peripheral

acting manner.

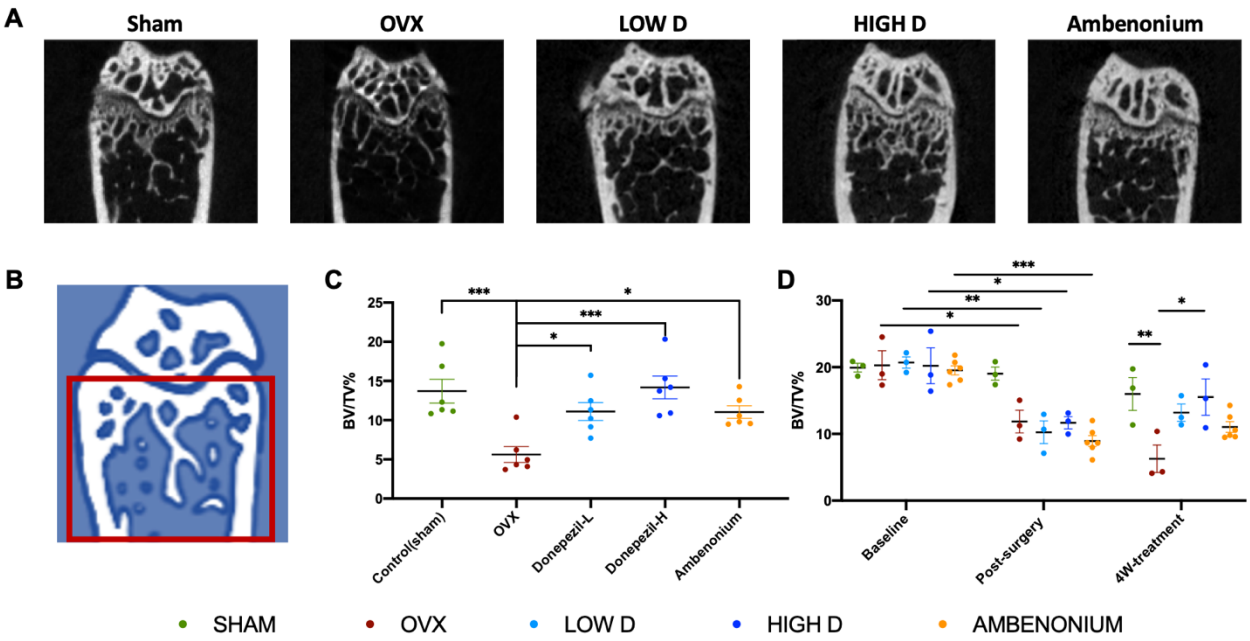

Fig 4.2 Both BBB permeable AChEI donepezil and BBB impermeable AChEI ambenonium were able to rescue OVX-induced osteoporosis in mice. (A) Representative microCT images of the femur from Control (Sham) group (n=6), OVX osteoporotic group (n=6), low dose donepezil treatment (0.2mg/kg bodyweight per day) group (n=6), high dose donepezil treatment (2mg/kg bodyweight per day) group (n=6), and ambenonium treatment (0.2mg/kg bodyweight per day) group (n=6) of Balb/c mice. (B) Schematic diagram of the region of interest where the microCT data was analyzed (red box). (C) End-point quantification results of BV/TV% of different groups. (D) Longitudinal quantification results of BV/TV% of different groups. All data are expressed as means ± SEM, and each data point represents an individual mouse. One-way ANOVA with Tukey's multiple-comparisons test was used for statistical analysis. * $p<0.05$; ** $p<0.005$; *** $p<0.001$.

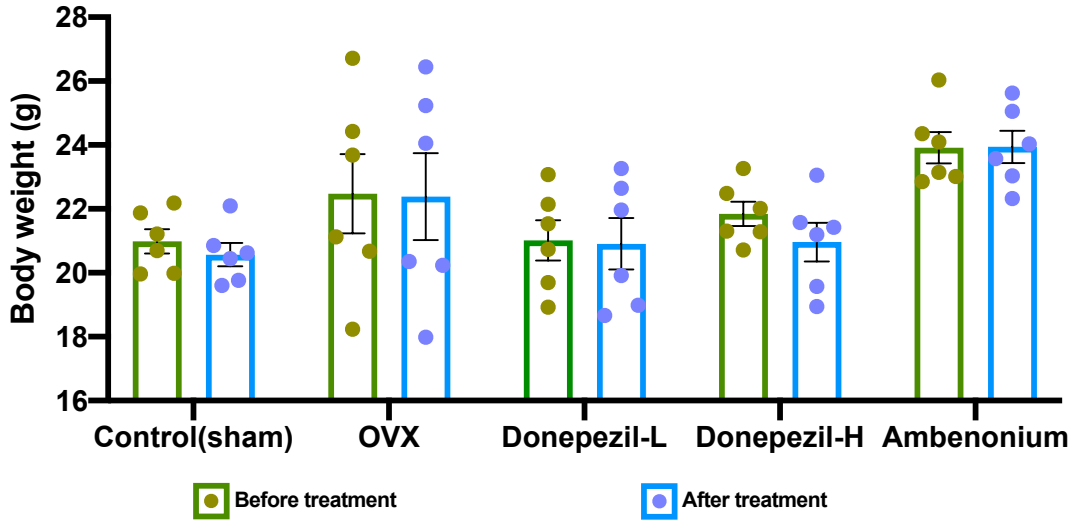

Fig 4.3 The body weight of mice before and after drug treatment did not change. Body weight data of all mice before and after 4-weeks treatment from Control (Sham) group (n=6), OVX osteoporotic group (n=6), low dose donepezil treatment (0.2mg/kg bodyweight per day) group (n=6), high dose donepezil treatment (2mg/kg bodyweight per day) group (n=6), and ambenonium treatment (0.2mg/kg bodyweight per day) group (n=6) of Balb/c mice. All data are expressed as means ± SEM, and each data point represents an individual mouse.

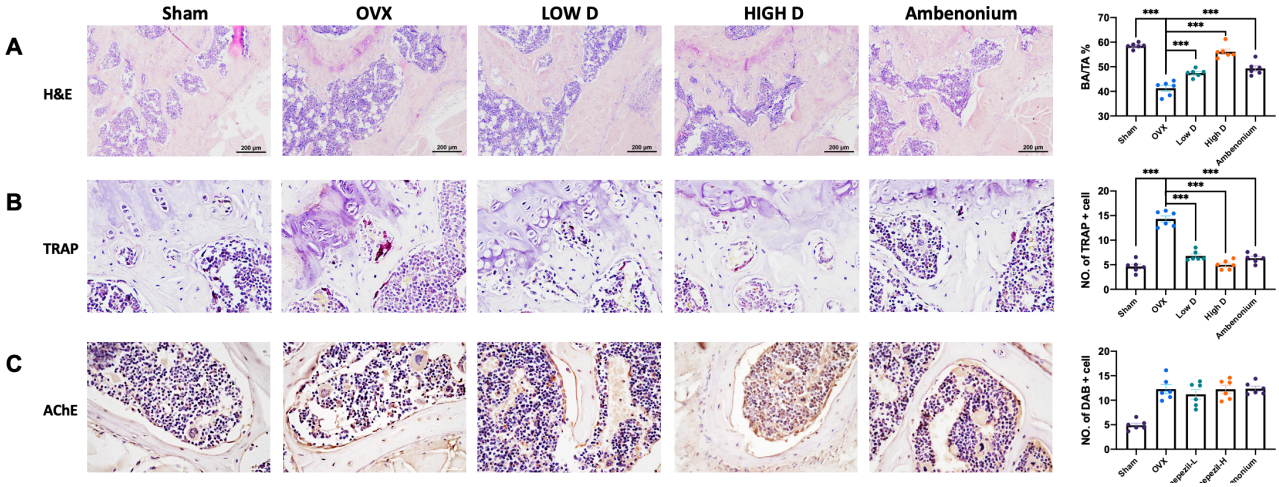

Fig 4.4 AChE expression and number of OCs increased after OVX osteoporotic induction and decreased with AChE inhibitors treatments *in vivo*. (A, B) Representative images of H&E staining, TRAP staining, and DAB staining for AChE(C) and (D) $p16^{INK4a}$ (brown) from Control (Sham) group (n=6), OVX osteoporotic group (n=6), low dose donepezil treatment (0.2mg/kg bodyweight per day) group (n=6), high dose donepezil treatment (2mg/kg bodyweight per day) group (n=6), and ambenonium treatment (0.2mg/kg bodyweight per day) group (n=6) of balb/c mice. Scale bar, 50 μm.

4.5 Discussion

AChE, the enzyme catalyzing the hydrolysis of acetylcholine, was associated with osteoporosis development. In chapter 2, we demonstrated that the expression of AChE in bone increased in aged osteoporotic mice, along with the increased number of osteoclasts in the femur. In this chapter, we observed the same phenomenon in the OVX bone loss model, after OVX surgery, both the number of osteoclasts and the AChE expression level in mice femur increased. Thirdly, we find that the peripheral acting AChE inhibitor ambenonium could rescue the OVX induced bone loss, which has a comparable protective effect to central acting inhibitor donepezil.

Previously, the expression pattern of AChE in the brain was well established [240-242]. For its expression in bone tissue, four studies identified AChE in embryo limbs[115], calvarias and femurs[125], maxilla[116] and ulnae[122]. All these studies pointed out that AChE expression increased during early embryo bone growth and then decreased during later embryo development and continuously declined during postnatal bone growth. This study was the first time to examine the expression of AChE in both age-related and postmenopausal bone degeneration.

For the osteoprotective effect of the AChE inhibitor, we used two AChEIs, donepezil and ambenonium. The binding ability to the AChE protein of these two inhibitors is similar[136, 153, 154]. The donepezil itself could cross the BBB barrier, whereas ambenonium was

BBB-impermeable. Our results indicated that donepezil treatment could inhibit bone loss *in vivo*. This is consistent with a previous study by Sato et al[124]. However, the RANKL-induced bone loss model used in that study was not a classical animal model to investigate osteoporosis. We confirmed this beneficial effect of donepezil in an OVX animal model. Furthermore, our data proved that under the same concentration, treatment of ambenonium reflected a comparable rescue effect to donepezil, suggesting the peripheral regulation effect of AChE in bone degeneration. However, a recent study claimed that the central acting AChE inhibitor galantamine did not alter the bone mass quantity in aged mice. We noticed that the galantamine only binds to the catalytic site of the AChE protein. We further investigated these controversial results in Chapter 2 and Chapter 3, our results showed that galantamine neither rescued osteoblastic senescence nor inhibited osteoclast differentiation. Pharmaceutical inhibition of AChE could attenuate bone loss in the mice model, indicating the potential therapeutic direction of osteoporosis.

As documented and illustrated in Fig 4.5, in the bone system, the AChE expression firstly elevated to promote osteogenesis in the early embryo development period, and later decreases and maintains a relatively low level for a long time after postnatal development. Here, we find that the expression of AChE increases after menopause or with aging. The increase of AChE level in bone leads to the process of bone degeneration and disorder.

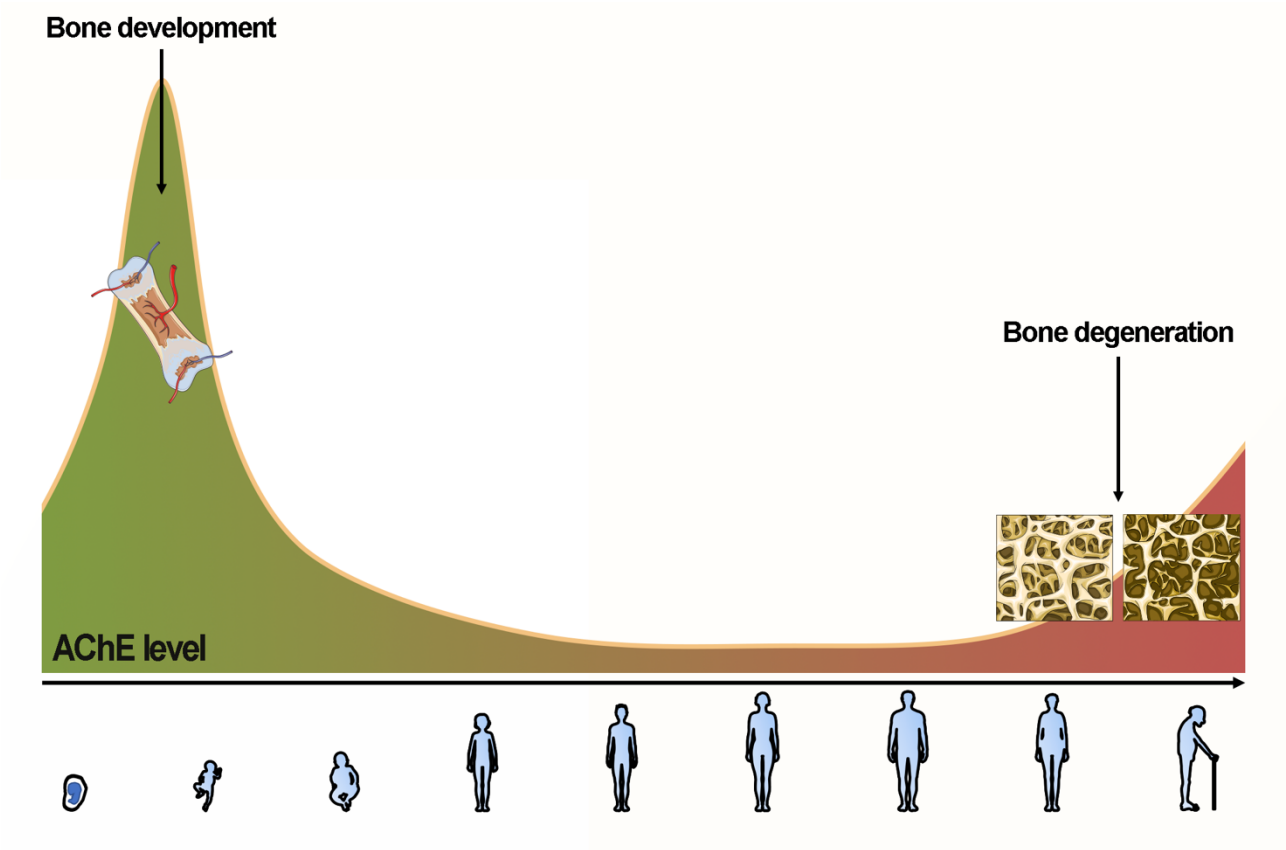

Fig 4.5 AChE expression during bone development and degeneration. In bone system, the AChE expression firstly elevated to promote osteogenesis in the early embryo development period, and later decreases and maintain a relative low level for a long time after postnatal development. Here, we find that the expression of AChE increases after menopause or with ageing. The increase of AChE level in bone leads to the process of bone degeneration and disorder.

Chapter 5 Conclusion and Future Perspectives

5.1 Conclusion

So, in this study, we explored the role of AChE on bone degeneration from three levels. At the tissue level, by using two inhibitors. We proved that peripheral acting inhibition of AChE could also rescue bone loss. At the cell level, by cell culture and microfluidic technics, we identified the non-neuronal role of AChE in both osteoblastic lineage and osteoclastic lineage. At the protein level, we used the dual binding or single binding AChE inhibitor as well as heat-inactivated AChE to confirm the effect of the ACHE peripheral anionic site.

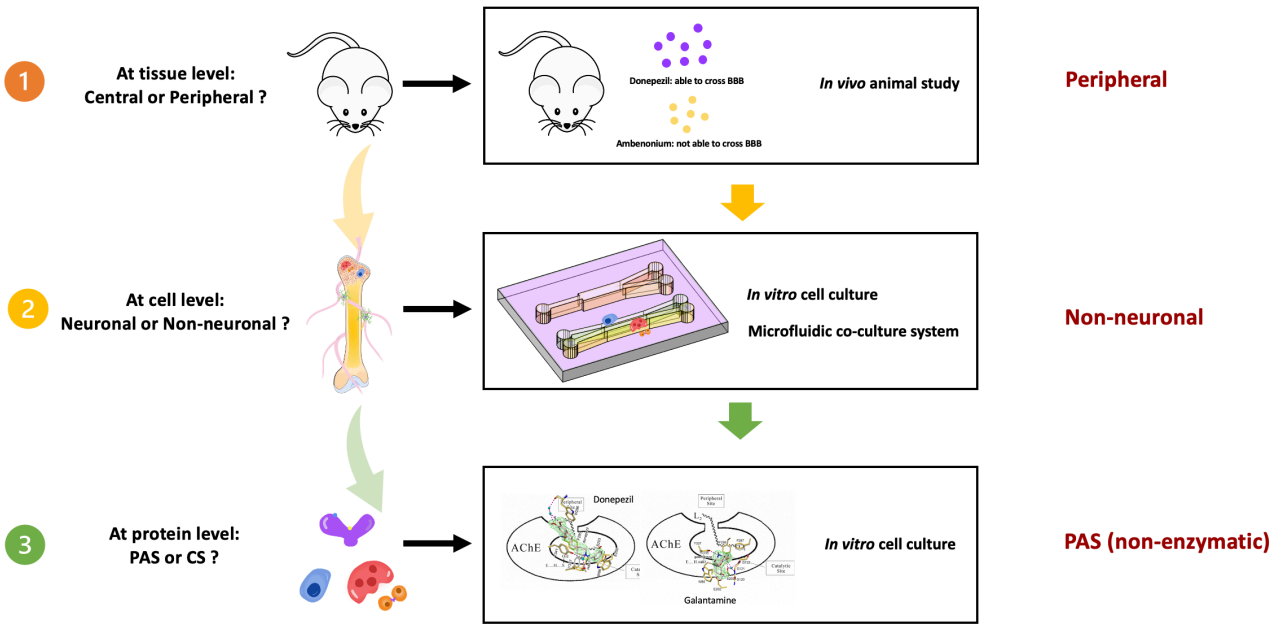

Fig 5.1 Overall framework of this research.we explored the role of AChE on bone degeneration from three levels. At the tissue level, by using two inhibitors. We proved that peripheral acting inhibition of AChE could also rescue bone loss. At the cell level, by cell culture and microfluidic technics, we identified the non-neuronal role of AChE in both osteoblastic lineage and osteoclastic lineage. At the protein level, we used the dual binding or single binding AChE inhibitor as well as heat-inactivated AChE to confirm the effect of the ACHE peripheral anionic site.

As mentioned in the introduction part of Chapter 4, cholinergic activity decreases and AChE level remains unchanged[259] with aging in brain tissue[260]. For the AChE level in the bone system, as documented in Chapter 1, AChE played an important role in regulating bone development. Briefly, the AChE level increased during chondrocyte remodeling and apoptosis in the early embryo bone development to favor osteoblast differentiation in endochondral ossification. Its expression level dramatically decreases in the later embryo development phase to support bone mineralization. AChE expression continues to reduce until the skeleton mature and maintains at a lower but stable level. In our study, we first time demonstrated that the expression of AChE increased after menopause or with aging, which contributes to pathological remodeling and osteoporosis development.

In Chapter 2, we illustrated that AChE expression was elevated during oxidative stress-induced osteoblast senescence. Reversely, the addition of AChE protein also triggered the pre-senescence of osteoblasts. We claimed that the osteoblast cells could form an autocrine loop of AChE, therefore constantly accelerating the process of their cellular senescence (Fig 5.1 A). We also confirmed that treatment of AChE inhibitor donepezil could suppress the AChE deposition and cellular senescence in osteoblast.

In Chapter 3, we proved that AChE protein, both intact and heat-inactivated, could promote the adhesion, migration, and cell-cell fusion of osteoclast precursors, therefore contributing to stronger osteoclastogenesis. The promotive effect of heat-inactivated AChE in osteoclastic differentiation suggested the non-enzymatic regulative function of AChE in bone resorption.

Both pharmaceutical inhibition and genetic inhibition of AChE hindered the process of osteoclastogenesis. In particular, we found that only the dual-binding (binding to both catalytic site and peripheral anionic site) inhibitor donepezil could attenuate the osteoclastogenesis but not the single binding inhibitor galantamine (only binding to the catalytic site). As the peripheral anionic site of AChE was associated with the non-enzymatic function of AChE in many studies, these results further suggested that AChE regulates osteoclastogenesis in a non-enzymatic manner.

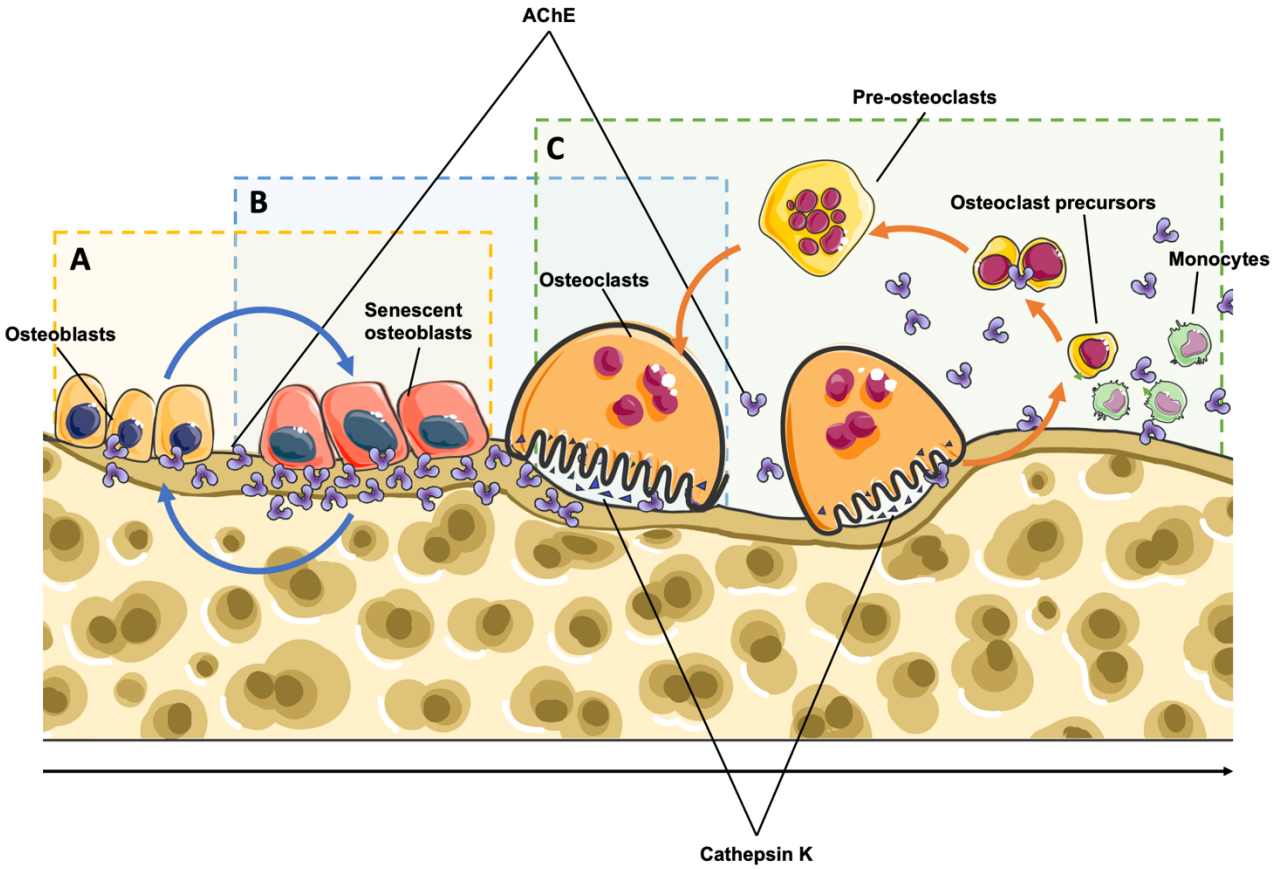

Fig 5.2 Proposed mechanisms of how AChE regulate osteoblasts, osteoclasts, and OB-OC crosstalk at cellular level. Osteoblast cells form an autocrine loop of AChE, therefore constantly accelerate the process of their cellular senescence. Evoked osteoclast resorption digested the bone matrix and released the osteoblast-deposited AChE to bone microenvironment. These released AChE promoted the fusion of osteoclast precursors, therefore resulted in stronger osteoclastogenesis.

5.2 Future Perspectives

Bone is an organ that is renewed constantly. It is critical for bone health that osteoblast-mediated bone formation and osteoclast-mediated bone resorption are coupled harmoniously. In case of an imbalance of bone formation or degradation, diseases occur associated with bone loss, i.e., osteoporosis, or excessive formation of new bone as is occurring in osteopetrosis. Osteoporosis is a degenerative disorder marked by low bone density and microarchitectural deterioration of bone tissue [261], which is caused by the uncoupling of bone formation and bone resorption, leading to huge medical and economic burdens to society [77, 262]. Although a primary understanding of this pathological process has been achieved, the underlying molecular mechanism remains unknown. Additionally, current prevention and treatment strategies (e.g., calcium and vitamin D supplement, bisphosphonates, parathyroid hormone) have limited effects, or unavoidable side effects [79, 82, 83, 85]. Therefore, new approaches to control or treat this disease need to be found.

As mentioned before, AChE regulates bone development and degeneration in both acetylcholine-dependent and acetylcholine-independent manners. In the bone development stage, the AChE expression firstly increased to promote osteogenesis in the early embryo development period, and later decreases and maintains a relatively low level for a long time after postnatal development. In the bone degeneration stage, osteoblast cells form an autocrine loop of AChE, therefore constantly accelerating the process of their cellular senescence. Evoked osteoclast resorption digested the bone matrix and released the osteoblast-deposited AChE to the bone microenvironment. This released AChE promoted the

fusion of osteoclast precursors, therefore resulting in stronger osteoclastogenesis. By targeting AChE, we may find a new approach to the treatment of the age-related bone disorder.

The pharmaceutical inhibition of AChE in both osteoblasts and osteoclasts indicates the emerging necessity of dual blockade of AChE (the non-enzymatic as well as the enzymatic functional sites) in order to achieve stronger anti-catabolic effects on bone. For dual blockade of AChE, the dimerization of available drugs can be an effective strategy as this is a good approach to developing novel multifunctional drugs [263-265]. Huperzine A is a potent AChE inhibitor originally isolated from the Chinese medicinal herb *Huperzia Serrata* [265]. Huperzine A has been approved as Alzheimer's therapy in China due to its specific anti-AChE activity. This component was reported to combine with itself to form bis(n)-hupyridone, or with previously FDA-approved anti-Alzheimer's drug tacrine to form hupyridone(n)-tacrine. Finally, the homodimer bis(n)-cognitin has been developed and synthesized as resulting of a computer model-based optimization strategy [266]. Pharmacokinetic studies demonstrate that these dimers could be well absorbed and readily cross the blood-brain barrier, suggesting that they might become applicable as drugs for both peripheral and central disorders [267], and could also represent emerging drug candidates for the treatment of osteoporosis.

For the non-enzymatic function of AChE in bone degeneration, we may pay our attention to the peripheral anionic site of AChE. The gene and protein sequence of the AChE PAS site

was clearly identified. Another area that needs investigation is the mechanism by which AChE affects the interactions of osteoblasts and osteoclasts[130]. Further mechanism analysis could focus the PAS site on both osteoblast and osteoclast. Moreover, although we know that AChE regulates proliferation and differentiation of both osteoblasts and osteoclasts, respectively, its effects on interactions of osteoblasts and osteoclasts leave relevant questions wide open.

References

1. Rodan, G.A., Introduction to bone biology, Bone, 1992. **13**: p. S3-S6.

2. Fukumoto, S. and T.J. Martin, Bone as an endocrine organ, Trends in Endocrinology and Metabolism, 2009. **20**(5): p. 230-236.

3. Karsenty, G. and E.N. Olson, Bone and muscle endocrine functions: Unexpected paradigms of inter-organ communication, Cell, 2016. **164**(6): p. 1248-1256.

4. Oury, F., L. Khrimian, C.A. Denny, A. Gardin, A. Chamouni, N. Goeden, et al., Maternal and offspring pools of osteocalcin influence brain development and functions, Cell, 2013. **155**(1): p. 228-241.

5. Rodan, G.A., Bone homeostasis, Proceedings of the National Academy of Sciences, 1998. **95**(23): p. 13361-13362.

6. Nijweide, P.J., E.H. Burger, and J. Feyen, Cells of bone: Proliferation, differentiation, and hormonal regulation, Physiological Reviews, 1986. **66**(4): p. 855-886.

7. Morgan, E.F. and L.C. Gerstenfeld, *The bone organ system: Form and function*, in *Marcus and feldman's osteoporosis*. 2021, Elsevier. p. 15-35.

8. Biga, L.M., S. Dawson, A. Harwell, R. Hopkins, J. Kaufmann, M. LeMaster, et al., Anatomy & physiology, 2020.

9. Martini, F., *Anatomy and physiology'2007 ed*. 2006: Rex Bookstore, Inc.

10. Fuchs, R.K., S.J. Warden, and C.H. Turner, *2 - bone anatomy, physiology and adaptation to mechanical loading*, in *Bone repair biomaterials*, J.A. Planell, S.M. Best, D. Lacroix, and A.

Merolli, Editors. 2009, Woodhead Publishing. p. 25-68.

11. Weiner, S. and W. Traub, Bone structure: From ångstroms to microns, The FASEB journal, 1992. **6**(3): p. 879-885.

12. Ramasamy, S.K., Structure and functions of blood vessels and vascular niches in bone, Stem Cells International, 2017. **2017**.

13. Prisby, R.D., Mechanical, hormonal and metabolic influences on blood vessels, blood flow and bone, Journal of Endocrinology, 2017. **235**(3): p. R77-R100.

14. Tomlinson, R.E. and M.J. Silva, Skeletal blood flow in bone repair and maintenance, Bone research, 2013. **1**(1): p. 311-322.

15. Marenzana, M. and T.R. Arnett, The key role of the blood supply to bone, Bone research, 2013. **1**(1): p. 203-215.

16. Sparks, D.S., D.B. Saleh, W.M. Rozen, D.W. Hutmacher, M.A. Schuetz, and M. Wagels, Vascularised bone transfer: History, blood supply and contemporary problems, Journal of Plastic, Reconstructive & Aesthetic Surgery, 2017. **70**(1): p. 1-11.

17. Sivaraj, K.K. and R.H. Adams, Blood vessel formation and function in bone, Development, 2016. **143**(15): p. 2706-2715.

18. Shen, C., J. Deng, R. Zhou, J. Chen, S. Fan, Z. Li, et al., Relation between bone mineral density, bone loss and the risk of cardiovascular disease in a chinese cohort, The American journal of cardiology, 2012. **110**(8): p. 1138-1142.

19. den Uyl, D., M.T. Nurmohamed, L.H. van Tuyl, H.G. Raterman, and W.F. Lems, (sub)

clinical cardiovascular disease is associated with increased bone loss and fracture risk; a systematic review of the association between cardiovascular disease and osteoporosis, Arthritis Research & Therapy, 2011. **13**(1): p. 1-19.

20. Sherman, M.S., The nerves of bone, JBJS, 1963. **45**(3): p. 522-528.

21. McCredie, J., Nerves in bone: The silent partners, Skeletal Radiology, 2007. **36**(6): p. 473-475.

22. Brazill, J.M., A.T. Beeve, C.S. Craft, J.J. Ivanusic, and E.L. Scheller, Nerves in bone: Evolving concepts in pain and anabolism, Journal of Bone and Mineral Research, 2019. **34**(8): p. 1393-1406.

23. Eimar, H., I. Tamimi, M. Murshed, and F. Tamimi, Cholinergic regulation of bone, Journal of Musculoskeletal & Neuronal Interactions, 2013. **13**(2): p. 124.

24. Togari, A., Adrenergic regulation of bone metabolism: Possible involvement of sympathetic innervation of osteoblastic and osteoclastic cells, Microscopy research and technique, 2002. **58**(2): p. 77-84.

25. Bonnet, N., D. Pierroz, and S.L. Ferrari, Adrenergic control of bone remodeling and its implications for the treatment of osteoporosis, Journal of Musculoskeletal & Neuronal Interactions, 2008. **8**(2): p. 94-104.

26. Katagiri, T. and N. Takahashi, Regulatory mechanisms of osteoblast and osteoclast differentiation, Oral Diseases, 2002. **8**(3): p. 147-159.

27. Florencio-Silva, R., G.R.d.S. Sasso, E. Sasso-Cerri, M.J. Simões, and P.S. Cerri, Biology of

bone tissue: Structure, function, and factors that influence bone cells, BioMed research international, 2015. **2015**.

28. Capulli, M., R. Paone, and N. Rucci, Osteoblast and osteocyte: Games without frontiers, Archives of biochemistry and biophysics, 2014. **561**: p. 3-12.

29. Buckwalter, J., M. Glimcher, R. Cooper, and R. Recker, Bone biology, Journal of Bone and Joint Surgery (American Volume), 1995. **77**(8): p. 1256-1275.

30. Peister, A., J.A. Mellad, B.L. Larson, B.M. Hall, L.F. Gibson, and D.J. Prockop, Adult stem cells from bone marrow (mscs) isolated from different strains of inbred mice vary in surface epitopes, rates of proliferation, and differentiation potential, Blood, 2004. **103**(5): p. 1662-1668.

31. Deng, Z.-L., K.A. Sharff, N. Tang, W.-X. Song, J. Luo, X. Luo, et al., Regulation of osteogenic differentiation during skeletal development, Frontiers in Bioscience, 2008. **13**(1): p. 2001-2021.

32. Yavropoulou, M.P. and J.G. Yovos, The role of the wnt signaling pathway in osteoblast commitment and differentiation, HORMONES-ATHENS-, 2007. **6**(4): p. 279.

33. Chen, G., C. Deng, and Y.-P. Li, Tgf-β and bmp signaling in osteoblast differentiation and bone formation, International Journal of Biological Sciences, 2012. **8**(2): p. 272.

34. Marie, P., Fibroblast growth factor signaling controlling osteoblast differentiation, Gene, 2003. **316**: p. 23-32.

35. Nakamura, T., T. Aikawa, M. Iwamoto-Enomoto, M. Iwamoto, Y. Higuchi, P. Maurizio, et

al., Induction of osteogenic differentiation by hedgehog proteins, Biochemical and biophysical research communications, 1997. **237**(2): p. 465-469.

36. Datta, N.S. and A.B. Abou-Samra, Pth and pthrp signaling in osteoblasts, Cellular Signalling, 2009. **21**(8): p. 1245-1254.

37. Miron, R. and Y. Zhang, Osteoinduction: A review of old concepts with new standards, Journal of Dental Research, 2012. **91**(8): p. 736-744.

38. Amarasekara, D.S., H. Yun, S. Kim, N. Lee, H. Kim, and J. Rho, Regulation of osteoclast differentiation by cytokine networks, Immune Network, 2018. **18**(1).

39. Kroemer, G., N. Zamzami, and S.A. Susin, Mitochondrial control of apoptosis, Immunology Today, 1997. **18**(1): p. 44-51.

40. Van Antwerp, D.J., S.J. Martin, T. Kafri, D.R. Green, and I.M. Verma, Suppression of tnf-α-induced apoptosis by nf-κb, Science, 1996. **274**(5288): p. 787-789.

41. Hock, J., V. Krishnan, J. Onyia, J. Bidwell, J. Milas, and D. Stanislaus, Osteoblast apoptosis and bone turnover, Journal of Bone and Mineral Research, 2001. **16**(6): p. 975-984.

42. Heino, T.J. and T.A. Hentunen, Differentiation of osteoblasts and osteocytes from mesenchymal stem cells, Current Stem Cell Research & Therapy, 2008. **3**(2): p. 131-145.

43. Franz-Odendaal, T.A., B.K. Hall, and P.E. Witten, Buried alive: How osteoblasts become osteocytes, Developmental dynamics: an official publication of the American Association of Anatomists, 2006. **235**(1): p. 176-190.

44. Brown, J.L., S.G. Kumbar, and C.T. Laurencin, *Chapter ii.6.7 - bone tissue engineering*, in

Biomaterials science (third edition), B.D. Ratner, A.S. Hoffman, F.J. Schoen, and J.E. Lemons, Editors. 2013, Academic Press. p. 1194-1214.

45. Everts, V., J. Delaisse, W. Korper, D. Jansen, W. Tigchelaar-Gutter, P. Saftig, et al., The bone lining cell: Its role in cleaning howship's lacunae and initiating bone formation, Journal of Bone and Mineral Research, 2002. **17**(1): p. 77-90.

46. Miller, S.C., L. de Saint-Georges, B.M. Bowman, and W.S. Jee, Bone lining cells: Structure and function, Scanning Microscopy, 1989. **3**(3): p. 27.

47. Boyle, W.J., W.S. Simonet, and D.L. Lacey, Osteoclast differentiation and activation, Nature, 2003. **423**(6937): p. 337-342.

48. Suda, T., N. Takahashi, and T.J. Martin, Modulation of osteoclast differentiation, Endocrine Reviews, 1992. **13**(1): p. 66-80.

49. Vaananen, H.K., H. Zhao, M. Mulari, and J.M. Halleen, The cell biology of osteoclast function, Journal of Cell Science, 2000. **113**(3): p. 377-381.

50. Tondravi, M., S. McKercher, K. Anderson, J. Erdmann, M. Quiroz, R. Maki, et al., Osteopetrosis in mice lacking haematopoietic transcription factor pu. 1, Nature, 1997. **386**(6620): p. 81-84.

51. Dai, X.-M., G.R. Ryan, A.J. Hapel, M.G. Dominguez, R.G. Russell, S. Kapp, et al., Targeted disruption of the mouse colony-stimulating factor 1 receptor gene results in osteopetrosis, mononuclear phagocyte deficiency, increased primitive progenitor cell frequencies, and reproductive defects, Blood, The Journal of the American Society of Hematology, 2002. **99**(1): p. 111-120.

52. Wada, T., T. Nakashima, N. Hiroshi, and J.M. Penninger, Rankl–rank signaling in osteoclastogenesis and bone disease, Trends in Molecular Medicine, 2006. **12**(1): p. 17-25.

53. Kong, Y.-Y., U. Feige, I. Sarosi, B. Bolon, A. Tafuri, S. Morony, et al., Activated t cells regulate bone loss and joint destruction in adjuvant arthritis through osteoprotegerin ligand, Nature, 1999. **402**(6759): p. 304-309.

54. Vignery, A., Macrophage fusion: The making of osteoclasts and giant cells, The Journal of experimental medicine, 2005. **202**(3): p. 337-340.

55. Ishii, M., J.G. Egen, F. Klauschen, M. Meier-Schellersheim, Y. Saeki, J. Vacher, et al., Sphingosine-1-phosphate mobilizes osteoclast precursors and regulates bone homeostasis, Nature, 2009. **458**(7237): p. 524-528.

56. Kim, K., S.H. Lee, J. Ha Kim, Y. Choi, and N. Kim, Nfatc1 induces osteoclast fusion via up-regulation of atp6v0d2 and the dendritic cell-specific transmembrane protein (dc-stamp), Molecular Endocrinology, 2008. **22**(1): p. 176-85.

57. Lee, S.-H., J. Rho, D. Jeong, J.-Y. Sul, T. Kim, N. Kim, et al., V-atpase v0 subunit d2–deficient mice exhibit impaired osteoclast fusion and increased bone formation, Nature Medicine, 2006. **12**(12): p. 1403-1409.

58. Yagi, M., T. Miyamoto, Y. Sawatani, K. Iwamoto, N. Hosogane, N. Fujita, et al., Dc-stamp is essential for cell-cell fusion in osteoclasts and foreign body giant cells, The Journal of experimental medicine, 2005. **202**(3): p. 345-351.

59. Vignery, A., Osteoclasts and giant cells: Macrophage–macrophage fusion mechanism, International Journal of Experimental Pathology, 2000. **81**(5): p. 291-304.

60. Yang, M., M.J. Birnbaum, C.A. MacKay, A. Mason-Savas, B. Thompson, and P.R. Odgren, Osteoclast stimulatory transmembrane protein (oc-stamp), a novel protein induced by rankl that promotes osteoclast differentiation, Journal of Cellular Physiology, 2008. **215**(2): p. 497-505.

61. Flores, M.E., M. Norgård, D. Heinegård, F.P. Reinholt, and G. Andersson, Rgd-directed attachment of isolated rat osteoclasts to osteopontin, bone sialoprotein, and fibronectin, Experimental Cell Research, 1992. **201**(2): p. 526-530.

62. Horton, M.A., M.A. Nesbit, and M.H. Helfrich, Interaction of osteopontin with osteoclast integrins, Annals of the New York Academy of Sciences, 1995. **760**: p. 190-200.

63. Faccio, R., D.V. Novack, A. Zallone, F.P. Ross, and S.L. Teitelbaum, Dynamic changes in the osteoclast cytoskeleton in response to growth factors and cell attachment are controlled by beta3 integrin, The Journal of cell biology, 2003. **162**(3): p. 499-509.

64. Olsen, B.R., A.M. Reginato, and W. Wang, Bone development, Annual review of cell and developmental biology, 2000. **16**(1): p. 191-220.

65. Yang, T.-L., H. Shen, A. Liu, S.-S. Dong, L. Zhang, F.-Y. Deng, et al., A road map for understanding molecular and genetic determinants of osteoporosis, Nature Reviews Endocrinology, 2019: p. 1-13.

66. Hauge, E.M., D. Qvesel, E.F. Eriksen, L. Mosekilde, and F. Melsen, Cancellous bone remodeling occurs in specialized compartments lined by cells expressing osteoblastic markers, Journal of Bone and Mineral Research, 2001. **16**(9): p. 1575-1582.

67. Sims, N.A. and T.J. Martin, Coupling the activities of bone formation and resorption: A

multitude of signals within the basic multicellular unit, BoneKEy reports, 2014. **3**.

68. Pettit, A.R., M.K. Chang, D.A. Hume, and L.-J. Raggatt, Osteal macrophages: A new twist on coupling during bone dynamics, Bone, 2008. **43**(6): p. 976-982.

69. Theoleyre, S., Y. Wittrant, S.K. Tat, Y. Fortun, F. Redini, and D. Heymann, The molecular triad opg/rank/rankl: Involvement in the orchestration of pathophysiological bone remodeling, Cytokine & Growth Factor Reviews, 2004. **15**(6): p. 457-475.

70. Li, X., L. Qin, M. Bergenstock, L.M. Bevelock, D.V. Novack, and N.C. Partridge, Parathyroid hormone stimulates osteoblastic expression of mcp-1 to recruit and increase the fusion of pre/osteoclasts, Journal of Biological Chemistry, 2007. **282**(45): p. 33098-33106.

71. Chen, X., Z. Wang, N. Duan, G. Zhu, E.M. Schwarz, and C. Xie, Osteoblast–osteoclast interactions, Connective Tissue Research, 2018. **59**(2): p. 99-107.

72. Raggatt, L.J. and N.C. Partridge, Cellular and molecular mechanisms of bone remodeling, Journal of Biological Chemistry, 2010. **285**(33): p. 25103-25108.

73. Department, D.S.S.C.a.S., *Hong kong population projections 2015 - 2064*. 2015: Hong Kong.

74. Rachner, T.D., S. Khosla, and L.C. Hofbauer, Osteoporosis: Now and the future, The Lancet, 2011. **377**(9773): p. 1276-1287.

75. Cawthon, P.M., Gender differences in osteoporosis and fractures, Clinical Orthopaedics and Related Research®, 2011. **469**(7): p. 1900-1905.

76. 中国健康促进基金会骨质疏松防治中国白皮书编委会, 骨质疏松症中国白皮书, 中华健康管理学杂志, 2009. **3**(3): p. 148-154.

77. P. Bonjour, P.C., C. Cooper, B. Dawson-Hughes, C. De Laet, P. Delmas, H. Johansson, O. Johnell, J. Kanis, J. Melton, P. Miller, A. Oden, N. Toroptsova, N. Khaltaev, B. A. Pfleger, *Who scientific group on the assessment of osteoporosis at primary health care level*. 2004: Brussels, Belgium.

78. Sharif, P.S., M. Abdollahi, and B. Larijani, Current, new and future treatments of osteoporosis, Rheumatology International, 2011. **31**(3): p. 289-300.

79. Jackson, R.D., A.Z. LaCroix, M. Gass, R.B. Wallace, J. Robbins, C.E. Lewis, et al., Calcium plus vitamin d supplementation and the risk of fractures, New England Journal of Medicine, 2006. **354**(7): p. 669-683.

80. Wells, G.A., A. Cranney, J. Peterson, M. Boucher, B. Shea, V. Welch, et al., Alendronate for the primary and secondary prevention of osteoporotic fractures in postmenopausal women, The Cochrane Library, 2008.

81. Wells, G.A., A. Cranney, J. Peterson, M. Boucher, B. Shea, V. Welch, et al., Risedronate for the primary and secondary prevention of osteoporotic fractures in postmenopausal women, The Cochrane Library, 2008.

82. Saita, Y., M. Ishijima, and K. Kaneko, Atypical femoral fractures and bisphosphonate use: Current evidence and clinical implications, Therapeutic Advances in Chronic Disease, 2015. **6**(4): p. 185-193.

83. Kneissel, M., A. Boyde, and J.A. Gasser, Bone tissue and its mineralization in aged estrogen-depleted rats after long-term intermittent treatment with parathyroid hormone (pth) analog sdz pts 893 or human pth(1-34), Bone, 2001. **28**(3): p. 237-250.

84. Borba, V.Z. and N.C. Mañas, The use of pth in the treatment of osteoporosis, Arquivos Brasileiros de Endocrinologia e Metabologia, 2010. **54**(2): p. 213.

85. Riek, A.E. and D.A. Towler, The pharmacological management of osteoporosis, Missouri Medicine, 2011. **108**(2): p. 118.

86. Michael Lewiecki, E., N.C. Wright, J.R. Curtis, E. Siris, R.F. Gagel, K.G. Saag, et al., Hip fracture trends in the united states, 2002 to 2015, Osteoporos Int, 2018. **29**(3): p. 717-722.

87. H Ferreira-Vieira, T., I. M Guimaraes, F. R Silva, and F. M Ribeiro, Alzheimer's disease: Targeting the cholinergic system, Current Neuropharmacology, 2016. **14**(1): p. 101-115.

88. Racké, K., U.R. Juergens, and S. Matthiesen, Control by cholinergic mechanisms, European Journal of Pharmacology, 2006. **533**(1-3): p. 57-68.

89. Weinstock, M., Possible role of the cholinergic system and disease models, 1997. **49**(49): p. 93.

90. Loewi, O., Über humorale übertragbarkeit der herznervenwirkung, Pflüger's Archiv für die gesamte Physiologie des Menschen und der Tiere, 1921. **189**(1): p. 239-242.

91. Oda, Y., Choline acetyltransferase: The structure, distribution and pathologic changes in the central nervous system, Pathology International, 1999. **49**(11): p. 921-937.

92. Erickson, J.D., H. Varoqui, M. Schäfer, W. Modi, M.-F. Diebler, E. Weihe, et al., Functional identification of a vesicular acetylcholine transporter and its expression from a" cholinergic" gene locus, Journal of Biological Chemistry, 1994. **269**(35): p. 21929-21932.

93. Bittner, E.A. and J.A.J. Martyn, *21 - neuromuscular physiology and pharmacology*, in

Pharmacology and physiology for anesthesia (second edition), H.C. Hemmings and T.D. Egan, Editors. 2019, Elsevier: Philadelphia. p. 412-427.

94. Fon, E.A. and R.H. Edwards, Molecular mechanisms of neurotransmitter release, Muscle & Nerve, 2001. **24**(5): p. 581-601.

95. Chuang, R., *Handbook of toxicology of chemical warfare agents, edited by ramesh c. Gupta*. 2010.

96. Dani, J.A. and D. Bertrand, Nicotinic acetylcholine receptors and nicotinic cholinergic mechanisms of the central nervous system, Annu. Rev. Pharmacol. Toxicol., 2007. **47**: p. 699-729.

97. Kramer, I.M., *Chapter 4 - cholinergic signaling and muscle contraction*, in *Signal transduction (third edition)*, I.M. Kramer, Editor. 2016, Academic Press: Boston. p. 263-327.

98. Rosenberry, T.L., Acetylcholinesterase, Advances in enzymology and related areas of molecular biology, 1975. **43**: p. 103-218.

99. Silver, A., The biology of cholinesterases, 1974.

100. Darvesh, S. and D.A. Hopkins, Differential distribution of butyrylcholinesterase and acetylcholinesterase in the human thalamus, Journal of Comparative Neurology, 2003. **463**(1): p. 25-43.

101. Chatonnet, A. and O. Lockridge, Comparison of butyrylcholinesterase and acetylcholinesterase, Biochemical Journal, 1989. **260**(3): p. 625-634.

102. Jbilo, O., C.F. Bartels, A. Chatonnet, J.-P. Toutant, and O. Lockridge, Tissue distribution of

human acetylcholinesterase and butyrylcholinesterase messenger rna, Toxicon, 1994. **32**(11): p. 1445-1457.

103. Manoharan, I., R. Boopathy, S. Darvesh, and O. Lockridge, A medical health report on individuals with silent butyrylcholinesterase in the vysya community of india, Clinica Chimica Acta, 2007. **378**(1-2): p. 128-35.

104. Li, B., E.G. Duysen, M. Carlson, and O. Lockridge, The butyrylcholinesterase knockout mouse as a model for human butyrylcholinesterase deficiency, Journal of Pharmacology and Experimental Therapeutics, 2008. **324**(3): p. 1146-1154.

105. Xie, W., J.A. Stribley, A. Chatonnet, P.J. Wilder, A. Rizzino, R.D. McComb, et al., Postnatal developmental delay and supersensitivity to organophosphate in gene-targeted mice lacking acetylcholinesterase, Journal of Pharmacology and Experimental Therapeutics, 2000. **293**(3): p. 896-902.

106. Beckmann, J. and K.S. Lips, The non-neuronal cholinergic system in health and disease, Pharmacology, 2013. **92**(5-6): p. 286-302.

107. Wessler, I. and C. Kirkpatrick, Acetylcholine beyond neurons: The non-neuronal cholinergic system in humans, British Journal of Pharmacology, 2008. **154**(8): p. 1558-1571.

108. Kurzen, H., I. Wessler, C. Kirkpatrick, K. Kawashima, and S. Grando, The non-neuronal cholinergic system of human skin, Hormone and Metabolic Research, 2007. **39**(02): p. 125-135.

109. Wessler, I., H. Kilbinger, F. Bittinger, R. Unger, and C.J. Kirkpatrick, The non-neuronal cholinergic system in humans: Expression, function and pathophysiology, Life Sciences,

2003. **72**(18-19): p. 2055-2061.

110. Klapproth, H., T. Reinheimer, J. Metzen, M. Münch, F. Bittinger, C.J. Kirkpatrick, et al., Non-neuronal acetylcholine, a signalling molecule synthezised by surface cells of rat and man, Naunyn-Schmiedeberg's Archives of Pharmacology, 1997. **355**(4): p. 515-523.

111. Kawashima, K. and T. Fujii, Extraneuronal cholinergic system in lymphocytes, Pharmacology & Therapeutics, 2000. **86**(1): p. 29-48.

112. Sato, T., T. Abe, D. Chida, N. Nakamoto, N. Hori, S. Kokabu, et al., Functional role of acetylcholine and the expression of cholinergic receptors and components in osteoblasts, FEBS Letters, 2010. **584**(4): p. 817-824.

113. En-Nosse, M., S. Hartmann, K. Trinkaus, V. Alt, B. Stigler, C. Heiss, et al., Expression of non-neuronal cholinergic system in osteoblast-like cells and its involvement in osteogenesis, Cell and tissue research, 2009. **338**(2): p. 203-215.

114. Mandl, P., S. Hayer, T. Karonitsch, P. Scholze, D. Győri, D. Sykoutri, et al., Nicotinic acetylcholine receptors modulate osteoclastogenesis, Arthritis Research & Therapy, 2016. **18**(1): p. 63.

115. Spieker, J., A. Ackermann, A. Salfelder, A. Vogel-Höpker, and P.G. Layer, Acetylcholinesterase regulates skeletal in ovo development of chicken limbs by ach-dependent and-independent mechanisms, PloS One, 2016. **11**(8): p. e0161675.

116. Guo, J., L. Wang, H. Xu, and X. Che, Expression of non-neuronal cholinergic system in maxilla of rat in vivo, Biological Research, 2014. **47**(1): p. 72.

117. Liu, P.-S., Y.-Y. Chen, C.-K. Feng, Y.-H. Lin, and T.-C. Yu, Muscarinic acetylcholine receptors present in human osteoblast and bone tissue, European Journal of Pharmacology, 2011. **650**(1): p. 34-40.

118. Zablotni, A., O. Dakischew, K. Trinkaus, S. Hartmann, G. Szalay, C. Heiss, et al., Regulation of acetylcholine receptors during differentiation of bone mesenchymal stem cells harvested from human reaming debris, International Immunopharmacology, 2015. **29**(1): p. 119-126.

119. Kauschke, V., K.S. Lips, C. Heiss, and R. Schnettler, Expression of muscarinic acetylcholine receptors m3 and m5 in osteoporosis, Medical science monitor: international medical journal of experimental and clinical research, 2014. **20**: p. 869.

120. Ternes, S., K. Trinkaus, I. Bergen, S. Knaack, M. Gelinsky, O. Kilian, et al., Impact of acetylcholine and nicotine on human osteoclastogenesis in vitro, International Immunopharmacology, 2015. **29**(1): p. 215-221.

121. Ma, Y., X. Li, J. Fu, Y. Li, L. Gao, L. Yang, et al., Acetylcholine affects osteocytic mlo-y4 cells via acetylcholine receptors, Molecular and Cellular Endocrinology, 2014. **384**(1-2): p. 155-164.

122. Inkson, C.A., A.C. Brabbs, T.S. Grewal, T.M. Skerry, and P.G. Genever, Characterization of acetylcholinesterase expression and secretion during osteoblast differentiation, Bone, 2004. **35**(4): p. 819-27.

123. Genever, P.G., M.A. Birch, E. Brown, and T.M. Skerry, Osteoblast-derived acetylcholinesterase: A novel mediator of cell-matrix interactions in bone?, Bone, 1999. **24**(4): p. 297-303.

124. Sato, T., Y. Enoki, Y. Sakamoto, K. Yokota, M. Okubo, M. Matsumoto, et al., Donepezil prevents rank-induced bone loss via inhibition of osteoclast differentiation by downregulating acetylcholinesterase, Heliyon, 2015. **1**(1): p. e00013.

125. Xu, M.L., C.W.C. Bi, E.Y.L. Liu, T.T.X. Dong, and K.W.K. Tsim, Wnt3a induces the expression of acetylcholinesterase during osteoblast differentiation via the runx2 transcription factor, J Biol Chem, 2017. **292**(30): p. 12667-12678.

126. Walker, L., M. Preston, J. Magnay, P. Thomas, and A. El Haj, Nicotinic regulation of c-fos and osteopontin expression in human-derived osteoblast-like cells and human trabecular bone organ culture, Bone, 2001. **28**(6): p. 603-608.

127. Dvir, H., I. Silman, M. Harel, T.L. Rosenberry, and J.L. Sussman, Acetylcholinesterase: From 3d structure to function, Chemico-biological interactions, 2010. **187**(1-3): p. 10-22.

128. Sussman, J.L., M. Harel, F. Frolow, C. Oefner, A. Goldman, L. Toker, et al., Atomic structure of acetylcholinesterase from torpedo californica: A prototypic acetylcholine-binding protein, Science, 1991. **253**(5022): p. 872-879.

129. Silman, I. and J.L. Sussman, Acetylcholinesterase: How is structure related to function?, Chemico-biological interactions, 2008. **175**(1-3): p. 3-10.

130. Johnson, G. and S. Moore, The peripheral anionic site of acetylcholinesterase: Structure, functions and potential role in rational drug design, Current Pharmaceutical Design, 2006. **12**(2): p. 217-225.

131. Sáez-Valero, J. and C.J. Vidal, Monomers and dimers of acetylcholinesterase in human meningioma are anchored to the membrane by glycosylphosphatidylinositol, Neuroscience

Letters, 1995. **195**(2): p. 101-104.

132. Massoulié, J., J. Sussman, S. Bon, and I. Silman, Structure and functions of acetylcholinesterase and butyrylcholinesterase, Progress in Brain Research, 1993. **98**: p. 139-139.

133. Colovic, M.B., D.Z. Krstic, T.D. Lazarevic-Pasti, A.M. Bondzic, and V.M. Vasic, Acetylcholinesterase inhibitors: Pharmacology and toxicology, Current Neuropharmacology, 2013. **11**(3): p. 315-335.

134. McGleenon, B., K. Dynan, and A. Passmore, Acetylcholinesterase inhibitors in alzheimer's disease, British Journal of Clinical Pharmacology, 1999. **48**(4): p. 471.

135. Galimberti, D. and E. Scarpini, Old and new acetylcholinesterase inhibitors for alzheimer's disease, Expert opinion on investigational drugs, 2016. **25**(10): p. 1181-1187.

136. Silva, M.A., A.S. Kiametis, and W. Treptow, Donepezil inhibits acetylcholinesterase via multiple binding modes at room temperature, Journal of Chemical Information and Modeling, 2020. **60**(7): p. 3463-3471.

137. Kim, M.H., H.J. Maeng, K.H. Yu, K.R. Lee, T. Tsuruo, D.D. Kim, et al., Evidence of carrier-mediated transport in the penetration of donepezil into the rat brain, Journal of Pharmaceutical Sciences, 2010. **99**(3): p. 1548-1566.

138. Jiang, Y., H. Gao, and G. Turdu, Traditional chinese medicinal herbs as potential ache inhibitors for anti-alzheimer's disease: A review, Bioorganic Chemistry, 2017. **75**: p. 50-61.

139. Dooley, M. and H.M. Lamb, Donepezil, Drugs and Aging, 2000. **16**(3): p. 199-226.

140. Bartolucci, C., E. Perola, C. Pilger, G. Fels, and D. Lamba, Three-dimensional structure of a complex of galanthamine (nivalin®) with acetylcholinesterase from torpedo californica: Implications for the design of new anti-alzheimer drugs, Proteins: structure, function, and bioinformatics, 2001. **42**(2): p. 182-191.

141. Scott, L.J. and K.L. Goa, Galantamine, Drugs, 2000. **60**(5): p. 1095-1122.

142. Marco-Contelles, J., M. do Carmo Carreiras, C. Rodríguez, M. Villarroya, and A.G. García, Synthesis and pharmacology of galantamine, Chemical Reviews, 2006. **106**(1): p. 116-133.

143. Anand, P. and B. Singh, A review on cholinesterase inhibitors for alzheimer's disease, Archives of pharmacal research, 2013. **36**(4): p. 375-399.

144. Bar-On, P., C. Millard, M. Harel, H. Dvir, A. Enz, J. Sussman, et al., Kinetic and structural studies on the interaction of cholinesterases with the anti-alzheimer drug rivastigmine, Biochemistry, 2002. **41**(11): p. 3555-3564.

145. Spencer, C.M. and S. Noble, Rivastigmine, Drugs and Aging, 1998. **13**(5): p. 391-411.

146. Gottwald, M.D. and R.I. Rozanski, Rivastigmine, a brain-region selective acetylcholinesterase inhibitor for treating alzheimer's disease: Review and current status, Expert opinion on investigational drugs, 1999. **8**(10): p. 1673-1682.

147. Raves, M.L., M. Harel, Y.-P. Pang, I. Silman, A.P. Kozikowski, and J.L. Sussman, Structure of acetylcholinesterase complexed with the nootropic alkaloid,(–)-huperzine a, Nature Structural Biology, 1997. **4**(1): p. 57-63.

148. Yamada, F., A.P. Kozikowski, E. Reddy, Y.P. Pang, J.H. Miller, and M. McKinney, A route

to optically pure (-)-huperzine a; molecular modeling and in vitro pharmacology, Journal of the American Chemical Society, 1991. **113**(12): p. 4695-4696.

149. Lian, W.-W., A.-L. Liu, and G.-H. Du, *Huperzine a*, in *Natural small molecule drugs from plants*. 2018, Springer. p. 271-275.

150. Marucci, G., M. Buccioni, D.D. Ben, C. Lambertucci, R. Volpini, and F. Amenta, Efficacy of acetylcholinesterase inhibitors in alzheimer's disease, Neuropharmacology, 2021. **190**: p. 108352.

151. Knapp, M.J., D.S. Knopman, P.R. Solomon, W.W. Pendlebury, C.S. Davis, S.I. Gracon, et al., A 30-week randomized controlled trial of high-dose tacrine in patients with alzheimer's disease, JAMA, 1994. **271**(13): p. 985-991.

152. Wlodek, S.T., T.W. Clark, L.R. Scott, and J.A. McCammon, Molecular dynamics of acetylcholinesterase dimer complexed with tacrine, Journal of the American Chemical Society, 1997. **119**(40): p. 9513-9522.

153. Bolognesi, M.L., A. Cavalli, V. Andrisano, M. Bartolini, R. Banzi, A. Antonello, et al., Design, synthesis and biological evaluation of ambenonium derivatives as ache inhibitors, Il Farmaco, 2003. **58**(9): p. 917-928.

154. Hodge, A.S., D. Humphrey, and T. Rosenberry, Ambenonium is a rapidly reversible noncovalent inhibitor of acetylcholinesterase, with one of the highest known affinities, Molecular Pharmacology, 1992. **41**(5): p. 937-942.

155. Lands, A., J. Hoppe, A. Arnold, and F.K. Kirchner, An investigation of the structure-activity correlations within a series of ambenonium analogs, Journal of Pharmacology and

Experimental Therapeutics, 1958. **123**(2): p. 121-127.

156. Xie, Q., Z. Zheng, B. Shao, W. Fu, Z. Xia, W. Li, et al., Pharmacophore-based design and discovery of (−)-meptazinol carbamates as dual modulators of cholinesterase and amyloidogenesis, Journal of Enzyme Inhibition and Medicinal Chemistry, 2017. **32**(1): p. 659-671.

157. Mehta, M., A. Adem, and M. Sabbagh, New acetylcholinesterase inhibitors for alzheimer's disease, International Journal of Alzheimer's disease, 2012. **2012**.

158. En-Nosse, M., S. Hartmann, K. Trinkaus, V. Alt, B. Stigler, C. Heiss, et al., Expression of non-neuronal cholinergic system in osteoblast-like cells and its involvement in osteogenesis, Cell Tissue Res, 2009. **338**(2): p. 203-15.

159. Xu, M.L., C.W. Bi, E.Y. Liu, T.T. Dong, and K.W. Tsim, Wnt3a induces the expression of acetylcholinesterase during osteoblast differentiation via the runx2 transcription factor, Journal of Biological Chemistry, 2017. **292**(30): p. 12667-12678.

160. Spieker, J., T. Mudersbach, A. Vogel-Hopker, and P.G. Layer, Endochondral ossification is accelerated in cholinesterase-deficient mice and in avian mesenchymal micromass cultures, PloS One, 2017. **12**(1): p. e0170252.

161. Kauschke, V., M. Kneffel, W. Floel, S. Hartmann, M. Kampschulte, L. Durselen, et al., Bone status of acetylcholinesterase-knockout mice, Int Immunopharmacol, 2015. **29**(1): p. 222-30.

162. Bourne, Y., P. Taylor, Z. Radić, and P. Marchot, Structural insights into ligand interactions at the acetylcholinesterase peripheral anionic site, The EMBO Journal, 2003. **22**(1): p. 1-12.

163. Layer, P.G., T. Weikert, and R. Alber, Cholinesterases regulate neurite growth of chick nerve cells in vitro by means of a non-enzymatic mechanism, Cell and tissue research, 1993. **273**(2): p. 219-226.

164. Small, D.H., G. Reed, B. Whitefield, and V. Nurcombe, Cholinergic regulation of neurite outgrowth from isolated chick sympathetic neurons in culture, Journal of Neuroscience, 1995. **15**(1): p. 144-151.

165. Lev-Lehman, E., V. Deutsch, A. Eldor, and H. Soreq, Immature human megakaryocytes produce nuclear-associated acetylcholinesterase, Blood, The Journal of the American Society of Hematology, 1997. **89**(10): p. 3644-3653.

166. Paoletti, F., A. Mocali, and A.M. Vannucchi, Acetylcholinesterase in murine erythroleukemia (friend) cells: Evidence for megakaryocyte-like expression and potential growth-regulatory role of enzyme activity, 1992.

167. Botti, S.A., C.E. Felder, J.L. Sussman, and I. Silman, Electrotactins: A class of adhesion proteins with conserved electrostatic and structural motifs, Protein Engineering, 1998. **11**(6): p. 415-420.

168. Scholl, F.G. and P. Scheiffele, Making connections: Cholinesterase-domain proteins in the cns, Trends in Neurosciences, 2003. **26**(11): p. 618-624.

169. Johnson, G. and S.W. Moore, Human acetylcholinesterase binds to mouse laminin-1 and human collagen iv by an electrostatic mechanism at the peripheral anionic site, Neuroscience Letters, 2003. **337**(1): p. 37-40.

170. Johnson, G. and S.W. Moore, Identification of a structural site on acetylcholinesterase that

promotes neurite outgrowth and binds laminin-1 and collagen iv, Biochemical and biophysical research communications, 2004. **319**(2): p. 448-455.

171. Paraoanu, L.E. and P.G. Layer, Acetylcholinesterase in cell adhesion, neurite growth and network formation, The FEBS journal, 2008. **275**(4): p. 618-624.

172. Xu, M.L., C.W.C. Bi, A.Y.Y. Kong, T.T.X. Dong, Y.H. Wong, and K.W.K. Tsim, Flavonoids induce the expression of acetylcholinesterase in cultured osteoblasts, Chem Biol Interact, 2016. **259**(Pt B): p. 295-300.

173. Vogel-Hopker, A., L. E Sperling, and P. G Layer, Co-opting functions of cholinesterases in neural, limb and stem cell development, Protein and peptide letters, 2012. **19**(2): p. 155-164.

174. Kennedy, B.K., S.L. Berger, A. Brunet, J. Campisi, A.M. Cuervo, E.S. Epel, et al., Geroscience: Linking aging to chronic disease, Cell, 2014. **159**(4): p. 709-713.

175. Candore, G., C. Caruso, E. Jirillo, T. Magrone, and S. Vasto, Low grade inflammation as a common pathogenetic denominator in age-related diseases: Novel drug targets for anti-ageing strategies and successful ageing achievement, Current Pharmaceutical Design, 2010. **16**(6): p. 584-596.

176. Schumacher, B., G.A. Garinis, and J.H. Hoeijmakers, Age to survive: DNA damage and aging, Trends in Genetics, 2008. **24**(2): p. 77-85.

177. Aubert, G. and P.M. Lansdorp, Telomeres and aging, Physiological Reviews, 2008. **88**(2): p. 557-579.

178. Wallace, D.C., Mitochondrial DNA in aging and disease, Scientific American, 1997. **277**(2):

p. 40-47.

179. Brignull, H.R., J.F. Morley, and R.I. Morimoto, The stress of misfolded proteins, Molecular aspects of the stress response: Chaperones, Membranes and Networks, 2007: p. 167-189.

180. Oh, J., Y.D. Lee, and A.J. Wagers, Stem cell aging: Mechanisms, regulators and therapeutic opportunities, Nature Medicine, 2014. **20**(8): p. 870-880.

181. Childs, B.G., M. Durik, D.J. Baker, and J.M. Van Deursen, Cellular senescence in aging and age-related disease: From mechanisms to therapy, Nature Medicine, 2015. **21**(12): p. 1424-1435.

182. Tchkonia, T. and J.L. Kirkland, Aging, cell senescence, and chronic disease: Emerging therapeutic strategies, JAMA, 2018. **320**(13): p. 1319-1320.

183. Sikora, E., A. Bielak-Żmijewska, and G. Mosieniak, What is and what is not cell senescence, Postepy Biochemii, 2018. **64**: p. 110-118.

184. Davalli, P., T. Mitic, A. Caporali, A. Lauriola, and D. D'Arca, Ros, cell senescence, and novel molecular mechanisms in aging and age-related diseases, Oxidative Medicine and Cellular Longevity, 2016. **2016**.

185. Von Zglinicki, T., G. Saretzki, J. Ladhoff, F.d.A. di Fagagna, and S. Jackson, Human cell senescence as a DNA damage response, Mechanisms of Ageing and Development, 2005. **126**(1): p. 111-117.

186. Marie, P.J., Bone cell senescence: Mechanisms and perspectives, Journal of Bone and Mineral Research, 2014. **29**(6): p. 1311-1321.

187. Kassem, M. and P.J. Marie, Senescence-associated intrinsic mechanisms of osteoblast dysfunctions, Aging Cell, 2011. **10**(2): p. 191-197.

188. Farr, J.N., D.G. Fraser, H. Wang, K. Jaehn, M.B. Ogrodnik, M.M. Weivoda, et al., Identification of senescent cells in the bone microenvironment, Journal of bone and mineral research, 2016. **31**(11): p. 1920-1929.

189. Farr, J.N., M. Xu, M.M. Weivoda, D.G. Monroe, D.G. Fraser, J.L. Onken, et al., Targeting cellular senescence prevents age-related bone loss in mice, Nature Medicine, 2017. **23**(9): p. 1072-1079.

190. Alber, R., O. Sporns, T. Weikert, E. Willbold, and P.G. Layer, Cholinesterases and peanut agglutinin binding related to cell proliferation and axonal growth in embryonic chick limbs, Anat Embryol (Berl), 1994. **190**(5): p. 429-38.

191. Spieker, J., A. Ackermann, A. Salfelder, A. Vogel-Hopker, and P.G. Layer, Acetylcholinesterase regulates skeletal in ovo development of chicken limbs by ach-dependent and -independent mechanisms, PLoS One, 2016. **11**(8): p. e0161675.

192. Bajayo, A., A. Bar, A. Denes, M. Bachar, V. Kram, M. Attar-Namdar, et al., Skeletal parasympathetic innervation communicates central il-1 signals regulating bone mass accrual, Proceedings of the National Academy of Sciences of the United States of America, 2012. **109**(38): p. 15455-60.

193. Eimar, H., S. Alebrahim, G. Manickam, A. Al-Subaie, L. Abu-Nada, M. Murshed, et al., Donepezil regulates energy metabolism and favors bone mass accrual, Bone, 2016. **84**: p. 131-138.

194. Edwards, J. and S. Brimijoin, Thermal inactivation of the molecular forms of acetylcholinesterase and butyrylcholinesterase, Biochimica et Biophysica Acta (BBA)-Protein Structure and Molecular Enzymology, 1983. **742**(3): p. 509-516.

195. Mu, X., C. Tseng, W.S. Hambright, P. Matre, C.Y. Lin, P. Chanda, et al., Cytoskeleton stiffness regulates cellular senescence and innate immune response in hutchinson–gilford progeria syndrome, Aging Cell, 2020. **19**(8): p. e13152.

196. Morgan, J.T., V.K. Raghunathan, Y.-R. Chang, C.J. Murphy, and P. Russell, The intrinsic stiffness of human trabecular meshwork cells increases with senescence, Oncotarget, 2015. **6**(17): p. 15362.

197. Keller, M., A. Robitzki, and P.G. Layer, Heterologous expression of acetylcholinesterase affects proliferation and glial cytoskeleton of adherent chicken retinal cells, Cell and tissue research, 2001. **306**(2): p. 187-198.

198. Humphries, M., Integrin structure, Biochemical Society Transactions, 2000. **28**(4): p. 311-340.

199. Humphries, J.D., A. Byron, and M.J. Humphries, Integrin ligands at a glance, Journal of Cell Science, 2006. **119**(19): p. 3901-3903.

200. Nakamura, I., l.T. Duong, S.B. Rodan, and G.A. Rodan, Involvement of αvβ3 integrins in osteoclast function, Journal of bone and mineral metabolism, 2007. **25**(6): p. 337-344.

201. Helfrich, M., S. Nesbitt, P. Lakkakorpi, M. Barnes, S. Bodary, G. Shankar, et al., B1 integrins and osteoclast function: Involvement in collagen recognition and bone resorption, Bone, 1996. **19**(4): p. 317-328.

202. Nesbitt, S., A. Nesbit, M. Helfrich, and M. Horton, Biochemical characterization of human osteoclast integrins. Osteoclasts express alpha v beta 3, alpha 2 beta 1, and alpha v beta 1 integrins, Journal of Biological Chemistry, 1993. **268**(22): p. 16737-16745.

203. Duong, L.T. and G.A. Rodan, Integrin-mediated signaling in the regulation of osteoclast adhesion and activation, Frontiers in Bioscience, 1998. **3**: p. d757-d768.

204. Nakamura, I., M.F. Pilkington, P.T. Lakkakorpi, L. Lipfert, S.M. Sims, S.J. Dixon, et al., Role of alpha (v) beta (3) integrin in osteoclast migration and formation of the sealing zone, Journal of Cell Science, 1999. **112**(22): p. 3985-3993.

205. Udagawa, N., M. Koide, M. Nakamura, Y. Nakamichi, T. Yamashita, S. Uehara, et al., Osteoclast differentiation by rankl and opg signaling pathways, Journal of bone and mineral metabolism, 2021. **39**(1): p. 19-26.

206. Boyce, B.F. and L. Xing, The rankl/rank/opg pathway, Current osteoporosis reports, 2007. **5**(3): p. 98-104.

207. Whitesides, G.M., The origins and the future of microfluidics, Nature, 2006. **442**(7101): p. 368-73.

208. Au, A.K., W. Huynh, L.F. Horowitz, and A. Folch, 3d-printed microfluidics, Angewandte Chemie-International Edition, 2016. **55**(12): p. 3862-3881.

209. Manz, A., D.J. Harrison, E.M.J. Verpoorte, J.C. Fettinger, H. Ludi, and H.M. Widmer, Miniaturization of chemical-analysis systems - a look into next century technology or just a fashionable craze, Chimia, 1991. **45**(4): p. 103-105.

210. Harrison, D.J., K. Fluri, K. Seiler, Z.H. Fan, C.S. Effenhauser, and A. Manz, Micromachining a miniaturized capillary electrophoresis-based chemical-analysis system on a chip, Science, 1993. **261**(5123): p. 895-897.

211. Whitesides, G.M. and A.D. Stroock, Flexible methods for microfluidics, Physics Today, 2001. **54**(6): p. 42-48.

212. Kauschke, V., M. Kneffel, W. Floel, S. Hartmann, M. Kampschulte, L. Dürselen, et al., Bone status of acetylcholinesterase-knockout mice, International Immunopharmacology, 2015. **29**(1): p. 222-230.

213. Klegeris, A., T.C. Budd, and S.A. Greenfield, Acetylcholinesterase activation of peritoneal macrophages is independent of catalytic activity, Cell Mol Neurobiol, 1994. **14**(1): p. 89-98.

214. Sato, T., Y. Enoki, Y. Sakamoto, K. Yokota, M. Okubo, M. Matsumoto, et al., Donepezil prevents rank-induced bone loss via inhibition of osteoclast differentiation by downregulating acetylcholinesterase, Heliyon, 2015. **1**(1): p. e00013.

215. Ma, Y. and F. Elefteriou, Brain-derived acetylcholine maintains peak bone mass in adult female mice, Journal of Bone and Mineral Research, 2020.

216. Maridas, D.E., E. Rendina-Ruedy, P.T. Le, and C.J. Rosen, Isolation, culture, and differentiation of bone marrow stromal cells and osteoclast progenitors from mice, JoVE (Journal of Visualized Experiments), 2018(131): p. e56750.

217. Taubenberger, A.V., D.W. Hutmacher, and D.J. Muller, Single-cell force spectroscopy, an emerging tool to quantify cell adhesion to biomaterials, Tissue Engineering Part B: Reviews, 2014. **20**(1): p. 40-55.

218. Friedrichs, J., K.R. Legate, R. Schubert, M. Bharadwaj, C. Werner, D.J. Müller, et al., A practical guide to quantify cell adhesion using single-cell force spectroscopy, Methods, 2013. **60**(2): p. 169-178.

219. Franz, C.M., A. Taubenberger, P.-H. Puech, and D.J. Muller, Studying integrin-mediated cell adhesion at the single-molecule level using afm force spectroscopy, Science's STKE, 2007. **2007**(406): p. pl5-pl5.

220. Puech, P.-H., K. Poole, D. Knebel, and D.J. Muller, A new technical approach to quantify cell–cell adhesion forces by afm, Ultramicroscopy, 2006. **106**(8-9): p. 637-644.

221. Kim, H., H. Arakawa, T. Osada, and A. Ikai, Quantification of cell adhesion force with afm: Distribution of vitronectin receptors on a living mc3t3-e1 cell, Ultramicroscopy, 2003. **97**(1-4): p. 359-363.

222. Galdeano, C., E. Viayna, P. Arroyo, A. Bidon-Chanal, J. Ramon Blas, D. Munoz-Torrero, et al., Structural determinants of the multifunctional profile of dual binding site acetylcholinesterase inhibitors as anti-alzheimer agents, Current Pharmaceutical Design, 2010. **16**(25): p. 2818-2836.

223. Ettinger, M.P., Aging bone and osteoporosis: Strategies for preventing fractures in the elderly, Archives of Internal Medicine, 2003. **163**(18): p. 2237-2246.

224. Jepsen, K.J., The aging cortex: To crack or not to crack, Osteoporosis international, 2003. **14**(5): p. 57-66.

225. Wang, X., X. Shen, X. Li, and C. Mauli Agrawal, Age-related changes in the collagen network and toughness of bone, Bone, 2002. **31**(1): p. 1-7.

226. Vashishth, D., G.J. Gibson, J.I. Khoury, M.B. Schaffler, J. Kimura, and D.P. Fyhrie, Influence of nonenzymatic glycation on biomechanical properties of cortical bone, Bone, 2001. **28**(2): p. 195-201.

227. BURR, D.B. and C.H. TURNER, *Biomechanical measurements in age-related bone loss*, in *The aging skeleton*. 1999, Elsevier. p. 301-311.

228. Simmons Jr, E.D., K. Pritzker, and M.D. Grynpas, Age-related changes in the human femoral cortex, Journal of Orthopaedic Research, 1991. **9**(2): p. 155-167.

229. Organization, W.H., *Dementia: A public health priority*. 2012: World Health Organization.

230. Zhou, R., H. Zhou, L. Rui, and J. Xu, Bone loss and osteoporosis are associated with conversion from mild cognitive impairment to alzheimer's disease, Current Alzheimer Research, 2014. **11**(7): p. -.

231. Tan, Z., S. Seshadri, A. Beiser, and et al., Bone mineral density and the risk of alzheimer disease, Archives of neurology, 2005. **62**(1): p. 107-111.

232. Fisher, A.A., M.W. Davis, W. Srikusalanukul, and M.M. Budge, Six-fold increased risk of hip fracture in older australians (≥60 years) with dementia, Archives of osteoporosis, 2006. **1**(1): p. 13-19.

233. Muir, J.L., Acetylcholine, aging, and alzheimer's disease, Pharmacology Biochemistry and Behavior, 1997. **56**(4): p. 687-696.

234. Haigler, H., L. Cahill, M. Crager, and E. Charles, Acetylcholine, aging and anatomy: Differential effects in the hippocampus, Brain Research, 1986. **362**(1): p. 157-160.

235. Corkin, S., Acetylcholine, aging and alzheimer's disease: Implications for treatment, Trends in Neurosciences, 1981. **4**: p. 287-290.

236. Nagai, T., P. McGeer, J. Peng, E. McGeer, and C. Dolman, Choline acetyltransferase immunohistochemistry in brains of alzheimer's disease patients and controls, Neuroscience Letters, 1983. **36**(2): p. 195-199.

237. Bird, T., S. Stranahan, S. Sumi, and M. Raskind, Alzheimer's disease: Choline acetyltransferase activity in brain tissue from clinical and pathological subgroups, Annals of Neurology: Official Journal of the American Neurological Association and the Child Neurology Society, 1983. **14**(3): p. 284-293.

238. Wilcock, G., M. Esiri, D. Bowen, and C. Smith, Alzheimer's disease: Correlation of cortical choline acetyltransferase activity with the severity of dementia and histological abnormalities, Journal of the Neurological Sciences, 1982. **57**(2-3): p. 407-417.

239. Pedata, F., J. Slavikova, A. Kotas, and G. Pepeu, Acetylcholine release from rat cortical slices during postnatal development and aging, Neurobiology of Aging, 1983. **4**(1): p. 31-35.

240. Haider, S., S. Saleem, T. Perveen, S. Tabassum, Z. Batool, S. Sadir, et al., Age-related learning and memory deficits in rats: Role of altered brain neurotransmitters, acetylcholinesterase activity and changes in antioxidant defense system, Age, 2014. **36**(3): p. 1291-1302.

241. Namba, H., M. lyo, H. Shinotoh, S.-i. Nagatsuka, K. Fukushi, and T. Irie, Preserved acetylcholinesterase activity in aged cerebral cortex, The Lancet, 1998. **351**(9106): p. 881-882.

242. Perry, E.K., The cholinergic system in old age and alzheimer's disease, Age and ageing, 1980. **9**(1): p. 1-8.

243. Eastell, R., T.W. O'Neill, L.C. Hofbauer, B. Langdahl, I.R. Reid, D.T. Gold, et al., Postmenopausal osteoporosis, Nature reviews Disease primers, 2016. **2**(1): p. 1-16.

244. Pacifici, R., Estrogen, cytokines, and pathogenesis of postmenopausal osteoporosis, Journal of Bone and Mineral Research, 1996. **11**(8): p. 1043-1051.

245. Newhouse, P. and J. Dumas, Estrogen-cholinergic interactions: Implications for cognitive aging, Horm Behav, 2015. **74**: p. 173-85.

246. Monteiro, S.C., C. Matte, D. Delwing, and A.T. Wyse, Ovariectomy increases na+, k+-atpase, acetylcholinesterase and catalase in rat hippocampus, Mol Cell Endocrinol, 2005. **236**(1-2): p. 9-16.

247. Basselin, M., H.N. Nguyen, L. Chang, J.M. Bell, and S.I. Rapoport, Acute but not chronic donepezil increases muscarinic receptor-mediated signaling via arachidonic acid in unanesthetized rats, J Alzheimers Dis, 2009. **17**(2): p. 369-82.

248. Nachlinger, R.J., V. Kauschke, K. Trinkaus, T. El Khassawna, C. Heiss, and K.S. Lips, Application of donepezil increased collagen 1 expression in mesenchymal stroma cells of an ovine osteoporosis model, Journal of Musculoskeletal & Neuronal Interactions, 2018. **18**(3): p. 354-365.

249. Sophocleous, A. and A.I. Idris, Rodent models of osteoporosis, BoneKEy reports, 2014. **3**.

250. Kalu, D.N., The ovariectomized rat model of postmenopausal bone loss, Bone and Mineral,

1991. **15**(3): p. 175-191.

251. Amouzougan, A., L. Lafaie, H. Marotte, D. Denarie, P. Collet, B. Pallot-Prades, et al., High prevalence of dementia in women with osteoporosis, Joint Bone Spine, 2017. **84**(5): p. 611-614.

252. Loskutova, N., R.A. Honea, E.D. Vidoni, W.M. Brooks, and J.M. Burns, Bone density and brain atrophy in early alzheimer's disease, J Alzheimers Dis, 2009. **18**(4): p. 777-85.

253. Chen, Y.-H. and R.Y. Lo, Alzheimer's disease and osteoporosis, Tzu-Chi Medical Journal, 2017. **29**(3): p. 138.

254. Tamimi, I., S.A. Madathil, A. Kezouh, B. Nicolau, I. Karp, and F. Tamimi, Effect of acetylcholinesterase inhibitors on post-surgical complications and mortality following a hip fracture: A cohort study, J Musculoskelet Neuronal Interact, 2017. **17**(2): p. 69-77.

255. Tamimi, I., T. Ojea, J.M. Sanchez-Siles, F. Rojas, I. Martin, I. Gormaz, et al., Acetylcholinesterase inhibitors and the risk of hip fracture in alzheimer's disease patients: A case-control study, J Bone Miner Res, 2012. **27**(7): p. 1518-27.

256. Eimar, H., A. Perez Lara, I. Tamimi, P. Marquez Sanchez, I. Gormaz Talavera, F. Rojas Tomba, et al., Acetylcholinesterase inhibitors and healing of hip fracture in alzheimer's disease patients: A retrospective cohort study, J Musculoskelet Neuronal Interact, 2013. **13**(4): p. 454-63.

257. Ogunwale, A.N., C.S. Colon-Emeric, R. Sloane, R.A. Adler, K.W. Lyles, and R.H. Lee, Acetylcholinesterase inhibitors are associated with reduced fracture risk among older veterans with dementia, Journal of Bone and Mineral Research, 2020. **35**(3): p. 440-445.

258. Won, D.Y., S.J. Byun, J.S. Jeong, and J.-Y. Shin, Association between acetylcholinesterase inhibitors and osteoporotic fractures in older persons with alzheimer's disease, Journal of the American Medical Directors Association, 2020.

259. Perry, E.K., The cholinergic system in old age and alzheimer's disease, Age Ageing, 1980. **9**(1): p. 1-8.

260. Namba, H., M. Iyo, H. Shinotoh, S. Nagatsuka, K. Fukushi, and T. Irie, Preserved acetylcholinesterase activity in aged cerebral cortex, Lancet, 1998. **351**(9106): p. 881-2.

261. Marcus, R., Clinical review 76: The nature of osteoporosis, The Journal of Clinical Endocrinology & Metabolism, 1996. **81**(1): p. 1-5.

262. Foundation, C.H.P., Editorial board of osteoporosis prevention and treatment (china white paper), Chinese Journal of Health Management, 2009. **3**: p. 148-154.

263. Carlier, P.R., D.M. Du, Y. Han, J. Liu, and Y.P. Pang, Potent, easily synthesized huperzine a-tacrine hybrid acetylcholinesterase inhibitors, Bioorg Med Chem Lett, 1999. **9**(16): p. 2335-8.

264. Carlier, P.R., D.M. Du, Y.F. Han, J. Liu, E. Perola, I.D. Williams, et al., Dimerization of an inactive fragment of huperzine a produces a drug with twice the potency of the natural product, Angewandte Chemie, 2000. **112**(10): p. 1845-1847.

265. Li, W.M., K.K. Kan, P.R. Carlier, Y.P. Pang, and Y.F. Han, East meets west in the search for alzheimer's therapeutics - novel dimeric inhibitors from tacrine and huperzine a, Curr Alzheimer Res, 2007. **4**(4): p. 386-96.

266. Pang, Y.-P., P. Quiram, T. Jelacic, F. Hong, and S. Brimijoin, Highly potent, selective, and low cost bis-tetrahydroaminacrine inhibitors of acetylcholinesterase steps toward novel drugs for treating alzheimer's disease, Journal of Biological Chemistry, 1996. **271**(39): p. 23646-23649.

267. Yu, H., W.M. Li, K.K. Kan, J.M. Ho, P.R. Carlier, Y.P. Pang, et al., The physicochemical properties and the in vivo ache inhibition of two potential anti-alzheimer agents, bis(12)-hupyridone and bis(7)-tacrine, J Pharm Biomed Anal, 2008. **46**(1): p. 75-81.